INAUGURAL-DISSERTATION

zur
Erlangung der Doktorwürde
der
Naturwissenschaftlich-Mathematischen
Gesamtfakultät
der
Ruprecht - Karls - Universität
Heidelberg

vorgelegt von

Diplom-Biologin Christine Hassler

aus Graz, Österreich

Tag der mündlichen Prüfung:

Characterization of developmental role and mechanistic function of Kremen proteins

Gutachter: Prof. Dr. Christof Niehrs

Prof. Dr. Renato Paro

Abbreviations

ACs	animal cap explants
a-p	antero-posterior
ARF	ADP-ribosylation factor
BMP	Bone morphogenetic protein
bp	base pairs
C. elegans	*Caenorhabditis elegans* (roundworm)
CNS	central nervous system
CoIP	Co-immunoprecipitation
CoMO	control Morpholino
DEPC	diethylpyrocarbonate
DIG	digoxygenin
DLMZ	dorso-lateral marginal zone
D. melanogaster	*Drosophila melanogaster* (fruit fly)
Dkk	Dickkopf
DNase	deoxyribonuclease
DTT	dithiothreitol
d-v	dorso-ventral
Dvl	Dishevelled
EDTA	sodium ethylendiaminotetraacetate
EGF	Epidermal growth factor
ER	endoplasmic reticulum
FGF	Fibroblast growth factor
Fz	Frizzled receptor
GFP	Green fluorescent protein
GNPTAG	N-Acetylglucosamine-1-Phosphotransferase gamma subunit
kDa	kiloDalton
Krm	Kremen
LDLR	Low density lipoprotein receptor
LRP	Lipoprotein receptor-related protein
LRP6ΔE1-4	LRP6 construct with deleted YWTD β-propeller/EGF modules

M	molar
M. lignano	*Macrostomum lignano* (flatworm)
mesd	*mesoderm development* (defective)
min	minutes
MO	Morpholino
MRH	mannose 6-phosphate receptor homology
NC	neural crest
OS-9	amplified in osteosarcoma
PC	prechordal plate
PCP	planar cell polarity
PCR	polymerase chain reaction
PPL	Preprolactin
PRKCSH	Glucosidase II beta subunit
rpm	rounds per minute
RT	room temperature
RT-PCR	Reverse transcriptase-PCR
sFRP	secreted Frizzled-related protein
S. purpuratus	*Strongylocentrotus purpuratus* (sea urchin)
SDS-PAGE	sodium dodecyl sulphate polyacrylamide gel electrophoresis
TCF	T-cell factor
UPR	unfolded protein response
X. laevis	*Xenopus laevis* (African clawed frog)
X. tropicalis	*Xenopus* (*Silurana*) *tropicalis* (western clawed frog)
Xnr3	*Xenopus* nodal-related3
YWTD	consensus amino acid motif of β-propeller of LDLR superfamily

Collaborators

C.C.	Cristina Cruciat
G.D.	Gary Davidson
R. Mayor	Roberto Mayor
W.W.	Wei Wu

Table of contents

1. SUMMARY

The Wnt/β-catenin signaling pathway plays pivotal roles during embryonic development and adult tissue homeostasis; these include the regulation of cell fate decisions during germ layer induction, axial patterning and organogenesis, as well as cell proliferation and stem cell maintenance. Wnt signaling is antagonized by Dickkopf (Dkk) proteins, which play an important role in antero-posterior patterning of the central nervous system. Dkks function by inhibiting the Wnt receptor LRP5/6. They act in conjunction with transmembrane proteins of the Kremen family (Krm1 and 2, collectively termed Krms). Dkk binds to both LRP5/6 and Krm and induces formation of a ternary complex, which is cleared from the cell surface by endocytosis, leading to shut down of Wnt signal transduction.

This study was initiated by several open questions: How do Krms function to mediate LRP6 clearance from the cell surface? Are there other proteins involved in this process? Do Krms have Dkk-independent roles during *Xenopus* development?

Towards a mechanistic analysis of Krm/Dkk mediated Wnt inhibition, several screens for Krm interaction/binding partners were undertaken which led to the identification and characterization of Erlectin, a novel secreted protein which (i) binds to N-glycans linked to Krm2; (ii) is a member of the endoplasmic reticulum (ER) synexpression group in *Xenopus*; (iii) is localized in the ER lumen; and (iv) is essential for normal *Xenopus* development. As a second major result of this study, I observed and established that Krm2 plays a Dkk1-independent role during *Xenopus* neural crest formation. The experimental data revealed that Krm2 (i) is co-expressed with Wnts and regulated by zygotic Wnt signaling; (ii) shows differential expression in the neural crest and can induce neural crest tissue when overexpressed; (iii) is required for neural crest formation; and (iv) promotes cell surface localization of LRP6, as well as LRP6-mediated Wnt signaling in cultured cells. Based on these findings I developed a model in which Krms may be considered as context-dependent inhibitors or activators of Wnt/LRP6 signaling, which are regulated by the presence or absence of Dkk, respectively.

2. ZUSAMMENFASSUNG

Der Wnt/β-catenin Signalweg hat als bedeutender Regulator der Embryonalentwicklung, aber auch der Gewebshomöostase im adulten Organismus, eine Schlüsselrolle inne; er kontrolliert Prozesse wie Keimblattinduktion, Musterbildung der Körperachsen, Zellproliferation und Stammzellerneuerung. Der Wnt Signalweg selbst wird streng reguliert, unter anderem von Proteinen der Dickkopf (Dkk) Familie, die als Inhibitoren wirken und die Signaltransduktion blockieren. Diese durch Dkk1 vermittelte Inhibition des Wnt Signalweges ist essentiell für die Entwicklung des Kopfes als Teil der Musterbildung entlang der antero-posterioren Körperachse. Dkk1 bindet an den Wnt Rezeptor LRP5/6 und blockiert ihn; dabei arbeitet Dkk1 mit einem weiteren Korezeptor zusammen, dem Transmembranprotein Kremen (Kremen1 bzw. 2, abgekürzt Krm1 bzw. 2). Zusätzlich zu LRP5/6 bindet Dkk1 auch an Krm, und gemeinsam bilden Dkk1, LRP5/6 und Krm einen ternären Komplex, der durch Endozytose von der Zelloberfläche entfernt wird – nun kann das Wnt Signal nicht mehr übermittelt werden.

Am Anfang dieser Studie standen folgende Fragen: Wie reguliert Krm die Entfernung bzw. den Abbau des Wnt Rezeptors LRP5/6 von der Zelloberfläche? Sind andere Proteine an diesem Prozess beteiligt, und wenn ja, welche? Weiters: Arbeitet Krm immer mit Proteinen der Dkk Familie zusammen, oder hat es auch eigene, Dkk-unabhängige Funktionen während der Embryonalentwicklung von *Xenopus*?

Ein Ziel dieses Arbeit ist die mechanistische Analyse der durch Krm und Dkk mediierten Inhibition des Wnt Signalweges. Es wurden mehrere Suchansätze unternommen um Binde- und Interaktionspartner von Krm zu finden; diese führten zur Isolierung und Charakterisierung von Erlectin, einem neuartigen sekretierten Protein. Erlectin (i) bindet an N-Glykangruppen auf Krm2; (ii) ist ein Mitglied der Synexpressionsgruppe des Endoplasmatischen Retikulums (ER); (iii) ist im Lumen des ER lokalisiert; und (iv) ist essentiell für die normale Entwicklung von *Xenopus* Embryonen.

Das zweite bedeutende Ziel dieser Arbeit umfasst die Analyse der Rolle von Krm2 während der Neuralleistenentwicklung in *Xenopus*. Meine Experimente zeigten dass Krm2 (i) mit Wnt Genen koexprimiert ist, und weiters dass die Expression von Krm2 vom Wnt Signalweg regulirt wird; (ii) differenziell in der Neuralleistenregion exprimiert wird und selbst Neuralleistengewebe induzieren kann; (iii) für die Neuralleisteninduktion unbedingt nötig ist; und (iv) in Zellkulturzellen sowohl den Wnt Signalweg stimulieren, als auch die vermehrte Lokalisierung von LRP6 an der Zelloberfläche bewirken kann. Aus diesen Ergebnissen habe ich ein hypothetisches Modell abgeleitet, in dem Kremen Proteine als kontextabhängige Inhibitoren oder Aktivatoren der Wnt Signalweges verstanden werden können, deren Wirkweise durch An- oder Abwesenheit von Dkk1 reguliert wird.

3. INTRODUCTION

Animal development progressively transforms a single cell (zygote) into a complex multicellular organism. Several closely interconnected processes form the basis of development; these include cleavage, embryonic pattern formation, morphogenesis, cell differentiation and growth [1]. Pattern formation lays down the body plan of an animal, and involves the induction of the main body axes and germ layers as well as the spatial and temporal organization of cell differentiation. Variations in pattern formation mainly account for the existing multitude of animal forms.

Cell to cell signaling is an essential and characteristic feature of all multicellular organisms, and core signaling pathways regulate most aspects of pattern formation. Such pathways are highly conserved throughout the animal kingdom, and thus must have evolved before the divergence of most of the modern phyla [2]. Only very few signaling pathways lie at the heart of all developmental regulation; they are repeatedly reused at different places and times during animal development to induce specific cellular responses, and ultimately establish the body plan [3]. The main signaling systems guiding early animal development are the TGFβ (including Nodal/BMP) [4], Hedgehog [5], Notch [6], receptor tyrosin kinase (EGF/FGF) [7] and Wnt [8] pathways; frequently, two or more of these pathways function cooperatively to elicit specific developmental responses [9-11]. The Wnt pathway - a main theme in this study – will be discussed in detail below.

To assure an orderly progression of development, these signaling pathways are themselves regulated at many levels by a variety of control mechanisms. To gain understanding of such regulatory mechanisms is a central question in developmental biology. Whereas phylogenetic variations in pathway regulation may account for evolutionary change, pathway misregulation during ontogeny inevitably leads to aberrant embryonic development, as well as disease, for example cancer.

A relatively small number of model organisms is used for experimental studies in developmental biology; theses include invertebrates such as the fruit fly (*D. melanogaster*) and roundworm (*C. elegans*), and vertebrate species such as amphibians, fish (*D. rerio*) and mice.

Traditionally, amphibians have been the model organisms of choice to address questions of embryology [12]. Their large and numerous embryos can be easily obtained, are accessible to manipulation already prior to fertilisation, and develop rapidly. The African clawed frog *Xenopus laevis* (*X. laevis*), an easy-to-keep freshwater animal, is today's prevalent amphibian model system in developmental biology; a combination of traditional experimental manipulations, such as microdissection, transplantation, microinjection and fate mapping, and advanced molecular methods, such as analysis of gene expression/protein expression patterns, transgenesis and manipulation of gene expression, is available to study its early development [13-15]. A major disadvantage of *X. laevis* is the lack of accessibility to genetic analysis; this frog has a long generation time (1-2 years) and is tetraploid (containing 4 homologous chromosomes). This prevents rapid breeding and entails the drawback of pseudoallelic compensation in loss-of-function studies. Recently, the diploid frog *Xenopus* (*Silurana*) *tropicalis*, a petite brother of *X. laevis*, is emerging as a useful alternative for genetic approaches in amphibians [16-18]. In the last decade, extensive analysis of complex developmental processes such as determination and patterning of the primary body axes, as well as induction of the neural crest, led to a comprehensive understanding of early *X. laevis* development.

Early *Xenopus* development I: Axis induction & patterning

The *Xenopus* egg is radially symmetrical along its animal-vegatal axis. Embryonic development starts with sperm entry, which breaks the egg's radial symmetry and initiates a directional cytoplasmic movement (referred to as cortical rotation). This movement translocates maternal components of the Wnt signaling pathway from the vegetal pole to the future dorsal side of the embryo, where Wnt signaling is activated. Simultaneously, the Nodal signaling pathway induces the mesodermal germ layer at the interface of animal (ectodermal) and vegetal (endodermal) hemispheres of the embryo. Dorsally, overlapping Wnt and Nodal pathway activation induces formation of the Spemann organizer (named

after its discoverer Hans Spemann [19]), a signaling center which establishes the dorso-ventral (d-v), and subsequently antero-posterior (a-p) body axes (Fig. 1) [20-22].

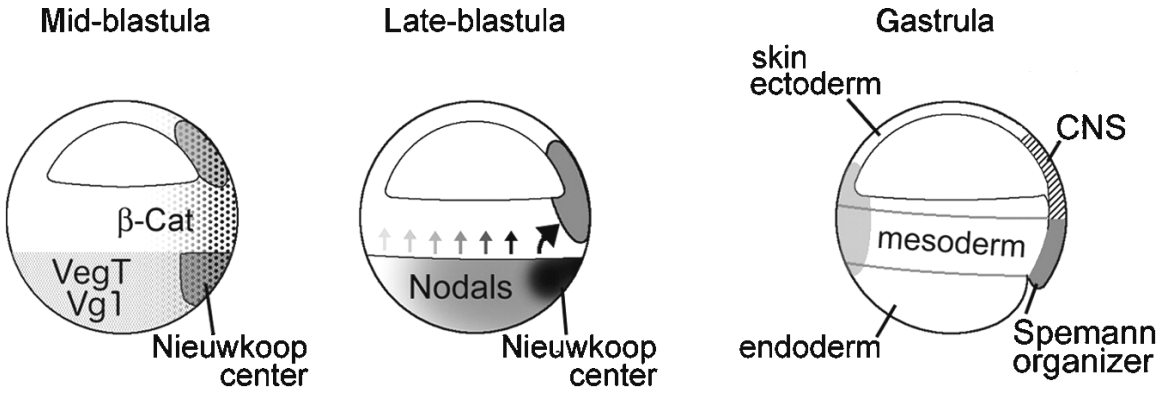

Figure 1. Establishment of the Spemann organizer. Activation of a maternal Wnt pathway on the dorsal side of the embryo leads to stabilization of the Wnt-mediator β-catenin. Nodal signals are induced by the maternal genes VegT and Vg1, and are secreted from vegetal cells to induce mesoderm. Dorsally, at the intersection of Nodal and Wnt signaling, the Nieuwkoop center forms and induces the Spemann organizer. CNS, central nervous system. Picture adapted from [21].

The Spemann organizer (dorsal blastopore lip) is the main signaling center of the early embryo and patterns all three germ layers along the d-v and a-p body axes [21, 23-25]. It initiates gastrulation and lengthens the a-p axis by undergoing extensive morphogenetic movements (convergent extension), which transform the ball-shaped organizer into a long, narrow rod [26, 27]. Based on distinct inductive abilities and gene expression domains the elongated organizer is subdivided into three main regions along the a-p axis: The anterior mesendoderm, which induces e.g. balancers, cement gland and heart, and differentiates into liver and foregut; the prechordal plate (PC), which e.g. induces forebrain and eyes, and differentiates into head mesenchyme and muscle; and the chordamesoderm, which e.g. induces mid-, hindbrain and spinal cord, and differentiates into notochord [24].

Molecularly, the organizer is defined by expression of a set of transcription factors as well as a 'cocktail' of secreted proteins, which mediate organizer activity. Albeit initially a surprise, it is now well established that these secreted proteins are mostly not instructive inducers, but act as inhibitors of major signaling pathways, namely the Wnt, BMP and

Nodal pathways [21, 24, 28]. They include: The Wnt inhibitors Dickkopf1 (Dkk1) [29] and secreted Frizzled-related proteins (sFRPs), including Frzb-1 [30, 31], sFRP2 [32] and Crescent [32, 33] (reviewed in [34-36]); the BMP inhibitors Chordin [37], Noggin [38], Follistatin [39] and *Xenopus* Nodal-related3 (Xnr3) [40, 41]; the Nodal inhibitors Lefty/Antivin proteins [42, 43] (reviewed in [44, 45]); and Cerberus, an inhibitor of all three (Wnt, BMP, Nodal) pathways [46, 47] (Fig. 2A).

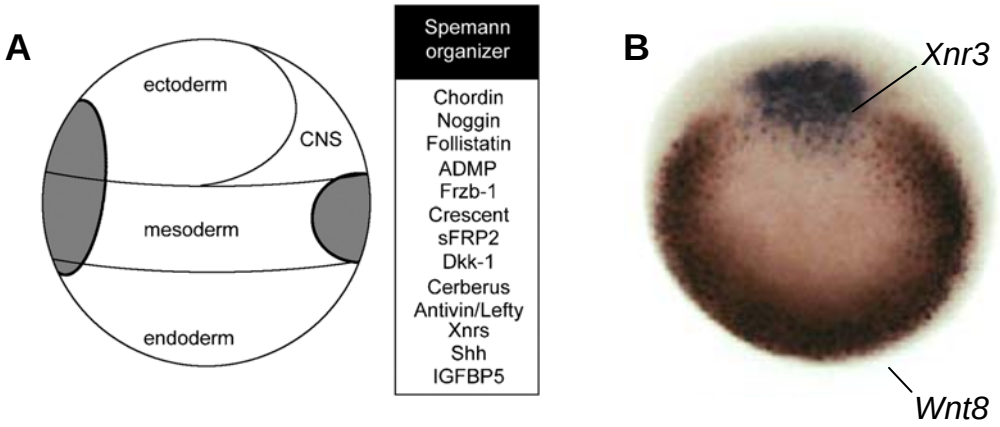

Figure 2. Overview of the Spemann organizer. (A) Secreted antagonists of the Spemann organizer. Left: Scheme of a late blastula stage embryo before the onset of gastrulation, shown in lateral view, with dorsal to the right. Indicated are the three germ layers: endoderm, mesoderm, which includes the organizer (grey), and ectoderm, which includes the future central nervous system (CNS). Right: The organizer secretes mainly Wnt, BMP and Nodal inhibitors (see text). Picture adapted from [21]. **(B)** Antagonistic gene expression domains define organizer and ventro-lateral mesoderm. Early gastrula stage embryo shown in vegetal view, with dorsal oriented to the top. A double *in situ* hybridization visualizes expression of the organizer gene *Xnr3* and the ventro-lateral mesodermal gene *Wnt8*. Picture taken from Xenbase [48]; expression patterns first published in [41, 49].

The distinct subregions of the organizer secret a specific combination of pathway antagonists [24]: Anterior mesendoderm and PC produce BMP and Wnt antagonists, which are required for anterior (head) development (two inhibitor model of head induction) [11, 50], and anti-Nodals, the requirement of which in head induction is still a matter of debate [47, 51]. The chordamesoderm secretes mainly BMP antagonists, whereas Nodals and Wnts are actively signaling here; this induces posterior (trunk) development [22]. Finally, tail

development is regulated by active BMP, Nodal and Wnt signaling, as shown for zebrafish [52].

The antagonism between dorsal, organizer-mediated inhibition and ventral activation of the Wnt and BMP pathways is well reflected by gene expression domains. Whereas organizer genes are expressed dorsally in a localized fashion, BMP and Wnt pathway ligands are expressed in the remaining ventro-lateral mesoderm, in a horseshoe-like pattern (Fig. 2B).

The secreted pathway antagonists of the organizer are expressed locally and form protein gradients; thereby, they create a counter-gradient of BMP and Wnt signaling, which in turn regulates tissue patterning in a concentration-dependent manner. The BMP gradient patterns ectoderm and mesoderm along the d-v axis; thereby, high signaling levels promote ventral fates (epidermis, blood), whereas low levels of BMP signals permit development of dorsal fates (neural plate, notochord) [21, 53]. Wnt signaling cooperates with BMP signaling in patterning of the ventral and lateral mesoderm, where it inhibits notochord formation and promotes muscle development [54-57].

Along the a-p axis, a Wnt gradient patterns the neuroectoderm in a direct and dose-dependent fashion [58-60]. Anteriorly, Wnt levels are kept low by secreted Wnt inhibitors emanating from the PC (see above) [61], and thereby anterior neuroectodermal cell fates (forebrain) are established; towards posterior, successively higher levels of Wnt signaling mediated by Wnts emanating from ventro-lateral mesoderm (candidates are Wnt8 and Wnt3a [58, 62]) specify midbrain, hindbrain and spinal cord fates [58].

Experimentally, inhibition of zygotic Wnt signaling leads to a prevalence of organizer-mediated effects, and thus to promotion of dorsal and anterior cell fates. Such embryos show enlarged notochord and forebrain, but reduced muscle tissue, and are generally termed ‘anteriorized’. Conversely, ectopic Wnt activation leads to reduced organizer function, and thus to promotion of ventral and posterior cell fates. Such embryos have enlarged muscle tissue, but reduced notochord and forebrain (termed ‘posteriorized’) [55, 56]. Phenotypically, perturbations of the zygotic Wnt pathway can be readily recognized as a ‘shift’ in a-p positional identity (Fig. 3).

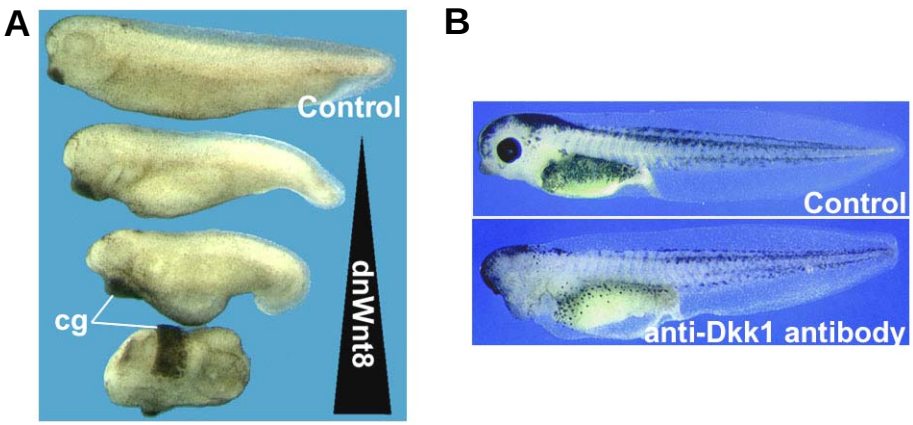

Figure 3. Phenotypes of embryos with perturbed zygotic Wnt signaling. (A) Wnt inhibition leads to anteriorization, characterized by increased head and cement gland (cg) tissue and shortened, towards ventral bent tail. Embryos were injected with increasing doses of dominant negative (dn) *Wnt8* mRNA; pictures were taken at tailbud stage (st. 34). **(B)** Wnt activation leads to posteriorization, characterized by missing head and cement gland tissue. The embryo shown in the lower panel was injected with anti-Dkk1 antibody, which blocks endogenous Dkk1 protein; pictures were taken at tadpole stage (approx. st. 43). Pictures adapted from: (A) my unpublished data; (B) [29] and [63].

Early *Xenopus* development II: Neural crest formation

Besides induction and patterning of the neural plate another event important for this study takes place in the ectoderm of the gastrulating embryo: Induction of the neural crest (NC).

Phylogenetically, the appearance of the NC was a key step in chordate evolution; it allowed formation of a new head and subsequent adaptation to an active predatory life style, ultimately giving rise to the vertebrate clade [64-66]. Thus, NC tissue is a defining feature of vertebrates and distinguishes them from non-vertebrate chordates (such as lancelets and ascidians).

The NC is a multipotent tissue arising at the border of neural plate and non-neural ectoderm. NC cells migrate throughout the embryo and differentiate into a variety of tissues, such as bone, cartilage and connective tissue of the head, melanocytes, peripheric nervous system (neurons and glia), epinephrine-producing cells of the adrenal gland, and fin

(in amphibians and fish) [67-69]. Due to its developmental importance, the NC has also been denominated the 'fourth germ layer'.

According to the variety of NC-derived tissues, perturbed NC development results in a set of pathological conditions, collectively termed neurocristopathies. These include facial abnormalities, pigmentation defects, heart defects and intestinal insufficiency (due to absence of enteric ganglia) [70-72].

Induction of NC. Since the discovery of NC [73] biologists have been interested in the process of its embryonic induction. Three tissues lie in close proximity to the future NC territory: Neural plate, non-neural ectoderm, and the underlying paraxial mesoderm, which later will form somites (Fig. 4). Initial embryological experiments established a pivotal role for interactions of these tissues during NC induction [74, 75]. In amphibians, experimental juxtaposition of paraxial mesoderm is sufficient to induce NC cells and derivatives in ectoderm, and paraxial mesoderm is required for NC induction *in vivo* [76, 77]. Similarly, juxtaposition of neural plate and non-neural ectoderm induces NC cells; interestingly, in this experiment both ectodermal tissues can generate NC, suggesting reciprocity of the inductive event [78].

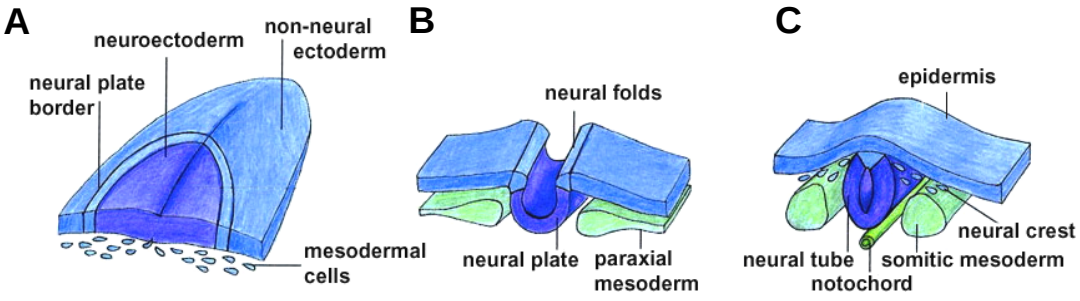

Figure 4. Overview of neurulation and neural crest formation. (A) The neural plate border forms at the interface of neuroectoderm and non-neural ectoderm, and **(B)** gives rise to the neural folds during neurulation. **(C)** Around the time of neural tube closure, NC cells undergo epithelial-to-mesenchymal transition, delaminate from the neural tube and start migrating along defined pathways. Picture taken and modified from [75].

In the last two decades, molecular studies have revealed the identity of signals emanating from NC inducing tissues. In *Xenopus*, induction of NC at the border of neural and non-

neural ectoderm takes place during late gastrulation and relies on the combined action of BMP, Wnt and FGF type signals (Fig. 5) [79-85].

It is well established that BMP signals pattern the ectoderm along the doso-ventral axis in a graded fashion [21]. Ventrally, high levels of BMP signaling establish epidermal cell fates. Dorsally, low levels of signaling activity, due to BMP inhibition by antagonists secreted from the dorsal mesoderm, permit induction of the neural plate (see above). At the interface of neural plate and ectoderm, intermediate levels of BMP activity provide the basis for NC induction [77, 79, 86, 87].

The pivotal role of Wnt/β-catenin signaling during NC induction is well established due to evidence coming from studies in *Xenopus*, as well as zebrafish [88], chicken [89] and mouse [90]; for reviews see [91-93]. In *Xenopus*, ectopic activation of the Wnt pathway, in conjunction with intermediate BMP levels, leads to NC induction in naïve ectoderm; similarly, Wnt activation in whole embryos expands the NC territory [81, 92, 94, 95]. Conversely, Wnt inhibition, e.g. by application of dominant negative constructs, or knock-down of pathway components, prevents NC formation [96-98].

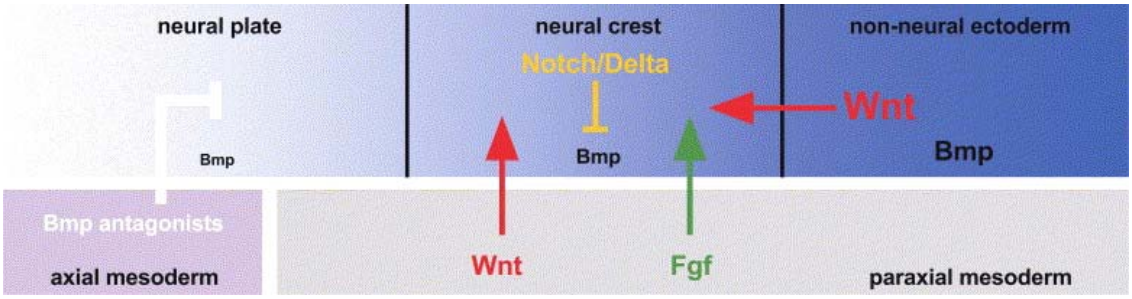

Figure 5. Signals involved in NC induction. NC is induced at the junction of neural plate and non-neural ectoderm, where intermediate levels of BMP signaling are present. Wnt signals emanating from paraxial mesoderm and/or non-neural ectoderm are required for NC induction. Furthermore, the FGF pathway regulats NC induction. Picture taken from [67].

NC induction by Wnts is a direct effect and not coupled to the posteriorizing influence of Wnts on the neural plate, since low levels of ectopic Wnt signals promote NC fates without affecting a-p patterning [97, 99]. It is yet unclear which Wnt ligand mediats NC induction in

Xenopus. Wnt8 ranks first as candidate, since it is expressed at the right time (throughout gastrulation) and place (in the paraxial mesoderm underlying the future NC region) [100]. In support of this, Wnt8 knock-down in zebrafish results in loss of NC tissue [88].

How are multiple signals from the BMP, Wnt and FGF pathways integrated to induce NC? It is emerging that sets of transcription factors are activated consecutively, and specify the prospective NC region in a successive manner. Initially, BMP, Wnt and FGF signals induce a set of transcription factors which broadly defines the prospective NC region (neural plate border specifiers); it includes Zic, Msx1/2, Dlx5 and Pax3/7 proteins, respectively. These transcription factors, in turn, activate a set of genes expressed only in the NC territory (NC specifiers); examples are Slug/Snail, the SoxE family members Sox9 and Sox10, Twist and FoxD3. As a next step, NC effector genes are activated; these regulate delamination, migration and lineage specific differentiation of the NC (Fig. 6) (e.g., Mitf, RhoB and Collagen 2a) [101-103]. In addition, various cross-regulatory events within the same level, as well as between different levels of this regulatory network exist, thus increasing complexity considerably (Fig. 6) [103]; a well-established example is the direct induction of *slug* transcription by Wnt signaling [104].

Migration of NC. After establishment of the NC cell fate and towards the end of neurulation (neural tube closure), NC cells delaminate from the neural tube and start migrating along defined routes throughout the embryo. Besides many other signals, both BMP and Wnt pathways have been implicated in these processes [91, 105, 106].

Differentiation of NC. NC cells are pluripotent and give rise to numerous differentiated cell types (see above), depending on their final location within the embryo. Both BMP and Wnt signals are involved in NC differentiation. Several studies suggest that during NC differentiation Wnt signals specify melanocytes at expense of neuronal cell fates [107, 108]. Wnt signaling activates transcription of *mitf*, a key regulator of the pigment cell lineage [109, 110], and *sox10*, a NC specifying transcription factor (see above) [111], which is also implicated specifically in melanocyte development (reviewed in [92, 112]). Conversely, BMP signals promote neuronal fates and inhibit pigment cell formation [91, 113].

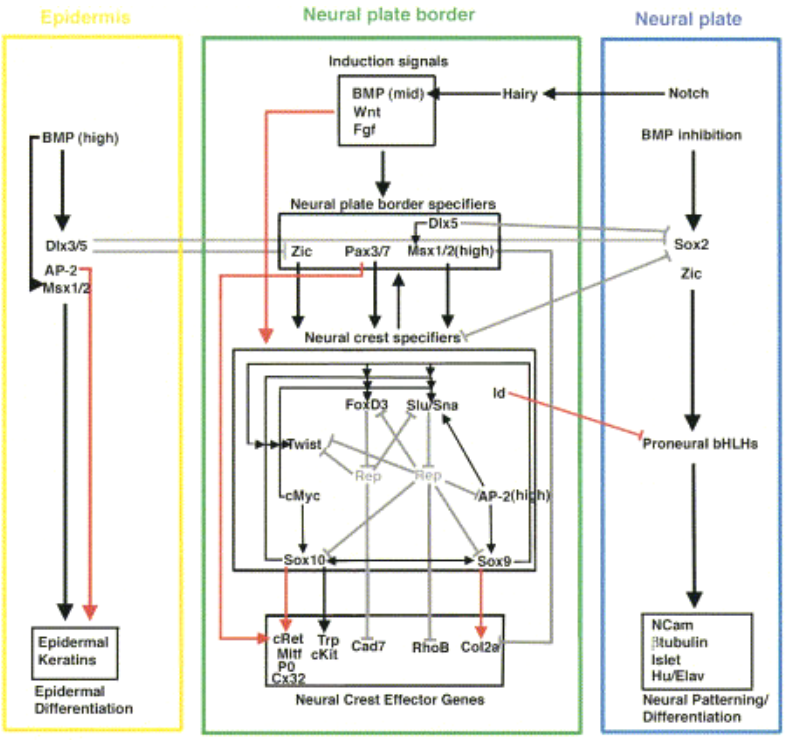

Figure 6. The putative gene regulatory network at the neural plate border is highly complex. At the neural plate border, Wnt and FGF signals, as well as intermediate levels of BMPs, induce expression of neural plate border genes, which subsequently induce NC specifiers. Extensive regulatory crosstalk between NC genes maintains their expression until migration and differentiation, when NC effector genes are expressed. Red arrows indicate direct regulatory interactions, whereas black arrows indicate genetic interactions suggested by gain- and loss-of-function analyses largely in *Xenopus*. Gray lines indicate repression. Picture taken from [103].

The Wnt signaling pathway in animal development

The above presented description of early *Xenopus* development highlights a prime role of Wnt signaling in vertebrate axis formation and patterning, as well as NC induction. The Wnt pathway is evolutionary highly conserved and ancient, and plays fundamental roles in the regulation of early developmental processes in most animal phyla.

In cnidarians, simple metazoans containing only two epithelial germ layers and one main body axis, the Wnt pathway is differentially activated along the body axis, and specifies the endodermal germ layer [114, 115]. Similarly, Wnts induce endoderm formation in the nematode *C. elegans* [116], pattern the endomesoderm along the animal-vegetal axis in sea

urchins (echinoderms) [117, 118], and regulate posterior specification and endoderm formation in protochordates, a basal non-vertebrate chordate group [119, 120]. Even sponges, which represent the simplest multicellular animals and completely lack body axes and differentiated tissues other than an epithelium, harbour homologs of Wnt signaling components, including a Wnt ligand. It was thus speculated that the Wnt pathway was already present in the last common ancestor of all multicellular animals [121].

Subsequent to their roles in early development, Wnts are extensively involved in the regulation of organogenetic processes such as myogenesis [122, 123], limb [124], lung [125], eye [126] and brain [127] development, and synaptogenesis [128, 129]. Throughout development, the Wnt pathway is furthermore an important regulator of cell survival and proliferation [130-133], as well as cell migration and polarity [134-136].

In adult animals, Wnt signaling is implicated in the regulation of tissue renewal, for example in the gut epithelium, skin, bone and hematopoetic system [137-140]. Misregulation of the Wnt pathway is a prime cause of several degenerative diseases and cancers, in particular colon cancer [8, 133, 141-143]. To gain a thorough understanding of Wnt pathway regulation is therefore of genuine biological interest as well as of considerable medical relevance.

According to different signaling mechanism and biological responses the Wnt pathway is divided into three branches:
1) The canonical Wnt/β-catenin pathway, which operates through transcriptional control of target genes, and regulates induction and patterning of germ layers/body axes, cell fate specification during organogenesis, and cell proliferation [8, 141, 144-146];
2) the non-canonical or Wnt/PCP pathway, which mainly elicits direct cytoskeletal changes, and is implicated in cell polarity and tissue movements [135, 136, 147-149]; and
3) the Wnt/Calcium pathway, which activates Calcium-dependent cellular responses, and is thought to antagonize Wnt/β-catenin signaling and regulate cell migration [134, 150, 151].

The Wnt/β-catenin pathway is the primary subject of this study, and its signaling mechanism and regulation will be discussed on the following pages.

The Wnt/β-catenin signal transduction pathway

Mechanistically, the Wnt/β-catenin pathway proves to be extraordinarily complex, involving a multitude of components and several, possibly parallel, signaling events [8, 141, 144, 146, 152, 153].

The key mechanism in the canonical Wnt pathway is the modulation of the stability of β-catenin, which acts as transcriptional co-activator. In the absence of a Wnt signal, cytosolic β-catenin is contained in a protein complex and constantly degraded. This so called degradation complex includes Glycogen synthase kinase3 (GSK3) and Casein kinase1α (CK1α), which phosphorylate β-catenin, and the scaffolding proteins Axin and Adenomatous polyposis coli (APC). Phosphorylated β-catenin is ubiquitinylated by β-TrCP, a component of the E3 ubiquitin ligase system, and rapidly degraded by the proteasome (Fig. 7A).

Activation of Wnt signaling leads to dephosphorylation and subsequent stabilisation of β-catenin, which translocates into the nucleus, where it replaces the transcriptional repressor Groucho and binds to LEF/TCF transcription factors to co-activate transcription of Wnt target genes. Signaling in initiated by binding of Wnt glycoproteins to Frizzled (Fz) and LRP5/6 (Low density lipoprotein receptor related protein) type receptors on receiving cells. Transduction of the signal induces recruitment of Axin to the cell membrane, where it binds to the cytoplasmic tail of LRP5/6. This event is dependent on LRP5/6 phosphorylation by GSK3β and CK1γ [154, 155], but how these kinases are activated in response to Wnts is still unknown. Axin recruitment disrupts the degradation complex, leading to stabilization of β-catenin. Wnts also induce phosphorylation of Dishevelled (Dvl), an essential cytoplasmic pathway component acting upstream of β-catenin. Phosphorylated Dvl is recruited to the membrane via interaction with Fz receptors (Fig. 7B).

The prevailing model of Wnt signaling suggests that these two signaling events, namely the recruitment of Axin and Dvl to their respective receptors, converge on β-catenin stabilisation. This is in agreement with experiments showing that forced association of Fz and LRP6 can induce β-catenin stabilization in the absence of Wnt ligands [156, 157].

Overexpression of the membrane-bound cytoplasmic tail of LRP5/6 activates the Wnt pathway without Fz/Dvl, suggesting that Axin recruitment alone may be sufficient for signal transduction [158]. However, much in favour of a mutual requirement and interdependence of Fz and LRP5/6 mediated signaling branches are recent results showing that under physiological conditions, Axin is recruited to the membrane in a Dvl-dependent manner, in flies as well as mammalian cells ([159] and Bilic et. al., submitted).

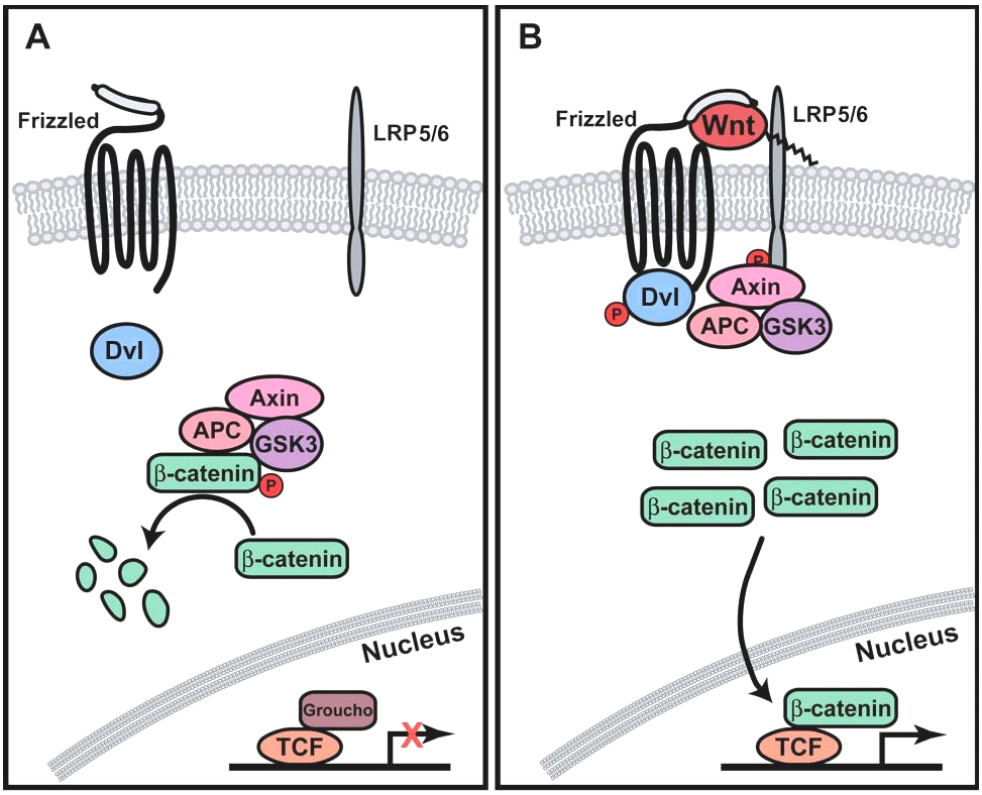

Figure 7. Overview of the Wnt/β-catenin signaling pathway. (A) In the absence of Wnt signals, cytoplasmic β-catenin is constantly degraded. **(B)** Binding of Wnt to Frizzled and LRP5/6 receptors induces recruitment of Axin and Dishevelled (Dvl) to the membrane, thereby disrupting the degradation complex. β-catenin can translocate into the nucleus and act as transcriptional co-activator. Image taken and modified from [146].

Regulation of Wnt/β-catenin signaling

Since the Wnt pathway elicits fundamental cellular responses it is not surprising that the pathway is under stringent regulatory control at various levels, including (i) upstream of

receptor-ligand interaction (biogenesis of receptors/ligands, see below), (ii) receptor-ligand interaction (extracellular space, see below), (iii) signaling in the cytoplasm, and (iv) target gene expression (feedback regulation) [8, 152, 153, 160, 161].

Regulation of Wnt signaling at the level upstream of receptor-ligand interaction

A variety of factors can regulate the Wnt pathway at a level upstream of receptor-ligand interaction, e.g. by specifically influencing maturation, secretion or stability of ligands or receptors, respectively (reviewed in [162-164]).

Wnt ligands. Well established examples are Porcupine [165, 166] and Evi/Wls [167, 168], which are required for acylation and secretion of Wnt, respectively. Furthermore, the retromer complex, which has a general role in retrograde transport of proteins from endosomes to the Golgi apparatus, is specifically involved in Wnt secretion [169, 170].

Wnt receptors. Shisa protein acts as Wnt antagonist by inhibiting Fz maturation in the endoplasmic reticulum (ER) [171].

Until recently, relatively little was known about the biogenesis of the Wnt receptor LRP5/6. However, in 2003, two studies in mouse and fly simultaneously identified a gene essential for LRP5/6 protein maturation (and thus Wnt signaling), termed *mesd*/*boca*, respectively [172, 173]. LRP5/6 proteins are essential components for Wnt/β-catenin signal transduction and their inactivation phenocopies loss of Wnt signaling in vertebrates and invertebrates [174-176]. They are members of the LDLR (low density lipoprotein receptor) superfamily, a group of cell surface receptors with diverse functions in cell metabolism and signal transduction [177, 178]. LRP5/6 proteins are characterized by an extracellular domain containing LDLR repeats and four YWTD β-propeller/EGF modules, a transmembrane domain, and a cytoplasmic tail carrying conserved signal transduction motifs (Fig. 8) [176, 179].

Like most secreted and transmembrane proteins, newly synthesized LRP6 protein enters the secretory pathway via translocation into the ER; there, general modifications/processes such as disulfide bond formation, N- and O- glycosylation, and quality control are performed,

until mature protein is finally transported to the cell surface. Upon ER entry, the YWTD β-propeller/EGF modules of LRP6 are prone to form inter-molecular disulfide bonds, thereby building aggregates and rendering LRP6 protein dysfunctional [180]. Here, Mesd/Boca protein comes into play; it is an ER resident chaperone and acts by specifically binding these YWTD β-propeller/EGF modules, thus reducing receptor aggregation and promoting LRP6 folding and surface localization [172, 173, 180]. Loss of Mesd/Boca function leads to reduced cell surface localization of LRP5/6 and thereby to a shut-down of Wnt signal transduction. Therefore, *mesd/boca* knock-out mice and flies display phenotypes mimicking the combined inactivation of several Wnts [172, 173].

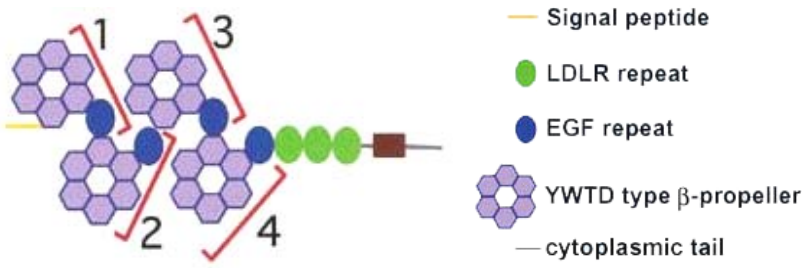

Figure 8. Modular domain structure of LRP6. The four YWTD β-propeller/EGF modules are targeted by Mesd. Picture taken from [180].

Extracellular regulation of Wnt signaling

In the extracellular space, Wnt signaling is mainly modulated by the regulation of Wnt ligand spread/availability, and receptor-ligand interaction.

Wnt proteins are lipid modified and likely do not diffuse easily in the extracellular space [181]; however, as morphogens they form concentration gradients, and can act in a long-range manner [58, 182, 183]. Several mechanisms have been suggested to explain how Wnts spread through tissues (reviewed in [184, 185]), including transport of Wnts by lipoprotein vehicles [186], transcytosis [187], and cytonemes, long membrane covered cellular protrusions [188]. The local concentration of Wnts on cell membranes is regulated by proteoglycans, low affinity Wnt co-receptors which are required for Wnt signaling *in vivo* (reviewed in [189]).

In vertebrates, a considerable set of secreted Wnt antagonists is present, which act by preventing ligand-receptor interaction; these include many of the classical Spemann organizer genes introduced above [34, 36]. According to their mechanism of function, secreted Wnt antagonists can be grouped in two classes (reviewed in [36]).

Antagonists binding to Wnt proteins

Secreted frizzled-related proteins (sFRPs) contain a domain similar to the cysteine-rich and Wnt binding domain of Fz receptors, which explains their function in sequestration of Wnts [190]. Of note, a sFRP (sFRP1) has been found to act both as Wnt antagonist and agonist in cultured cells, suggesting a dual, context-dependent mechanism of action [191].
Wnt inhibitory factor1 (WIF1) contains a unique, Wnt-binding WIF domain, inhibits Wnt signaling *in vitro*, and plays a role in *Xenopus* somitogenesis, a Wnt-dependent process [192]. The *D. melanogaster* ortholog of WIF is a regulator of Hedgehog signaling [193].
Cerberus/Coco is a multivalent growth factor antagonist, which binds and sequesters Wnt, BMP and Nodal ligands [46, 47, 194].

Antagonists binding to Wnt receptors

Wise (Wnt modulator in surface ectoderm) binds to LRP6 and can compete for Wnt binding, or alternatively mimic Wnt activity. It thus acts as context-dependent Wnt inhibitor or activator in *Xenopus* ectoderm, where it is also expressed [195].
Sclerostin (Sost) binds to LRP5/6 receptors and plays a role in Wnt antagonism during bone formation and remodelling [196].
Dickkopf (Dkk) proteins bind and antagonize LRP5/6 [197-199]; their developmental roles and mechanism of action will be discussed in the following chapter.

Dickkopf proteins as Wnt antagonists

In vertebrates, the Dkk family contains four members (Dkk1-4). All Dkks contain an N-terminal signal peptide as well as two conserved cysteine rich domains, which are defining for the Dkk family. Functionally, Dkk1/2/4 are implicated in Wnt antagonism, whereas Dkk3 does not modulate Wnt signaling [35].

In the genomes of the protostome organisms *D. melanogaster* and *C. elegans* no Dkk homologs are present. Recently, however, a cnidarian Dkk1 homolog was shown to act as

Wnt inhibitor, pinpointing the ancient role of Wnt-Dkk antagonism [200]. Thus, the lack of Dkk1 homologs in protostome genomes is believed to be due to gene loss events during evolution [35].

Dkk1 is the founding member of the family and was first characterized in *Xenopus*, where it acts as Wnt inhibitor secreted from the Spemann organizer and is required for PC specification and maintenance as well as forebrain induction [29, 201, 202]. Since then, Dkk1 was shown to antagonize Wnt signaling in developmental processes as diverse as a-p patterning [29, 201, 203, 204], bone formation [205, 206], vertebral development [207] and limb formation [204, 208], in many species.

Dkk2 is expressed during organogenesis stages in *Xenopus* and mouse; it acts as Wnt antagonist during eye formation in mouse [209]. While Dkk1 exclusively inhibits Wnt signaling, Dkk2 was also shown to act as Wnt agonist in *Xenopus* embryos and cultured cells [210]. However, since Dkk2-mediated Wnt agonism was only analyzed in overexpression studies, so far its physiological relevance is unclear.

Dkk1 binds to LRP6 in a 1:1 stochiometric manner [197]. Simultaneously, Dkk1 binds as well to another transmembrane protein, Kremen. Thereby, Dkk1 forms a ternary complex with LRP6 and Kremen, which is cleared from the cell surface by endocytosis (Fig. 9) [211].

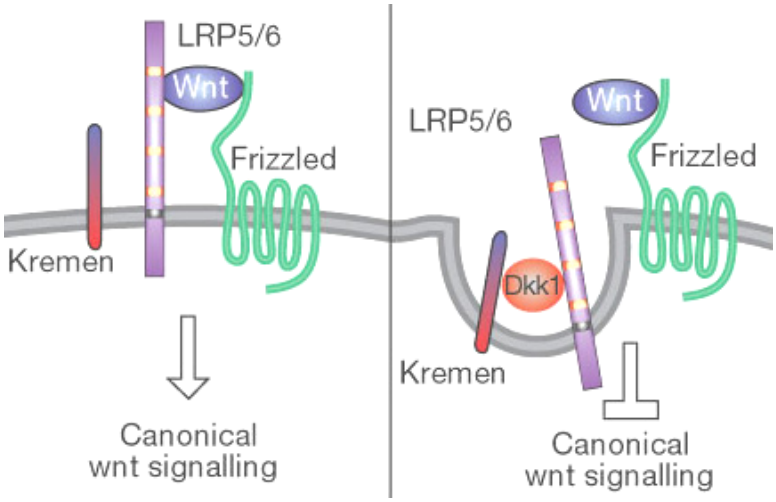

Figure 9. Dkk1 forms a ternary complex with LRP6 and Kremen, which is removed from the cell surface by endocytosis. (Left) In absence of Dkk1, Wnt binds to LRP5/6 and Frizzled receptors and activates signaling. **(Right)** Dkk1 induces formation of a ternary complex containing LRP5/6 and Kremen, which is removed from the cell surface by endocytosis. As a consequence, Wnt signaling is inhibited. Picture taken from [211].

Kremen proteins as Wnt antagonists

Kremen was found in our laboratory in a screen for Dkk1 binding partners, and established as Wnt antagonist which cooperates with Dkk1 in LRP6 clearance [211].

Prior to that, Kremen (Kringle-coding gene marking the eye and the nose) proteins were first identified in a screen for Kringle domain containing proteins [212]. The two family members Kremen1 and 2 (Krm1 and 2, collectively termed Krms) are single-span transmembrane proteins characterized by an extracellular domain composition encompassing a Kringle, WSC and CUB domain (Fig. 10) [212]. Kringle [213] and CUB [214] domains are mainly involved in protein-protein interaction, and occur in several secreted structural proteins and growth factors of higher animals, respectively [215-217]. WSC [218] is a rarely occurring, carbohydrate-binding domain conserved from yeast to humans [219]. Of note, albeit all these domains are individually found in other proteins, the composition as well as organization of all three domains in Krm proteins is unique. The short cytoplasmic tail of Krms contains no conserved motives, but is highly conserved across species (*Xenopus* and mouse) in case of Krm1 [220].

The extracellular domain architecture of Krms is evolutionary conserved in vertebrates, but no homologs are present in *D. melanogaster* and *C. elegans* [220]. Recently, Krm homologs have also been suggested for the sea urchin *S. purpuratus* and the flatworm *M. lignano* [221, 222]; however, these genes only show similarity to one discrete domain of Krm, and it is unclear if they comprise the same domain composition and thus are true Krm orthologs.

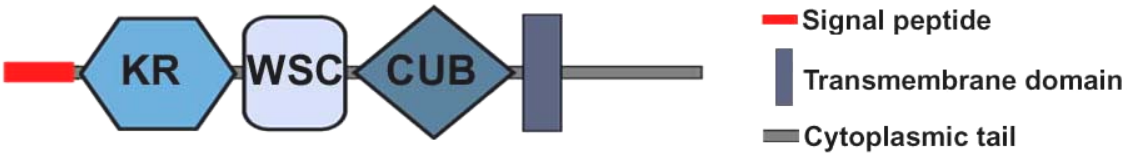

Figure 10. Domain structure of Krm proteins. KR, kringle domain.

Krms are differentially expressed during embryonic development in mouse and frog. In the mouse, expression of *krm* genes during early development (prior to day 8 post fertilization) has not been analyzed. During later developmental stages, *krm1* and *2* transcripts are

detected in limbs, brain, mesanephros, nose, otic and optic vesicle [212, 220]. In *Xenopus*, *krm1* transcript is present maternally and is transiently downregulated during gastrulation, whereas *krm2* expression starts at MBT (mid-blastula transition, the onset of zygotic transcription) and persists until tailbud stages at a similar level. During gastrulation, *krm2* is strongly expressed in the ventro-lateral mesoderm. In neurula stage embryos, *krm1* and *2* transcripts similarly localize to the lateral neural plate and to the PC, where they co-localize with *dkk1* transcript. During tailbud stages both *krm1* and *2* are expressed in the hatching gland; *krm1* transcript is also detected in the notochord, whereas *krm2* is additionally expressed in branchial arches, otic vesicle and pronephric duct [220].

Functionally, the main characteristic of Krm proteins is that they strongly enhance the potency of Dkk1 to inhibit Wnt/LRP6 in *Xenopus* embryos as well as cultured cells [211, 223]. This was also nicely shown in an experiment in *D. melanogaster*, an organism devoid of Dkk and Krm homologs. Whereas ectopic expression of mouse Dkk1 in the developing fly wing is not able to perturb wing formation, a process dependent on Wnt signaling, ectopic co-expression of Dkk1 and Krm2 blocks wing formation due to Wnt inhibition [211]. However, since all these experiments involve overexpressed genes, they do not allow conclusions about the requirement of Krms for Dkk1 function.

In *Xenopus* embryos, Dkk1 and co-expressed Krms in the PC cooperate in Wnt inhibition to regulate a-p patterning of the central nervous system (CNS). In this context, Krms are required for Dkk1-mediated Wnt inhibition and forebrain development [220]. Beyond that, it is yet unclear if Krms are generally essential co-receptors for Dkk1, in *Xenopus* and other species, or if they modulate Dkk1 activity more specifically during selected developmental processes.

It is also unknown if Krms are involved in developmental processes independent of Dkk1/2-mediated Wnt antagonism. Indeed, recently it was shown that Krm1 is required for formation of thymic architecture in mice by acting as Wnt inhibitor, possibly in a Dkk1-independent manner [224].

Furthermore, even though a function of Krms in Dkk-mediated LRP5/6 clearance is established, many open questions remain. For example, the cytoplasmic tail of Krms is dispensable for clearance of the ternary complex from the cell surface [211]. Thus, Krms

are likely not direct regulators of endocytosis, raising the question of the exact role of Krms in Dkk1 induced internalisation of LRP6. Membrane attachment of Krms is essential for functional cooperation with Dkk1 in Wnt inhibition [211]; this raises the possibility that further, so far uncharacterized proteins are recruited by Krm and contained in the ternary complex as well, contributing to the regulation of LRP5/6.

Aims of the thesis

The aim of this thesis was to address some of these open questions regarding the mechanistic function and developmental role of Kremen proteins. Towards this end I have followed two main lines of research:

1) Identification and analysis of Krm interacting proteins. It was previously shown that Krm and Dkk1 recruit the Wnt receptor LRP6 into a ternary complex, which is cleared from the cell surface, and thereby inhibit Wnt signaling. Upon the beginning of this study, it was unclear i) which other proteins are involved in this process, and ii) how Krms mediate LRP6 clearance from the cell surface. To answer this, I employed an *in vivo* screen to identify functional Krm interaction partners, as well as *in vitro* approaches to isolate Krm binding proteins. The latter led to the identification of the Krm2 binding protein Erlectin. Further analysis of Erlectin included combined *in vitro* and *in vivo* experimental approaches and revealed that Erlectin, albeit not specifically involved in Wnt/Krm signaling, is a novel ER protein involved in N-glycan recognition and essential for *Xenopus* development.

2) Analysis of the role of Krm2 during *Xenopus* development. In *Xenopus*, Krms have been shown to cooperate with Dkk1 in Wnt inhibition to regulate a-p patterning of the CNS. It was unknown if Krms have further roles during development. Thus, the second focus of this work was to characterize the developmental role of Krm2 during neural crest formation. This also included an extended analysis of Krm activity in Wnt pathway regulation. Together, *in vivo* and *in vitro* approaches revealed that Krm2 is required for neural crest formation in *Xenopus*, and than Krms can promote LRP6-mediated Wnt signaling in the absence of Dkk1.

4. RESULTS

Bacterial and yeast two-hybrid assays to identify Krm binding proteins

Bacterial two-hybrid assay

To identify novel binding partners of Krm2 I employed a bacterial two-hybrid screen kit (BacterioMatch® I, Stratagene). Bacterial systems are thought to have several advantages over classical yeast two-hybrid assays, including more rapid transformation procedure and DNA isolation, as well as fewer false-positives and less toxic effects due to the reduced chance of bacteria harboring eukaryotic homologs (cited from [225]). In the BacterioMatch® system, bait and target clones are fused to the DNA binding domain of γcl protein and the catalytic α-subunit of RNA polymerase, respectively. Upon interaction of bait and target, transcription of a reporter is activated (for more details, see [225]).

As *krm2* is expressed in the brain of mouse embryos [212, 220], I screened a human fetal brain plasmid cDNA library, using the C-terminal cytoplasmic tail of human Krm2 as bait. In total, $6x10^6$ colonies were screened, which corresponds to 1.8 fold coverage of clones present in the library ($3,3x10^6$ cfu). After reselection, 50 positive colonies were obtained and sequenced.

45 clones (90%) show an incorrect open reading frame (ORF) due to out-of-frame fusion to the RNA polymerase subunit, and therefore do not result in correctly translated proteins. The 5 clones with correct ORF (10%) are: NADH dehydrogenase subunit III, Ribosomal protein L28, ATPase subunit 1, Actin γ1, and SRY-box 13. Importantly, for none of these

clones could an interaction with Krm2 be verified by retransformation within the bacterial system (not shown). I conclude that all isolated clones are false-positives.

Yeast two-hybrid assay

To identify novel binding partners of Krms in a well-established approach, we assigned a company (Dualsystems Biotech AG, Switzerland) to perform a yeast two-hybrid assay. A mouse whole embryo (11 days) library was screened for candidates, using the C-termini of mouse Krm1 and 2 as baits.

Whereas screening of the bait Krm2 yielded no positive clones, for Krm1 one potential binding partner was identified, and verified within the yeast system. Tax1 binding protein1 (TAX1BP1, GeneID 8887) contains a calcium binding and coiled-coil domain (Pfam: CALCOCO1) and two zink finger domains (SMART), and is likely localized in the cytoplasm. Its molecular function is not characterized.

To analyze the role of TAX1BP1 in Wnt/Krm signaling *in vivo*, I injected *TAX1BP1* mRNA in *Xenopus* embryos. Injected embryos are stunted and show various pleiotropic defects. Importantly, co-injection of *TAX1BP1* and *krm2* mRNA does not induce significant phenotypic changes, indicating that the two genes do not functionally interact. In cultured cells *TAX1BP1* DNA co-transfection has no effect on a Wnt responsive reporter (results not shown). I conclude that very likely TAX1BP1 neither interacts with Krm2 in Wnt inhibition, nor elsewise regulates the Wnt pathway.

Notably, TAX1BP1 has so far solely been studied as candidate retrieved from yeast two-hybrid screens. It binds to a multitude of functionally diverse proteins including HTLV-1 Tax protein [226], zinc finger protein A20 [227], TNF-receptor associated factor 6 [228], RhoGAP [229] and $GABA_C$ receptor [230]. Although it cannot be excluded that the binding promiscuity of TAX1BP1 is physiological, this rather suggests that TAX1BP1 may be a 'sticky' protein in yeast two-hybrid assays, whose interactions with various unrelated proteins are not of physiological importance [231].

A *Xenopus* injection screen to identify functional interaction partners of Krm2

Xenopus embryos are a well suited system for expression cloning screens, in which a large number of cDNAs is assayed for a particular biological activity. Genes are easily overexpressed and evaluation of embryos for specific phenotypes is straightforward. Furthermore, expression screens can be adapted to make use of the fact that functional interaction between two genes can lead to a strongly enhanced, or even unprecedented phenotypic effect [232-236]. A major advantage of such functional interaction screens, when compared to classical binding assays, is that a wide range of candidates can be identified. These include not only physical but also genetic interaction partners, e.g. components of other signaling pathways. In addition, the use of an *in vivo* system such as the *Xenopus* embryo increases the likeliness of identifying physiologically relevant interactions. This principle has been successfully used to discover numerous genes (summarized in [237]).

Overview of the injection screen

To screen for functional interaction partners of Krm2, mRNA pools of a cDNA library were injected with or without *Xkrm2* mRNA and embryos were analyzed at various stages. The functional interaction of Krm2 and a clone contained in a library pool was expected to become manifest in a specifically enhanced or different phenotype, in comparison to the phenotype induced by the library pool on its own (Fig. 11). *Xkrm2* mRNA was used at low dose which does not induce a phenotype. In proof of principle, co-injection of a similarly low dose of *krm2* and *dkk1* mRNA results in a strikingly enhanced phenotype, due to functional cooperation (not shown and [223]), indicating that Krm2 is a suitable bait for this type of screen.

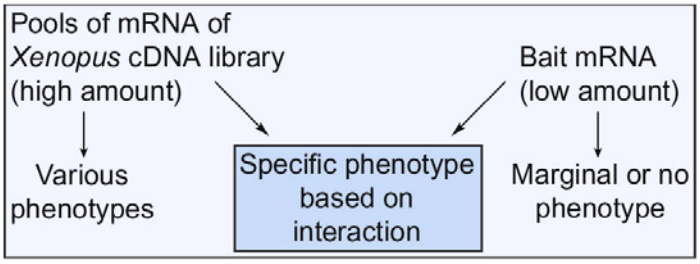

Figure 11. Scheme of the injection screen.

In total, 96 pools of a *X. laevis* eye library and 33 pools of a *X. tropicalis* embryonic library were screened for Krm2 interacting candidates. In addition, 76 eye library pools and 33 *X. tropicalis* library pools were screened for candidates interacting with Rspo-2, a novel secreted Wnt activator [238]. For a summary of general features of the screen, see Fig. 12.

Baits	Libraries	Mode of injection	Phenotypic analysis
Xkremen2 *XRspo-2*	*X.l.* eye library 200 clones/pool *X.t.* embryonic library 96 clones/pool	2- and 4-cell stage, equatorial region	at gastrula, neurula and tailbud stages

Figure 12. General features of the injection screen.

Identification of a library pool interacting with Krm2 and Dkk1

Only one pool (pool 5A) showed, albeit weak, functional interaction with Krm2, leading to embryos with enlarged cement glands (Fig. 13C, arrows). Importantly, embryos injected with pool 5A mRNA alone (Fig. 13B), or *krm2* mRNA alone (not shown), had similarly sized cement glands as control embryos (Fig. 13A). Rspo-2 did not interact with any pool tested.

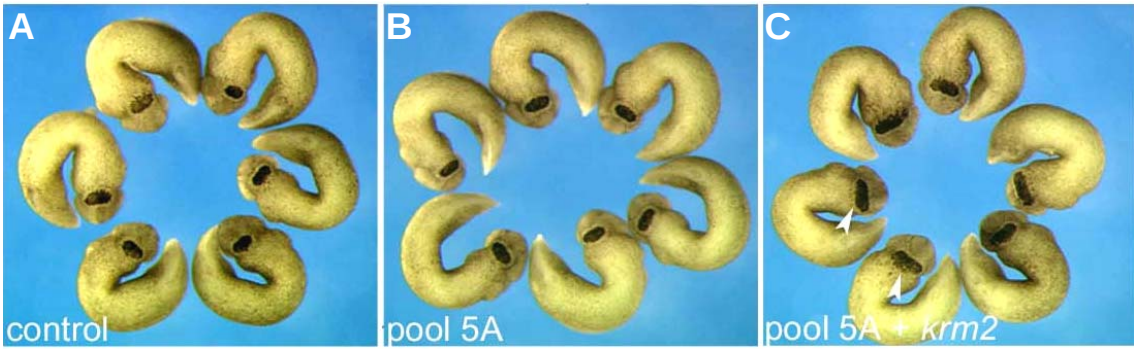

Figure 13. Functional interaction of a library pool with Krm2. Tailbud embryos shown in ventral view. **(A)** Uninjected control embryos. **(B)** Embryos injected with 4-5 ng pool 5A mRNA look normal. **(C)** Embryos co-injected with pool 5A mRNA and low amounts (200 pg) of *krm2* mRNA display enlarged cement glands (arrows).

To identify the single clone conferring activity to the pool interacting with Krm2, a sib selection process was performed. Thereby, a pool is repeatedly split into smaller subpools, which are each selected for activity, until a single active clone is isolated [239]. During sib selection of the pool interacting with Krm2, the activity was lost, and could not be detected in any of the subpools tested (~50 clones/subpool).

Such a loss of an active clone during sib selection can have several causes: 1) The interaction with the protein of interest may be weak and therefore insignificant; 2) the clone can be physically lost; 3) the activity of the pool may be based on the effect of two genes within the same pool, which become separated during sib selection; or 4) some smaller subpools may start giving pronounced phenotypes by themselves, which would mask a weak interaction phenotype. One or a combination of several of these causes may explain why the active clone of the Krm interacting pool was lost; the precise reason, however, remains unknown.

Krms and Dkk1 functionally cooperate and act in the same pathway [220]; I therefore reasoned that a factor interacting with Krm2 may also interact with Dkk1. Since the original pool 5A containes a clone (or a combination of clones) weakly interacting with Krm2, I tested if pool 5A also functionally interacts with Dkk1. Co-injection of low doses of *dkk1* mRNA with mRNA of pool 5A results in strongly anteriorized embryos, with strikingly expanded cement glands and shortened body axes; in contrast, embryos injected with *dkk1* mRNA alone are only weakly anteriorized (Fig. 14A). Based on this robust phenotypic readout I performed sib selection and successfully identified a single active clone, *Xenopus nodal-related 3* (*Xnr3*).

Xenopus nodal-related 3 functionally interacts with Dkk1

Dkk1 and Xnr3 cooperate to induce strongly anteriorized embryos (Fig. 14B). However, Krm2 and Xnr3 do not functionally interact (not shown).

Xnr3 is expressed in the Spemann organizer epithelium in response to early Wnt signals [41]. Several studies have shown that Xnr3 acts as neural inducer through inhibition of BMP signaling [40, 236, 240]. It is well established that simultaneous inhibition of Wnt and

BMP signaling leads to strong anteriorization, and induction of complete secondary embryonic axes (two inhibitor model of head induction, see also Introduction, p. 7) [11]. Thus, the enhanced anteriorization resulting from co-injection of *Xnr3* and *dkk1* mRNAs is likely due to simultaneous inhibition of BMP and Wnt signaling by these genes, respectively. The functional interaction of Xnr3 and Dkk1 was therefore not studied any further.

Figure 14. Xnr3 functionally interacts with Dkk1. Tailbud embryos shown in lateral view. Control, uninjected embryos. **(A)** Functional interaction of the Krm2-interacting library pool with Dkk1. Embryos were injected with 4-5 ng pool mRNA (top right) or 10 pg *dkk1* mRNA (bottom left). Embryos co-injected with pool mRNA and *dkk1* mRNA are strongly anteriorized (bottom right). **(B)** Functional interaction of Xnr3 with Dkk1. Embryos were injected equatorially with 100 pg *Xnr3* mRNA (top right) or 10 pg *dkk1* mRNA (bottom left). Embryos co-injected with *Xnr3* mRNA and *dkk1* mRNA are strongly anteriorized (bottom right).

Analysis of factors modifying LRP6, Krm2 and Wnt3a proteins

Overview of the modification screen

To identify novel genes that specifically regulate the Wnt pathway at the level of receptor/ ligand biogenesis, a cell-based modification screen for factors that affect protein expression of LRP6, Krm2, and Wnt3a (baits) was carried out in the lab (by G.D) [154]. In brief, plasmids encoding baits were co-transfected with library pools in cultured cells, and bait protein expression was analyzed by Western blotting (Fig. 15). Any alteration of a bait protein band induced by a co-transfected library pool, e.g. up- or downshift, increase, decrease, or appearance of additional bands, was monitored, and pools conferring activity were further analyzed by sib selection.

In total, 10^6 clones (in pools of 96) of a *X. tropicalis* embryonic library were screened; 37 single clones were identified by sib selection, and after subtraction of duplicates 28 candidate clones were selected for further study (Table 1).

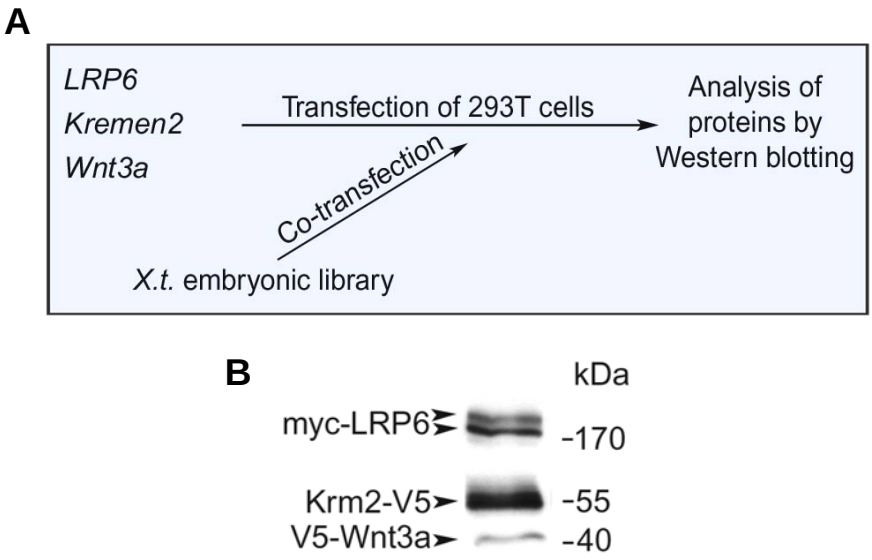

Figure 15. Overview of the modification screen. (A) Scheme of the screen. **(B)** Western blot analysis as readout of the screen (example). The three baits LRP6, Krm2 and Wnt3a were co-transfected and analyzed in the same sample. Note that LRP6 protein is detected as two bands: An upper band (cell surface form) and a lower band (intracellular form) [173].

No	Pool/ clone	Gene name	Protein modification	R	RT	mRNA overexpression		Morpholino injection	REFs
1	79-4,A3	*Xenopus laevis* Hatching enzyme	E/ 30 kDa	-	l	n		/	
2	80-4,B6	Ubiquit. carboxyl-terminal hydrolase family2	E/ 50, 55 kDa	i	m	n		/	
3	253-1,G5	Embryonic serine protease-1 (Xesp-1)	E/ 35, 100, 180 kDa	i	g	gd, short embryos, deformed		**T**delayed development	[241]
4	103-3,F9	Embryonic serine protease-2 (Xesp-2)	Loss/ uLRP6; Red/ Krm2	i	l	strong gd, pleiot.		/	
5	199-3,H1	Sim. to far upstream element binding prot.1, FUSE	Loss/ Wnt3a	-	/	strong gd, d		/	
6	72-1,C11	*X.laevis* nuclear orphan receptor XGCNF	Loss/ Wnt3a	-	g	n		/	
7	24-2,H1	hnRNA binding protein	Loss/ Wnt3a	-	/	gd, pleiot.	F	/	
8	146-1,A1	RNA-binding protein XlhnRNPL	Loss/ Wnt3a	i	/	strong gd		/	
9	153-1,C11	Cold-inducible RNA binding protein 2 (CIRP2)	Loss/ uLRP6, Red/ others	-	/	pleiot.	F	/	[242]
10	153-1,H11	Serine/threonine-protein kinase ANKRD3	Red/ all	i	m	extended abdomen, head defects	F	/	[243]
11	130-2,D7	Receptor tyrosine kinase, c-mer like	Incr/ LRP6; E/ 30 kDa	i	g	posteriorized, extra tails		n	[244]
12	199-3,F11	Protein transport protein SEC61 alpha subunit	Red/ Krm2	i	/	pleiot.		/	
13	48-1,D8	Protein transport protein SEC61 beta subunit	Red/ Krm2	-	/	n			
14	20-4,H7	Small GTPase; ADP-ribosylation factor 4, ARF-4	Loss/ uLRP6; Red/ Krm2	i	m	enlarged head and cg	F	**N**elong; **T**head defects	[245-248]
15	146-1,B4	Similar to arfaptin 1	Loss/ uLRP6	i	/	pleiot., slightly bigger cg		/	[249]
16	96-1,G4	Glycosyl transferase	Up-shift/ LRP6	i	m	n		/	
17	238-4,H2	Sialyltransferase	Up-shift/ LRP6	i	m	n		/	
18	36-3,H1	Signal peptide peptidase-like 3, SPP-like 3	Loss/ uLRP6; Red/ others	i	m	pleiot.	F	**N**elong; **T**ventralized	[250, 251]
19	24-2,B2	Similar to DnaJ (Hsp40) homolog	Loss/ uLRP6	i	m	blisters	F	**G**d	[252, 253]
20	47-1,B4	Embryonic 7-span transmembrane protein-like	Loss/ uLRP6, Red/ others	i	m	mildly anteriorized; growth on belly		**G**d	[254, 255]
21	42-4,F10	Similar to thioredoxin domain containing 4	Red/ uLRP6	-	m	n		/	
22	74-2,H6	Weak sim. to putat. G-prot. coupled receptor TRC8	Loss/ uLRP6, Krm2	i	m	blisters, protrusions		**N**elong; **T**stunted axis	[256, 257]
23	20-4,G1	Potential novel G-protein-coupled receptor	Loss/ uLRP6; Red/ others	i	m	bent; otherwise n		/	
24	30-3,H1	Uncharacter. multi TM protein - hemolytic activity	Loss/ uLRP6, Krm2	i	m	pleiot.	F	**N**elong;	[258]
25	179-3,E2	Similar to presenilin stabilisation factor b, APH1	Loss/ uLRP6, Red/ Krm2	i	m	n		/	[259]
26	44-3,H10	Hypot. Vitamin K-dependent carboxyl. dom. cont.	Loss/ Wnt3a; Red/ others	i	/	n		/	
27	12-1,B7	Unknown WD40 repeat containing protein	Incr/ Wnt3a	s	m	pleiot.	F	**T**ventrally bent tails	[260]
28	199-3,B12	No significant match	E/ 50, 55 kDa	i	/	reduced cg; altered body shape		/	

Table 1. Overview of clones identified in the modification screen. The colors mark different functional classes of clones (compare Table 2). **No**, running number. **Pool/clone** refers to identity within *X. tropicalis* library. **Gene names** were assigned by sequence BLAST and database search. **Protein modifications** as determined by G.D.: E, extra band; Loss/Red, loss/reduction of band, respectively; Incr, quantitative increase of band; Up-shift, up-shift of band; uLRP6, upper (cell surface) band of LRP6; others refers to both other baits not mentioned. **R**, Wnt reporter assay stimulated with Wnt1/Fz8 (by W.W.): -, no effect; i, inhibition of signal; s, stimulation of signal. **RT**, RT-PCR analysis, indicated is onset of expression: m, maternal; g, gastrulation; l, late tailbud stages; /, not determined. **mRNA overexpression**: n, normal; gd, gastrulation defects; pleiot, pleiotropic defects; d, dead; cg, cement gland; F, picture contained in Fig. 16. **Morpholino injection**: **G**, **N**, **T**, gastrula, neurula, tailbud stage, respectively; n, normal; d, dead; elong, elongation defects; /, not determined. **REFs**, relevant references.

Functional classes of identified clones. The 28 identified clones can be grouped into several classes according to gene function: 1) Proteases, 2) DNA/ RNA binding proteins, 3) kinases, 4) proteins involved in protein modification and transport, and 5) others (Table 2).

Total	28
Proteases	4
DNA/ RNA binding	5
Kinases	2
Protein modification & transport	10
Others	7

Table 2. Functional classes of identified clones. Indicated is the number of clones per class. Data were extracted from Table 1. The color code is the same as in Table 1.

Effect of clones on protein expression of LRP6, Krm2, and Wnt3a. Since all three baits were co-expressed in the same sample, it is possible to distinguish between clones affecting one, two, or all three baits (Table 3).

	Modified baits						
	LRP6	Krm2	Wnt3a	Two baits LRP6+Krm2	Two baits (other)	All baits	Unknown/ extra bands
Clones	5	2	5	5	1	6	4

Table 3. Overview of numbers of clones affecting each of the baits. Data were extracted from Table 1.

Types of bait modifications

- **LRP6 (16 clones).** The most prevalent type of LRP6 protein modification is the loss/reduction of the upper band, which represents the cell surface-localized protein ([173] and Hassler et. al., submitted). Cell surface LRP6 is affected either solely (three clones) or in combination with a reduction of Krm2 and/or Wnt3a protein (10 clones). Loss/reduction of cell surface LRP6 is mainly induced by protein modification/transport components, and uncharacterized genes. Further modifications are: Up-shift of LRP6 protein bands (two clones, both are glycan transferases), and increase of LRP6 protein amount (one clone, a tyrosine kinase) (Table 1).

- **Modifications of Krm2 (13 clones).** The only modification of Krm2 protein is reduction, mostly in combination with loss of surface LRP6 (five clones), or reduction of both other baits (six clones). Specific reduction of Krm2 protein expression is induced by two clones; both are components of the SEC61 translocon. Krm2 modifying clones are mainly members of the protein modification/transport group, and uncharacterized genes (Table 1).

- **Modifications of Wnt3a (11 clones).** The most prevalent modification type of Wnt3a protein is loss or reduction, often in combination with reduction of other baits (six clones). Four clones specifically reduce Wnt3a protein expression; all are members of the DNA/ RNA binding class. One clone (class 'others') induces an increase of Wnt3a protein (Table 1).

In vivo analysis of identified clones

Since inhibition of zygotic Wnt signaling in *Xenopus* leads to anteriorization, whereas Wnt activation results in headless embryos, axial patterning defects provide a specific phenotypic readout for genes affecting the Wnt pathway. Therefore, to analyze the identified clones regarding their role in the Wnt pathway *in vivo*, I performed mRNA overexpression and Morpholino-mediated loss-of-function experiments in *Xenopus* embryos, and screened for phenotypes mimicking Wnt activation or inhibition.

Gain-of-function analysis. I first injected mRNA of each of the 28 genes in *X. laevis* embryos, and evaluated phenotypes for axial patterning defects at various stages. See Table 1 for overview of all obtained phenotypes.

In summary, overexpression of nine genes has no effect; 11 genes induce pleiotropic or gastrulation defects (Fig. 16a', b'', c', c'', d''). Of the remaining eight genes, several induce specific phenotypes like blisters, extra tails, or extended abdomen (Fig. 16a'', d'); one gene, identified as ADP-ribosylation factor 4 (ARF4), induces anteriorized embryos with enlarged heads and cement glands, thus mimicking Wnt inhibition (Fig. 16b'). Therefore, phenotypes are randomly distributed throughout functional gene classes as grouped above (Table 2), and related gene function is not reflected in similar phenotypes.

Figure 16. Gain-of-function analysis of selected genes in *X. laevis*. (a-d) Uninjected control embryos relate to experimental embryos shown in the same column. **(a'-d'')** 2-cell stage embryos were injected equatorially with titrated mRNAs of the indicated genes. Bottom left, clone numbers as defined in Table 1 as 'No'. Arrows indicate phenotypic features mentioned in the main text.

Loss-of-function analysis. In a complementary approach, I performed Morpholino (MO)-mediated loss-of-function analyses of selected genes. As a purchase of MOs for each of the 28 genes was not feasible, nine candidate genes were chosen according to 1) phenotypic analysis by gain-of-function 2) onset of expression during early development (as determined by RT PCR, Table 1) and 3) research of literature with main focus on novelty of genes (Table 1). MOs were targeted against *X. tropicalis* genes to avoid redundancy of pseudoalleles, which is common in *X. laevis*; however, several MOs target at least one *X. laevis* allele as well (see Materials & Methods for details; see Table 1 for overview of all obtained phenotypes).

In summary, injection of one MO does not alter the embryonic phenotype (not shown), whereas the remaining eight MOs induce phenotypic changes. Injection of two MOs is lethal at gastrula stages (not shown). Injection of four MOs leads to elongation defects during neurula stage (not shown); at tadpole stage these embryos show a variety of phenotypic changes, including ventralization, stunted axis and head defects (Fig. 17A, B). Injection of two MOs affects phenotypes only at late tailbud stage, leading to ventrally bent tails and generally delayed development, respectively (Fig. 17A). Injection of one MO induces a phenotype partially reminiscent of Wnt pathway perturbation. The MO targeting ADP-ribosylation factor4 (ARF4) induces elongation defects during neurula stage and head

defects at tadpole stage (Fig. 17B), thus in part mimicking Wnt pathway activation. However, ARF4 MO injected embryos show a range of other defects as well, including impaired gastrulation and generally delayed development.

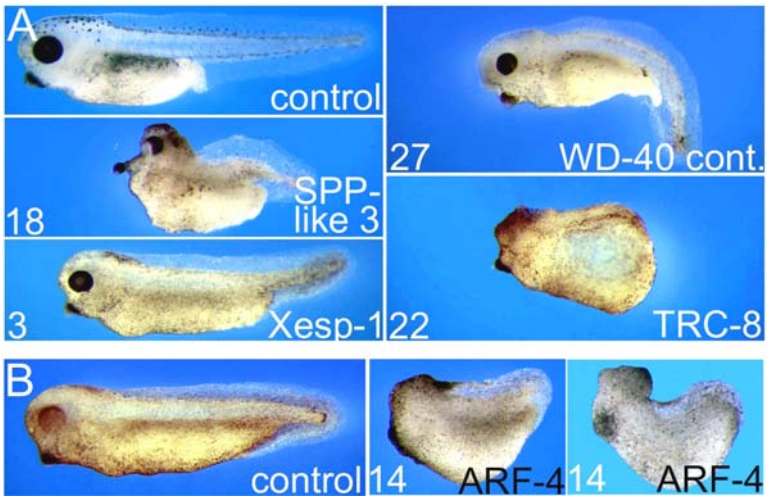

Figure 17. Loss-of-function analysis of selected genes in *X. tropicalis*. 2-cell embryos were injected equatorially with 10-25 ng MO targeting the indicated gene (numbers/ names on panel bottom refer to Table 1) and photographed at tadpole **(A)** and tailbud **(B)** stages. Control, control MO injected embryos.

Conclusion: Of the 28 candidates analyzed in gain- and loss-of-function analysis, only one gene, ARF4, partially mimics the effects of a Wnt regulator in *Xenopus* embryos.

Selection of ADP-ribosylation factor4 for further study

ADP-ribosylation factor4 (ARF4) was chosen for further study on account of: 1) Overexpression of mRNA, which leads to anteriorized embryos, suggesting Wnt inhibition (Fig. 16b'); 2) MO mediated knock-down, which induces gastrulation and head defects, possibly due to Wnt activation (Fig. 17B); 3) inhibition of Wnt1/Fz8 stimulated reporter assays by ARF4 (by W.W., Table 1), suggesting that it may act as Wnt inhibitor; 4) co-transfection in cultured cells, where ARF4 leads to loss of cell surface LRP6 protein, suggesting a possible mechanism for Wnt inhibition (by G.D., Table 1). In the light of these initial results, my working hypothesis was that ARF4 may specifically inhibit Wnt signaling by negatively regulating the amount of cell surface-localized LRP6.

ARFs are highly conserved, ras-like cytoplasmic GTPases widely implicated in regulation of protein/vesicle traffic, endocytosis and organelle maintenance. Inhibition of ARF

function efficiently blocks protein transport through the early secretory pathway [245-248, 261, 262]. Since ARFs mediate such broad effects on the general cell machinery, it is possible that they indirectly co-affect Wnt signaling, e.g. by influencing homeostasis of the membrane compartment, where LRP6 is localized. Thus, my prime focus was the analysis of the specificity of ARF4-mediated effects on Wnt/LRP6 signaling.

Analysis of the role of ARF4 in Wnt signaling: Selected results

As main tools to study ARF4 function, I constructed constitutive active (Q71L; GTP associated) and dominant negative (T31N; GDP associated) mutants of ARF4, which are well established to activate and inhibit ARF4 function, respectively [247]. The following results were obtained:

- *Xenopus* embryos injected with ARF4 T31N as well as ARF4 Q71L mRNA show gastrulation defects and stunted body axes, but do not mimic phenotypes induced by Wnt activation and inhibition, respectively (not shown). This indicates that ARF4 mutants do not specifically affect the Wnt pathway *in vivo*.
- ARF4 MO injection does not affect a Wnt reporter in embryos, indicating that MO-induced effects are not due to Wnt pathway perturbation (not shown).
- In cultured cells, a Wnt reporter (stimulated with Wnt1/LRP6) is mildly inhibited by wild type ARF4, whereas co-transfection of either mutant strongly inhibits the reporter (not shown). Since the Q71L and T31N mutants have opposing molecular functions, this result is in contrast to a hypothesis suggesting specific Wnt regulation by ARF4.
- Co-transfection of ARF4, or either mutant, in cells reduces expression of cell surface LRP6 (Table 1), but also expression of several control proteins, indicating an unspecific effect on protein trafficking rather that a specific effect on LRP6 (not shown).
- Co-transfection of ARF4, or either mutant, in cells reduces expression of cell surface LRP6ΔC, an LRP6 construct which lacks the cytoplasmic C-terminus [176], indicating that the effect is not mediated through the C-terminus of LRP6, and thus indirect (not shown).

Conclusion. The hypothesis that ARF4 may be a specific Wnt inhibitor, acting by negatively regulating the amount of cell surface-localized LRP6, could not be validated. Rather, my results are in agreement with a general function of ARF4 in membrane/protein traffic. Therefore, this project was not continued further.

Characterization of the Krm2 binding protein Erlectin

Identification of Erlectin as binding partner of Krm2 in a proteomic approach

To identify binding partners of Krm2, C.C. performed a large-scale affinity purification of a Krm2 protein complex from cellular membrane lysates [263]. One of the proteins found was a novel protein we termed Erlectin (for ER lectin, see below; other GenBank designations are XTP3-B, C2orf30, CL25084).

Domain structure and homologies of Erlectin

The open reading frame of *erlectin* (GeneID 27248) consists of 483 amino acids with a calculated molecular weight of 53 kDa (Fig. 18A). Database searches revealed homologs of *erlectin* in deuterostomes (chordates, echinoderms) and protostomes including *D. melanogaster* and *C. elegans* (Fig. 18B). Erlectin contains a signal peptide and two Mannose-6-phosphate receptor homology (MRH) domains (Fig. 18C). MRH domain containing proteins represent a subfamily of the Mannose-6-phosphate receptor superfamily and include four members [264-266] (Fig. 18C), three of which have been described before: OS-9 [267-272], the gamma subunit of N-Acetylglucosamine-1-Phosphotransferase (GNPTAG) [273, 274] and Glucosidase II beta subunit (PRKCSH) [275-280]. Interestingly, the latter two play a role in N-glycan recognition and processing in the secretory pathway.

Binding of Erlectin to Krm2 is N-glycan-dependent

Since other MRH domain proteins are implicated in N-glycan recognition, C.C. analyzed if binding of Erlectin to Krm2 is glycan-dependent. Deglycosylation of Krm2 by treatment with N-glycosidase F leads to a shift in apparent molecular weight of Krm2, indicating that it is indeed N-glycosylated. Furthermore, deglycosylated Krm2 fails to bind Erlectin *in vitro* (not shown) [263]. These results suggest that Erlectin recognizes and binds to oligosaccharides linked to Krm2. Consistent with this, the Krm2 kringle domain contains one potential N-glycosylation site (N48 in mouse, N55 in *X. laevis*).

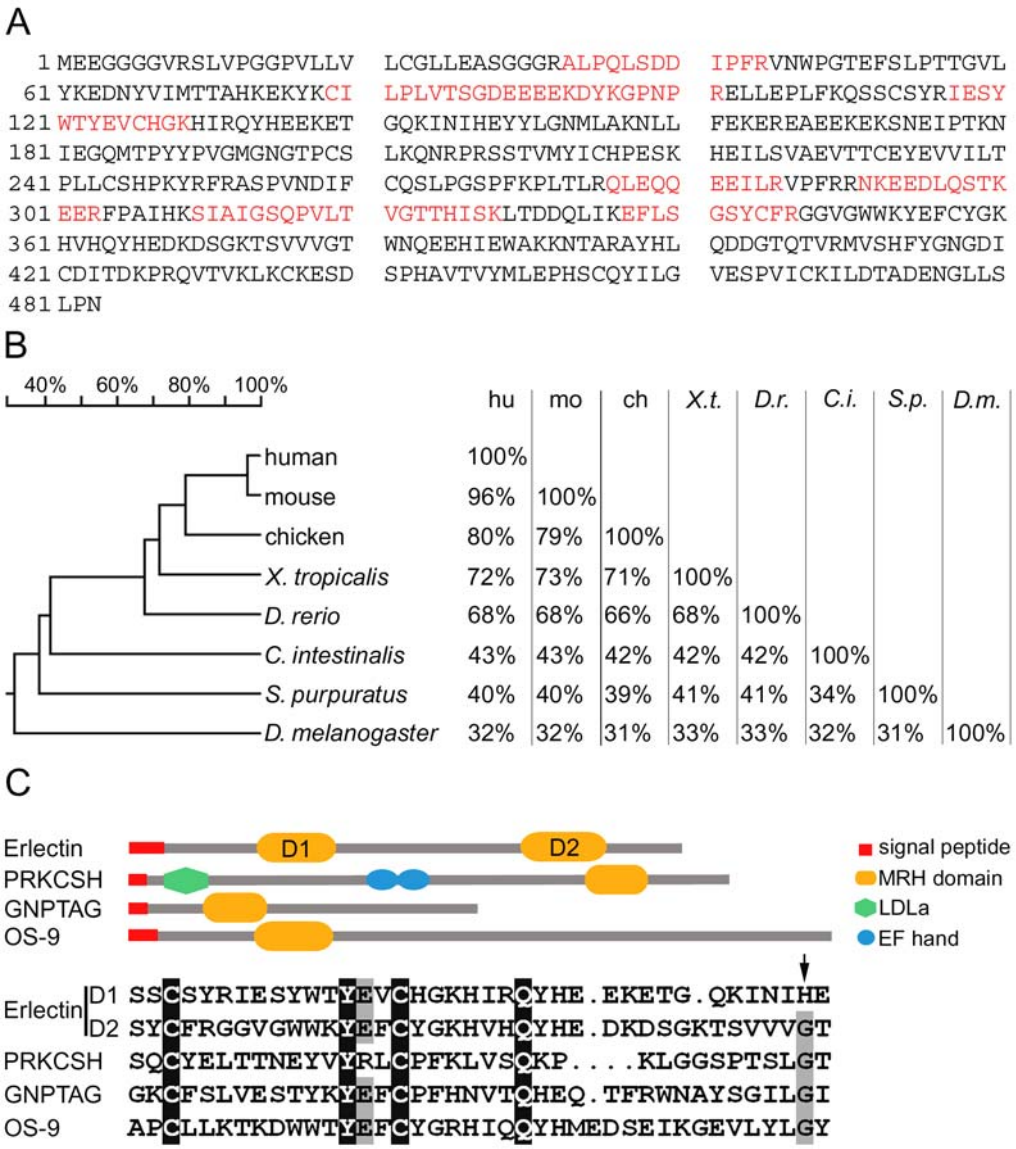

Figure 18. Erlectin is a novel protein related to oligosaccharide processing proteins. (A) Amino acid sequence of Erlectin. Highlighted in red are peptides identified in the Krm2 affinity purification. **(B)** Erlectin homology tree and matrix showing amino acid identity between indicated species. **(C)** Structure of Erlectin and comparison with domain relatives (adapted from SMART). Erlectin contains a signal peptide and two MRH domains (PRKCSH by SMART/InterPro, indicated as D1, D2). The scheme shows a comparison of all four human proteins containing an MRH domain. Also shown is an alignment of a conserved region of the MRH domains, with conserved residues labeled in black and grey. A point mutation in a conserved residue (G106S, arrow) of GNPTAG leads to a lysosomal storage disease [273]. Abbreviations: hu, human; mo, mouse; ch, chicken; *X.t.*, *Xenopus tropicalis*; *D.r.*, *Danio rerio*; *C.i.*, *Ciona intestinalis*; *S.p.*, *Strongylocentrotus purpuratus*; *D.m.*, *Drosophila melanogaster*; PRKCSH, β-subunit of Glucosidase II; GNPTAG, γ-subunit of GlcNAc-1-phosphotransferase.

A point mutation of Erlectin abolishes binding to Krm2

Since Erlectin contains two MRH domains, C.C. and I combined our efforts to test the requirement of either MRH domain for Krm2 binding. Deletion of the MRH domain 2 but not 1 impairs binding of Erlectin to Krm2, indicating that MRH domain 2 alone mediates Krm2 binding (Fig. 19, lanes 1-3).

A point mutation in the MRH domain of GNPTAG (see Fig. 18, arrow) leads to the lysosomal storage disease mucolipidosis type III in humans [273]. It affects a conserved residue (G106S) which is present in the MRH domains of OS-9 and PRKCSH as well as in MRH domain 2 of Erlectin (G379S), but not MRH domain 1 (Fig. 18, arrow). Therefore, C.C. and I tested if the homologous mutation of Erlectin affects binding to Krm2. Interestingly, this mutation abolishes binding of Erlectin to Krm2 (Fig. 19, lane 5).

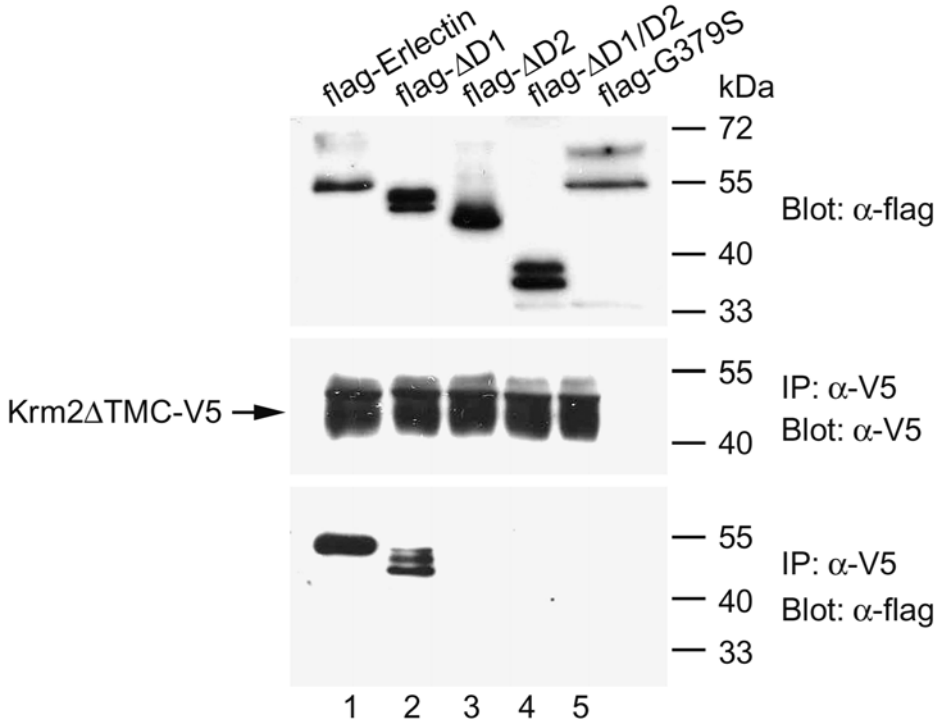

Figure 19. A point mutation of Erlectin abolishes binding to Krm2. *In vitro* binding assay with flag-Erlectin constructs as indicated. IPs were performed with anti-V5 antibody and analyzed by SDS-PAGE and Western blotting. D1/D2, MRH domains 1 and 2, respectively. Top panel: Protein expression, lower two panels: IPs. The binding assay was performed by C.C. I discovered the point mutation and cloned all Erlectin deletion constructs.

Erlectin is a member of the ER synexpression group in *Xenopus*

I studied the expression pattern of *erlectin* during *Xenopus* development by *in situ* hybridization and RT-PCR. Two alleles are present in *X. laevis* showing 82% identity in their open reading frames. I therefore designed PCR primer pairs as well as *in situ* probes specific for each allele. RT-PCR analysis shows no difference in the expression pattern of both alleles. Likewise, *in situ* hybridization indicates a comparable expression pattern of both alleles.

RT-PCR analysis shows that *erlectin* is expressed maternally. Levels of mRNA decrease during gastrulation (stages 10.5 – 13) and are then increasingly upregulated during neurulation (st. 17 – 21) and tailbud stages (Fig. 20A). By whole-mount *in situ* hybridization, *erlectin* expression is observed in the animal hemisphere of blastula stage embryos (Fig. 20C). During neurula stages expression is seen in the notochord (Fig. 20E). At late neurula stage strong expression is also detected in the anlagen for cement gland and hatching gland and is very similar to the expression of *XAG*, a marker for this tissues [281] (Fig. 20F, G). In tailbud embryos *erlectin* expression occurs in otic vesicle and pronephros and continues in cement and hatching gland (Fig. 20I). A weak ubiquitous expression of *erlectin* is observed at all stages. This expression is highly reminiscent of the expression pattern of the endoplasmic reticulum (ER) synexpression group [282], which comprises a group of genes characterized by predominant expression in actively secreting tissues. The ER synexpression group so far includes 38 annotated members [263], of which the KDEL receptor is one example (Fig. 20H). These genes are not only co-expressed in a characteristic pattern encompassing organs with high secretory activity, but also function in ER-related processes [282, 283]. I conclude that *erlectin* is a member of the ER synexpression group, which strongly suggests that the protein plays a role in secretory protein traffic.

The expression pattern of Erlectin is conserved in zebrafish (D. rerio)

Expression of the zebrafish *erlectin* homolog is detected in notochord and hatching gland (Fig. 21) as well as the otic vesicle (not shown) [284], thus being spatially conserved in *Xenopus* and zebrafish (compare Figs. 20E and 21D).

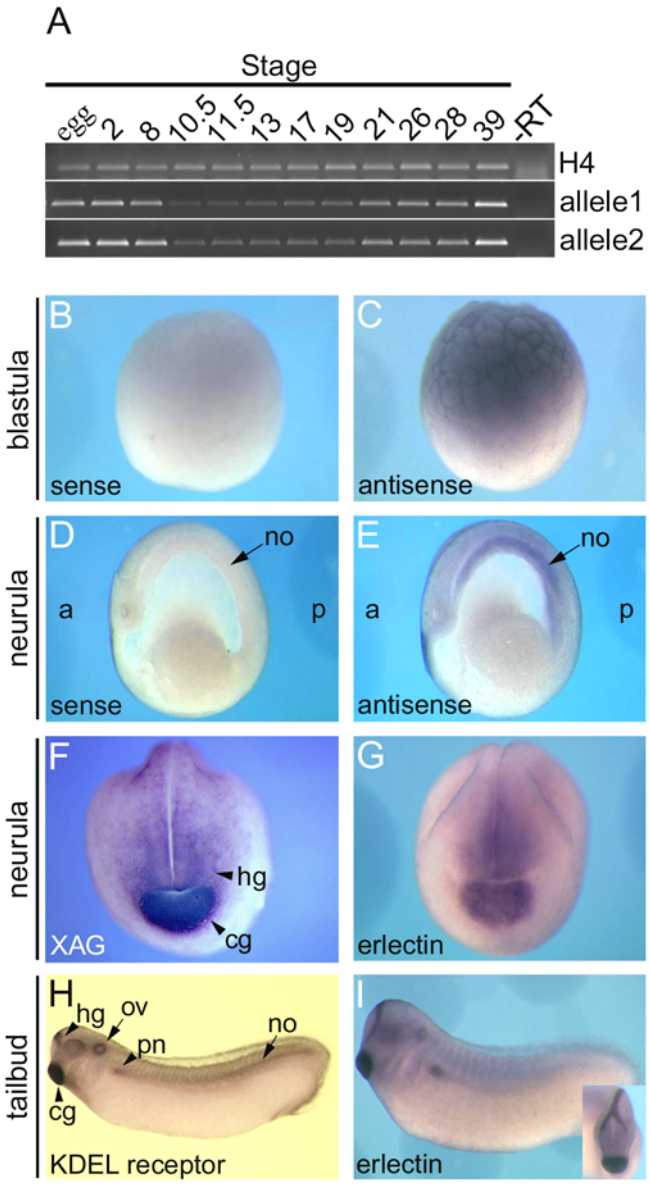

Figure 20. Erlectin is a member of the endoplasmic reticulum synexpression group. (A) Expression of *erlectin* analyzed by RT-PCR at the indicated stages. Histone H4 was used for normalization. **(C)** Blastula stage embryo (st. 8) showing *erlectin* expression in the animal hemisphere. **(E)** During neurula stages *erlectin* is expressed in the notochord. Embryo was sagittally cut, anterior (a) towards the left. (p), posterior. **(F, G)** Anterior view of late neurula stage embryos showing expression of *XAG* and *erlectin*, respectively. **(I)** Tailbud stage (st. 28). The inset shows the same embryo in anterior view. **(H)** Expression of the KDEL receptor, member of the ER synexpression group. **(B, D)** Control hybridizations using sense riboprobe. Abbreviations: Cg, cement gland; hg, hatching gland; no, notochord; ov, otic vesicle; pn, pronephros.

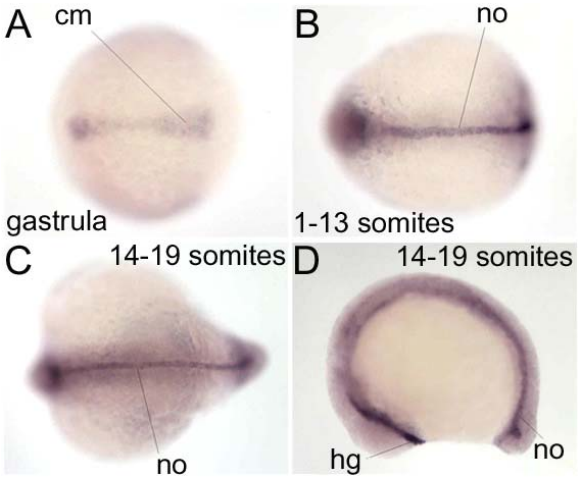

Figure 21. *Erlectin* expression in the zebrafish *Danio rerio*. Whole mount *in situ* hybridizations. **(A-C)** Dorsal view, anterior to the left. During gastrula **(A)** and segmentation **(B-D)** stages *erlectin* is expressed in axial chordamesoderm (cm) and notochord (no), respectively. **(D)** Sagittal section, anterior to the left. Expression is also detected in the hatching gland (hg). Pictures taken from [284].

Erlectin transcription is not induced by ER stress

Cells with high unfolded protein load of the ER (ER stress) due to disturbed homeostasis or professional secretory activity (e.g. plasma cells, pancreatic cells, hepatocytes) activate an intracellular signal transduction cascade, which leads to transcription of numerous target genes (in particular ER chaperones) and is termed unfolded protein response (UPR) [285-288]. Members of the ER synexpression group in *Xenopus* are mainly expressed in tissues that show a high demand for secretory activity [282]; I therefore hypothesized that regulatory elements of ER synexpression group genes may be shared with ER stress inducible genes.

Indeed, the 5' UTR of the *erlectin* gene contains a conserved binding site for ATF6 (in mouse, zebrafish, *X. tropicalis*, not shown), a transcription factor mediating UPR [286, 287, 289]. Hence, I tested if *erlectin* transcription can be activated by ER stress in *Xenopus* animal cap explants (ACs). Treatment of ACs with the glycosylation inhibitor tunicamycin induces transcription of the ER stress-inducible chaperone BiP/GRP78 (glucose-regulated protein, 78kDa) in a dose-dependent manner [290], whereas transcription of the cytoplasmic chaperone Hsp70 is not affected (Fig. 22); this indicates that induction of ER stress by tunicamycin is specific. However, transcription of *erlectin* is not induced by tunicamycin treatment, indicating that *erlectin* is not a direct ER stress target (Fig. 22).

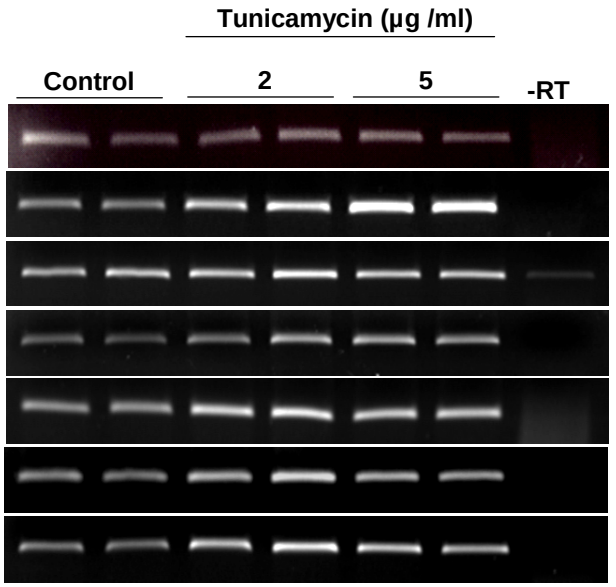

Figure 22. *Erlectin* transcription is not induced by ER stress. RT PCR analysis of tunicamycin treated ACs using the indicated primers. Explants were cut at stage 9, grown for 9 hours and then incubated with indicated amounts of tunicamycin for 12 hours. Samples were prepared in duplicates. Control, untreated explants. H4 was used for normalization. The expression of *keratin*, *integrin* and *krm2* was analyzed as further control.

Erlectin is a luminal protein of the ER

To further corroborate an involvement of Erlectin in ER function, we next studied its subcellular distribution in cultured cells.

C.C. showed by immunofluorescence analysis that Erlectin co-localizes with the ER-marker Calnexin, but not with the *trans*-Golgi marker TGN38 [291] or the endosome marker EEA1 [292] (not shown). To clarify the membrane topology of Erlectin, I performed a protease protection assay with membranes prepared from transfected cultured cells. I compared the protease accessibility of the luminal domain of the ER chaperone Calnexin [293] and Erlectin. Erlectin is protease resistant in the absence of non-ionic detergent as is Calnexin, while both are degraded in the presence of Triton X-100 (Fig. 23). The change of the gel migration of Calnexin upon protease treatment in the absence of detergent reflects the removal of its short (87 amino acids) cytoplasmic domain [293]. Together, these results indicate that Erlectin is ER-localized and resides on the luminal side of the ER membrane.

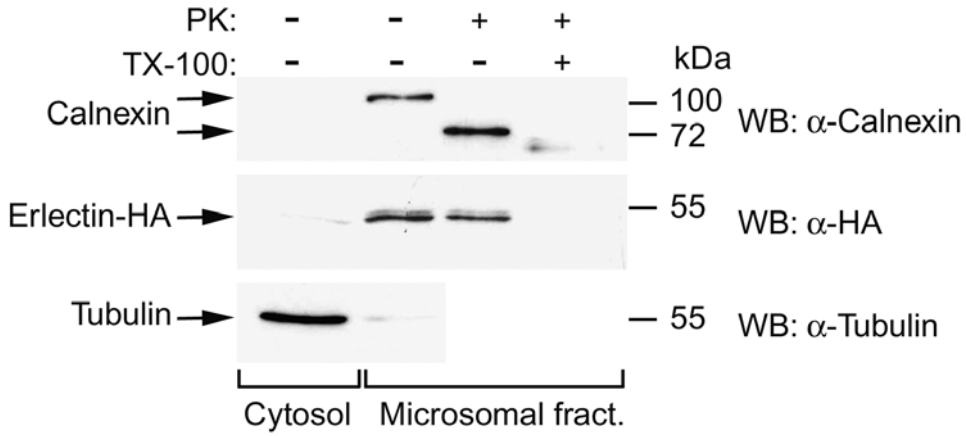

Figure 23. Erlectin is localized in the ER lumen. Protease protection assay followed by SDS-PAGE analysis and Western blotting. Microsomal membranes from HEK293T cells transfected with Erlectin-HA were subjected to Proteinase K (PK) digestion in the presence or absence of TritonX-100 (TX-100).

Role of Erlectin during *Xenopus* development

To study the function of Erlectin *in vivo* I first overexpressed mRNA in *Xenopus* embryos. Analysis of tagged Erlectin protein by Western blotting confirmed that the injected mRNA

was translated into protein (not shown). Embryos injected with up to 4 ng of mRNA develop normally (not shown).

To further investigate the role of Erlectin during development I focused on a MO-mediated loss-of-function approach. I designed two MOs targeting each of the two alleles found in *X. laevis*. Both MOs also target the *X. tropicalis erlectin* allele (two mismatches each) (Fig. 24).

Injection of both MOs at 4-cell stage leads to a very similar, characteristic phenotype in *X. laevis* and *X. tropicalis* embryos, although at different doses (Fig. 25A). Embryos develop morphologically normal until late tailbud stage. Tadpole embryos show axial defects including anterior head defects and shorter, bent tails, as well as retarded development and consequently reduced size. Histological analysis of MO injected embryos shows reduced size of axial organs including somites and notochord. Embryos exhibit microcephaly, with reduced brain tissue which lacks a ventricle. The cement gland is present but abnormally shaped and the heart is absent (Fig. 25B). The specificity of this phenotype is supported by two different MOs that give the same characteristic phenotype in both *X. laevis* and *X. tropicalis*. I next asked if the observed axial defects in Erlectin MO injected embryos are due to a requirement of Erlectin during early a-p patterning. I injected Erlectin MO1 into *Xenopus* embryos and analyzed *bf1* (forebrain) [294] and *krox20* (hindbrain) [295] expression (Fig. 25D). Neither of these markers is affected by Erlectin MO1 injection. Likewise, other a-p markers such as *XAG* (cement/hatching gland) [281], *otx2* (fore/midbrain) [296] and *Xnot2* (notochord) [37] are unaffected (not shown). Taken together, these results indicate that Erlectin plays an essential, pleiotropic role during late *Xenopus* development, after initial a-p patterning is established.

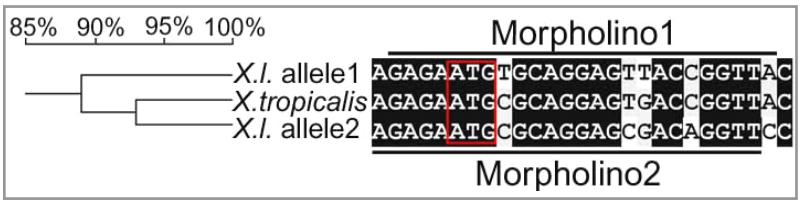

Figure 24. Homology tree of *erlectin* alleles in *X. laevis (X.l.)* and *X. tropicalis.* Also shown is an alignment of nucleotide sequences around the ATG (red), which are targeted by two Morpholinos as indicated.

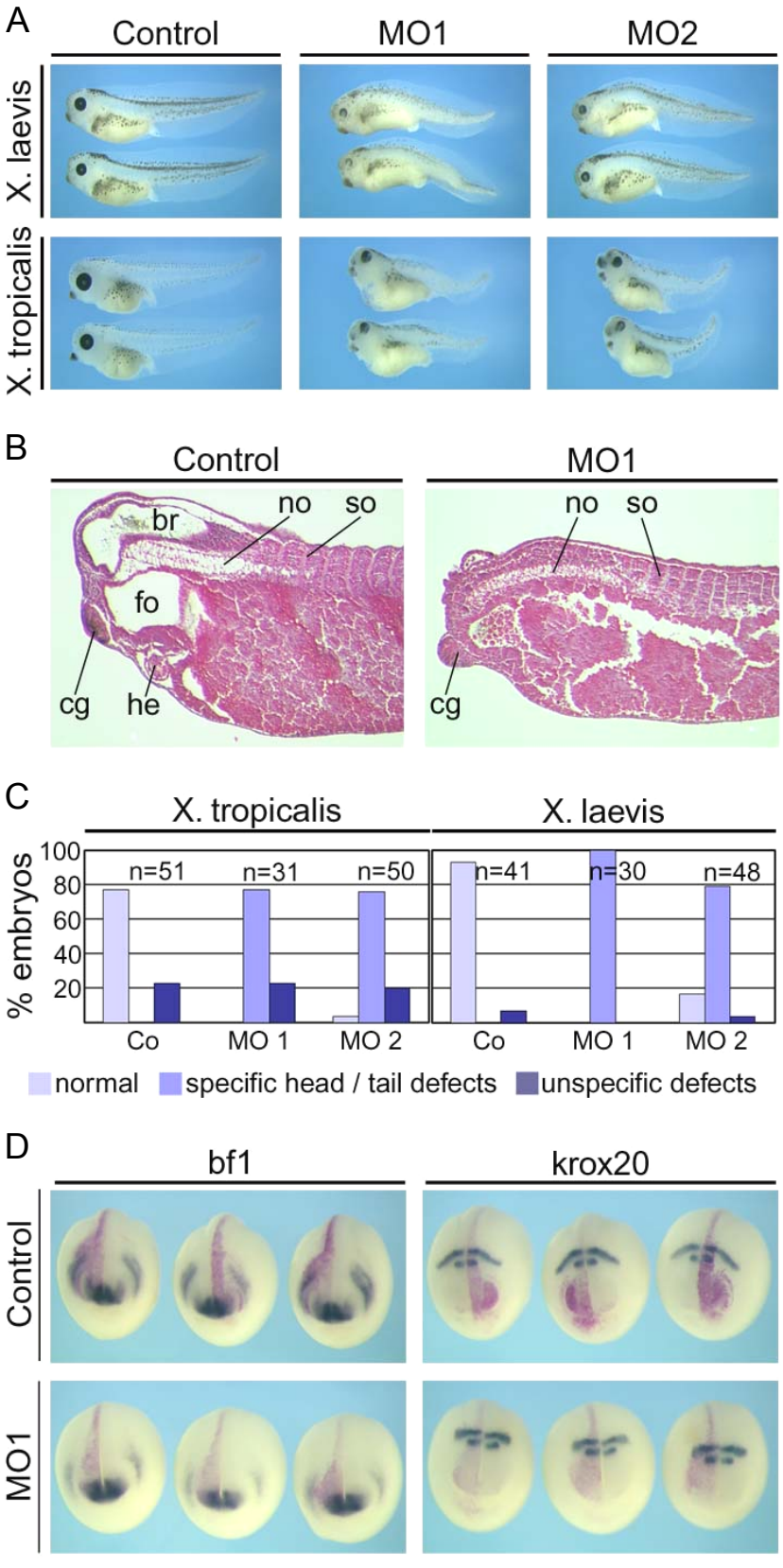

Figure 25. Erlectin Morpholino (MO) injection induces head and axial defects in *Xenopus* embryos. (A) MO1 and MO2 injected embryos show similar phenotypes. *X.* laevis and *X. tropicalis* embryos were injected with 30 ng and 10 ng of MO1 and 60 ng and 20 ng of MO2, respectively. Control embryos were injected with 60 ng (*X. laevis*) and 20 ng (*X. tropicalis*) control Morpholino. **(B)** Histological analysis of MO1 injected *X. laevis* embryos. Note that notochord (no) and somites (so) are reduced and the brain (br) and heart (he) are virtually absent. Cg, cement gland, fo, foregut. **(C)** Statistical overview of one representative MO injection experiment. Shown is the percentage of embryos with the indicated phenotype. (n), total number of embryos. **(D)** Early anterior neural markers are not affected by injection of MO1. 8-cell stage embryos were injected with 10 ng MO1 or control MO into one dorsal animal blastomere. Embryos were harvested at stage 20 and processed for *in situ* hybridization. Co-injected ß-gal was used as lineage tracer.

Erlectin does not cooperate with Krm2 in Wnt inhibition in *Xenopus*

As Erlectin specifically binds to the Wnt inhibitor Krm2, I analyzed a potential functional interaction of these proteins in Wnt inhibition during *Xenopus* development. A summary of approaches and obtained results is presented below.

- **Erlectin and Krm2 do not interact in gain-of-function.** Since Krm2 overexpression anteriorizes embryos [220], I tested if overexpression of Erlectin can modify this Krm2 gain-of-function phenotype by co-injecting *erlectin* and *krm2* mRNA. Neither an enhancement nor a rescue of the embryonic phenotype was observed (not shown).
- **Erlectin loss-of-function does not mimic Krm2 loss-of-function.** Krm1+2 MO injected embryos show microcephaly and reduced expression of the forebrain marker *bf1* due to a role of the proteins in early a-p patterning [220]. As detailed above, early a-p markers are unaffected by Erlectin MO1 injection in embryos (Fig. 25D) and animal caps (not shown).
- **Erlectin and Krm2 do not interact in loss-of-function.** Co-injection of Erlectin MO1 and Krm2 MO [220] does not lead to a significantly and specifically enhanced phenotype; rather, the phenotype of co-injected embryos is a superimposition of independent effects induced by Erlectin MO1 and Krm2 MO (not shown).
- **Erlectin loss-of-function is not rescued by Krm2 overexpression.** If two genes cooperate in the same pathway, loss-of-function of one gene may be compensated by overexpression of the other. Co-injection of *krm2* mRNA does not rescue the phenotype induced by Erlectin MO1 injection. Furthermore, co-injection of several other Wnt inhibitors, including *dkk1* or *dnWnt8* mRNA, or β-catenin MO [297], does not rescue the phenotype induced by Erlectin MO1 injection (not shown).

Taken together, these results clearly indicate that although Erlectin binds to Krm2 *in vitro*, in *Xenopus* embryos Erlectin (i) does not mimic Krm2 in gain- and loss-of-function analysis, and (ii) does not functionally interact with Krm2 in Wnt inhibition.

However, my MO-mediated knock-down experiments clearly indicate that Erlectin function is required during *Xenopus* development. Since Erlectin is a member of the ER synexpression group, localizes to the ER lumen and binds N-glycans, this strongly suggests an essential, possibly general role of Erlectin in an ER-related process.

Kremen is required for neural crest induction in *Xenopus* and promotes LRP6-mediated Wnt signaling

Xkrm2 is co-expressed with and regulated by Wnts

This laboratory previously reported that *Xkrm1* and *2* are co-expressed with *dkk1* in the *Xenopus* prechordal plate during mid-neurula stages, where they cooperate to regulate a-p CNS patterning [220]. However, *krm2* shows additional expression in regions devoid of *dkk1* transcripts. At gastrula stages *Xkrm2* expression occurs in the ventro-lateral marginal zone of the embryo (Fig. 26A). During neurula stages *krm2* is expressed in the lateral neural plate, overlapping with the neural crest marker *slug* (Fig. 26B). Furthermore, *krm2* is co-expressed with Wnt genes such as *Wnt8* and *Wnt3a* (Fig. 26A), raising the possibility that *krm2* expression is regulated by Wnt signaling. Indeed, local inhibition of Wnt signaling by injection of dominant negative *XWnt8* mRNA abolishes the expression of *krm2* in the marginal zone (Fig. 27A, C). Conversely, injection of *Wnt8* and *Wnt3a* DNA leads to ectopic expression of *krm2* (Fig. 27B, C).

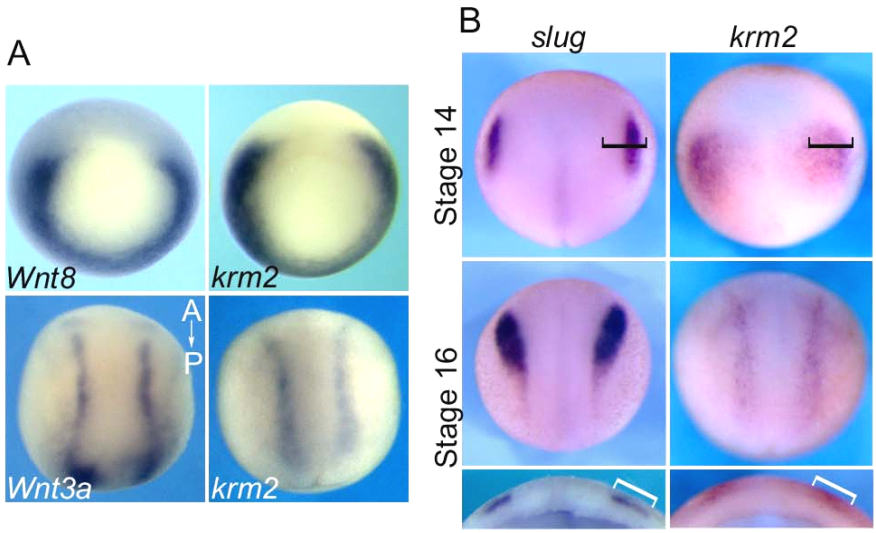

Figure 26. *Xkrm2* is co-expressed with Wnts and neural crest (NC) markers. Whole mount *in situ* hybridizations. **(A)** Comparison of *Xkrm2*, *XWnt8* and *XWnt3a* expression patterns in gastrula and early neurula stage embryos. Top, gastrula stage. Vegetal view, dorsal is up. Bottom, neurula stage. Dorsal view, anterior is up. **(B)** Comparison of *Xkrm2* and *slug* expression patterns at the indicated stages. Dorsal view, anterior is up. Lowermost panel: View of frontally cut stage 16 embryos, dorsal is up. Brackets indicate overlapping expression domains of *krm2* and *slug*. This experiment was done by R. Mayor lab members.

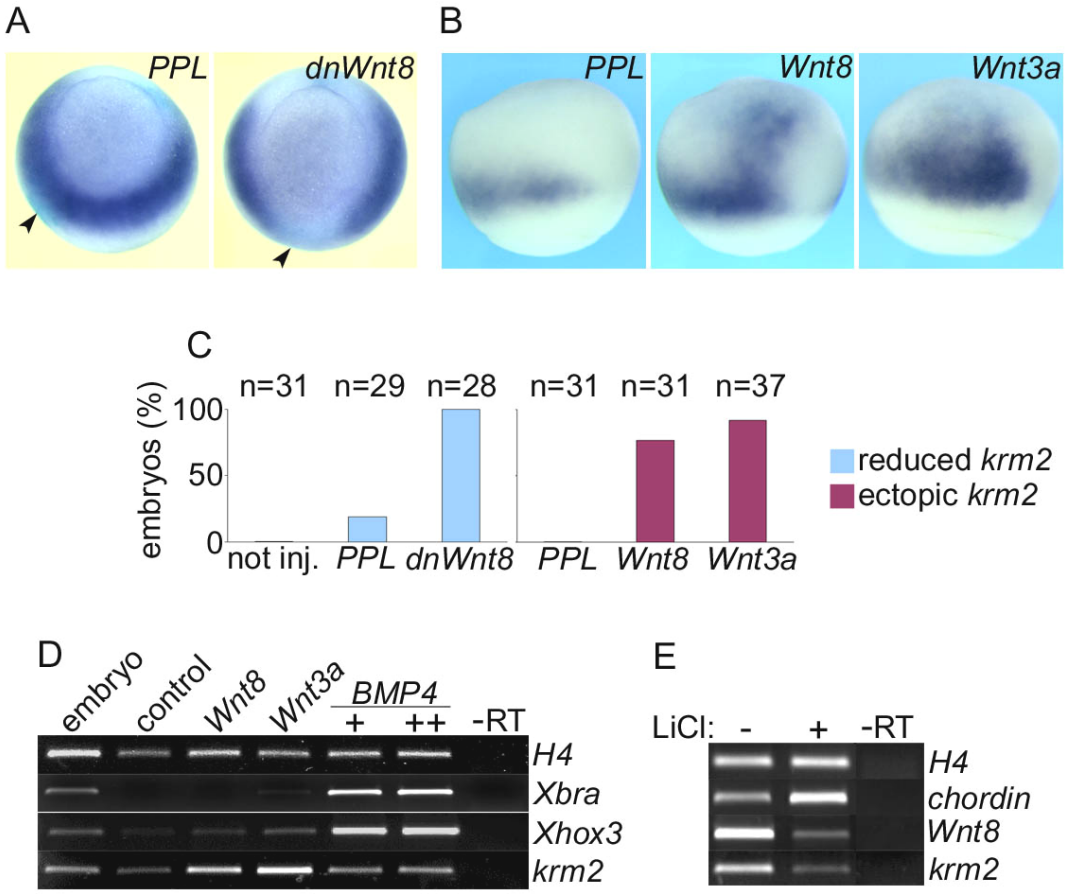

Figure 27. *Xkrm2* expression is regulated by Wnt signaling. (A-C) Effect of Wnt pathway perturbations on *krm2* expression. **(A, B)** Whole mount *in situ* hybridizations. **(A)** 32-cell stage embryos were injected equatorially in two opposite blastomeres with 1 ng *PPL* or *dnWnt8* mRNA and analyzed at gastrula stage. Arrowheads indicate ß-gal lineage tracer staining (blue). Vegetal view, dorsal is up. **(B)** 4-cell stage embryos were injected animally with 200 pg pCS2-*PPL* or pCSKA-*Wnt8* DNA or 100 pg pCS2-*Wnt3a* DNA in one blastomere and analyzed at gastrula stage. Lateral view, dorsal to the right. **(C)** Statistical overview of experiments shown in (A) and (B). **(D)** 4 to 8-cell stage embryos were injected animally with 100 pg *XWnt8* or *Wnt3a* mRNA, or 1 or 2 ng *BMP4* mRNA. Animal caps were cut at stage 8-9, cultured until stage 20 equivalent, and analyzed by RT-PCR for expression of the indicated genes. **(E)** 32-cell stage embryos were treated with 120 mM LiCl for 50 min, cultured until stage 11.5, and analyzed by RT-PCR. **(D, E)** Histone H4 was used for normalization. –RT, minus reverse transcriptase control.

I furthermore analyzed the effect of Wnt and BMP pathway activation on *krm2* expression in animal caps. In control caps *krm2* is expressed at moderate levels. *Wnt8* and *Wnt3a* mRNA injections increase *krm2* expression, whereas *BMP* mRNA has no effect (Fig. 27D).

LiCl treatment of early embryos, which leads to dorso-anteriorization, downregulates *krm2* expression along with *Wnt8* and other ventro-laterally expressed genes (Fig. 27E, and not shown). I conclude that (i) *krm2* at gastrula stages is expressed and regulated like a classical ventro-lateral gene; (ii) *krm2* is co-expressed with Wnts and regulated by zygotic Wnt signaling; (iii) *krm2* at neurula stages shows differential expression in the neural crest.

Overexpression of *krm2* induces NC markers and NC-derived structures

To study potential Dkk1-independent roles of Krm2, I first analyzed gain-of-function effects. Localized injection of *krm2* mRNA into anterior embryonic regions induces ectopic cement glands (Fig. 28A, arrowhead) and retinal pigment epithelium (Fig. 28B, arrowhead). Ventral injection of *krm2* mRNA leads to induction of protrusions containing melanocytes and fin-like structures (Fig. 28C, arrowhead). Widespread *krm2* overexpression leads to hyper-pigmented embryos due to overproduction of melanocytes, which have normal morphology (Fig. 28E). Embryos frequently also show eye and tail defects (not shown).

Melanocytes are neural crest (NC) derivatives, which in *Xenopus* are characteristically overproduced when NC regulators such as *slug* or *sox10* are overexpressed [81, 111, 298]. I therefore tested if *krm2* overexpression can induce NC markers. Localized *krm2* injection leads to ectopic expression of the NC marker *sox10* (Fig. 28F, G, arrowheads). *Krm2* overexpression affects NC markers in a region-specific fashion: Posterior *krm2* injection leads to expansion of *slug* and *sox10* (Fig. 28L, N, black arrowheads). In contrast, anterior *krm2* injection reduces *slug* and *sox10* expression (Fig. 28M, O, black arrowheads). Thus, the region of *krm2* expression determines its effect on NC markers (summarized in Fig. 28P). This may be explained by the local interaction of injected Krm2 with Dkk1 anteriorly, to inhibit Wnt signaling and NC induction. In posterior regions, where Dkk1 is absent, Krm2 has a stimulatory effect on NC development.

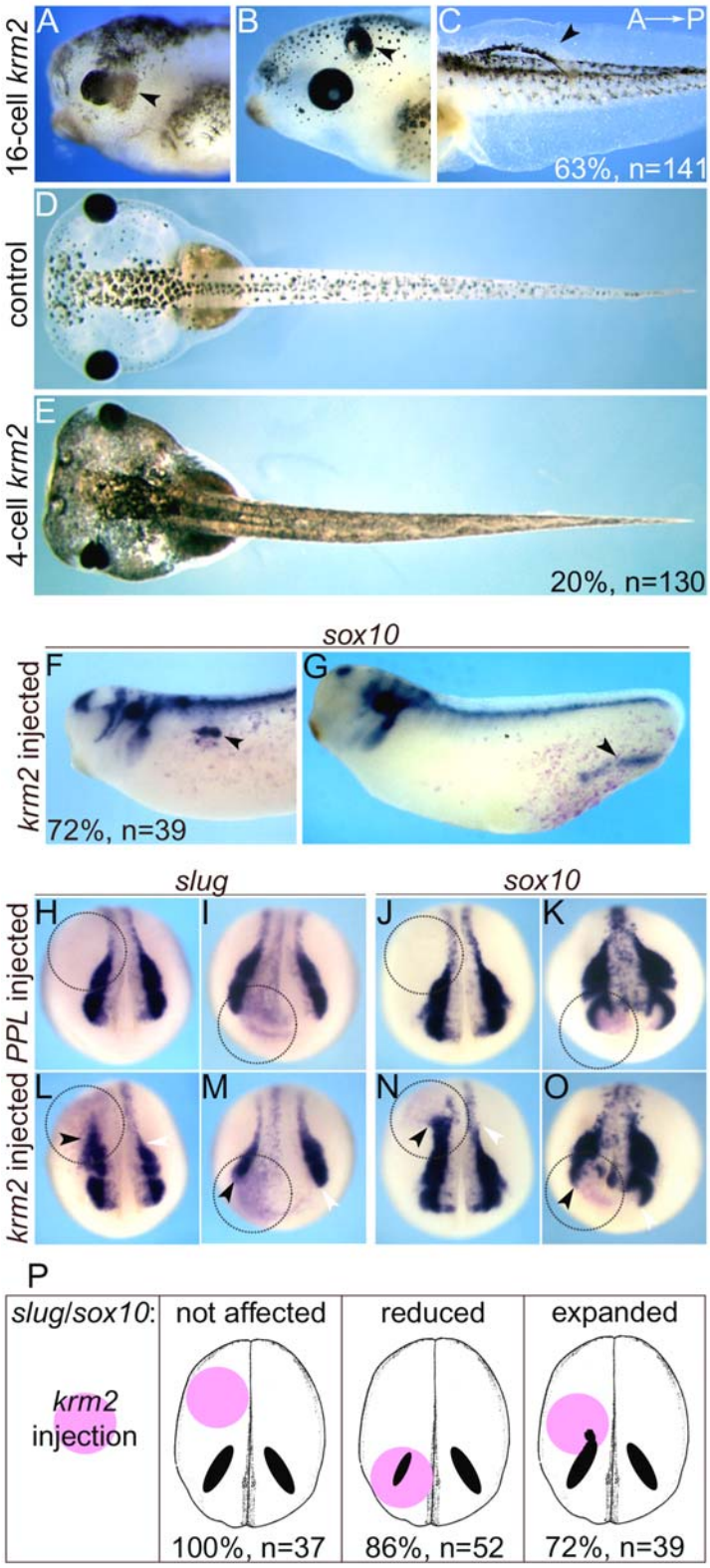

Figure 28. *Xkrm2* over-expression induces NC-derived structures and NC markers. (A-E) Phenotypic analysis of *krm2* overexpression. Anterior to the left. **(A-C)** 16-cell stage embryos were injected in a single animal **(A, B)** or ventral equatorial **(C)** blastomere with 400 pg *krm2* mRNA and photographed at tadpole stages. Arrowheads indicate ectopic pigment containing structures. **(D)** Uninjected control embryo at tadpole stage. **(E)** 4-cell stage embryos were injected equatorially in both dorsal blastomeres with 400 pg *krm2* mRNA each. **(F, G)** 16-cell stage embryos were injected in a single ventral equatorial blastomere with 400 pg *krm2* mRNA and *sox10* expression was analyzed at tailbud stage by *in situ* hybridization. Arrowheads indicate ectopic *sox10* expression. Co-injected ß-gal was used as lineage tracer (red). **(H-O)** Neurula stage embryos, shown in anterior view. Embryos were injected with 400 pg *PPL* **(H-K)** or *krm2* **(L-O)** mRNA into one ventral equatorial blastomere at 16-cell stage **(H, J, L and N)** or one dorsal animal blastomere at 8 to 16-cell stage **(I, K, M and O)**. *In situ* hybridizations were performed using *slug* and *sox10* probes as indicated. ß-gal lineage tracer is stained in red. **(H-O)** Circles indicate lineage tracer positive cells. Black and white arrowheads indicate altered and control marker gene expression, respectively. **(P)** Scheme and statistical overview of experiment shown in (H-O). Red area indicates region of *krm2* injected cells.

Morpholino-mediated knock-down of Krm2 inhibits NC formation

Since *krm2* is expressed in the prospective NC region and is sufficient to induce NC tissue, I next asked if it is also required for NC development. I made use of the previously characterized Morpholino antisense oligonucleotide targeting the ATG codon of *Xkrm2* (MO-1) [220].

Besides the previously described microcephaly I found that Krm2 MO-1 injection strongly reduces the pigmentation of embryos (Fig. 29A). Furthermore, Krm2 MO-1 inhibits *slug* expression (Fig. 29B, C). This is also the case for a second Krm2 MO (Krm2 MO-2), which targets the 5' untranslated region of *krm2* (Fig. 29B, C), thus corroborating the specificity of the effect.

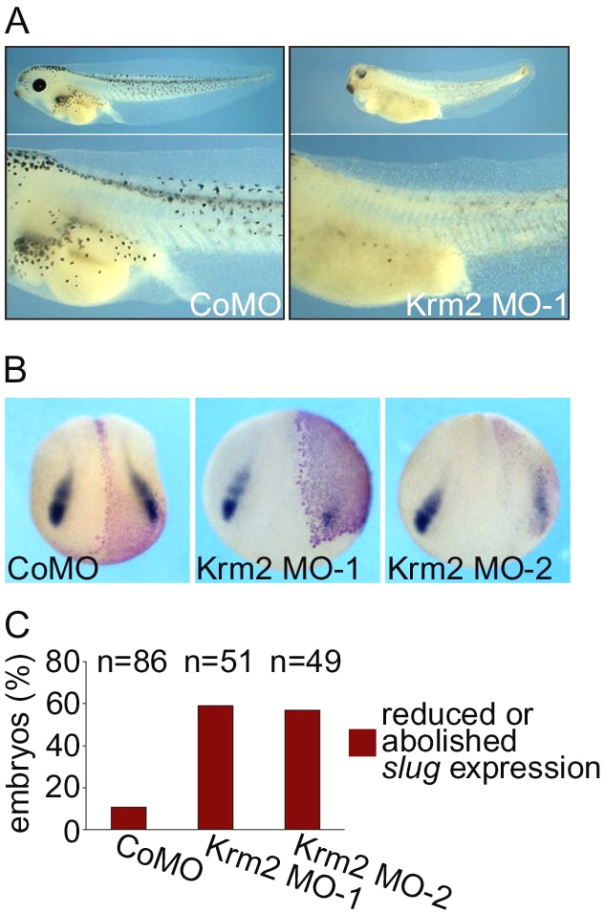

Figure 29. Morpholino-mediated knock-down of *krm2* expression. (A) 8-cell stage embryos were injected animally with 20 ng control MO (CoMO) (left panel) or Krm2 MO-1 (right panel). **(B)** 4 to 8-cell stage embryos were injected animally with 10 ng Krm2 MO-1 or 20 ng Krm2 MO-2 or (CoMO), respectively. Shown are whole-mount *in situ* hybridizations for *slug* expression at neurula stage in anterior view. ß-gal lineage tracer is stained in red. **(C)** Statistical overview of MO injection experiment.

To analyze if Krm2 is required specifically in the ectoderm for NC formation, or in the underlying, inducing mesoderm, members of the Mayor lab combined Krm2 MO-1 injected animal caps with uninjected dorso-lateral marginal zones (DLMZs) and analyzed NC

induction. Whereas DLMZs can induce *slug* in control caps in 62% of cases (n=42), *slug* induction is completely abolished upon injection of Krm2 MO-1 into the responding ectoderm (0%, n=43) (Fig. 30). These results indicate that Krm2 is required directly in the ectoderm for NC formation, where it is also expressed.

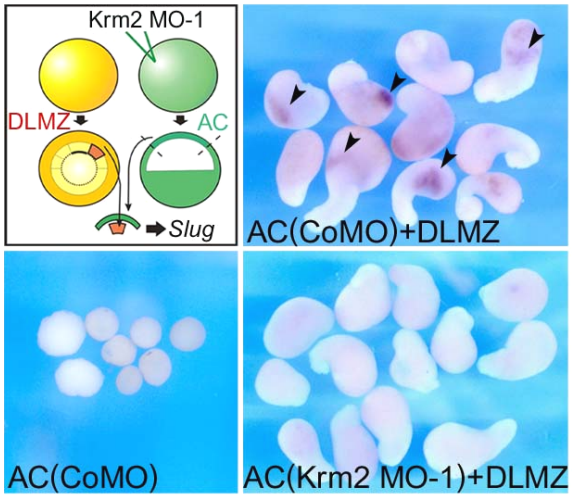

Figure 30. Krm2 is required in the ectoderm for NC formation. Top left: Diagram of experiment. 2-cell stage embryos were injected animally with 10 ng CoMO or Krm2 MO-1 and animal caps (ACs) were explanted at stage 8-9 and combined with dorso-lateral marginal zones (DLMZs) of uninjected gastrula stage embryos. Conjugates were assayed at stage 20 for *slug* expression by *in situ* hybridization. **Top right**: Conjugates of DLMZs and CoMO injected ACs. Arrowheads indicate *slug* expression. **Bottom left**: ACs injected with CoMO and processed for *slug in situ*. **Bottom right**: Conjugates of DLMZs and Krm2 MO-1 injected ACs. This experiment was performed by members of R. Mayor's lab.

Morpholino-mediated knock-down of LRP6 inhibits NC formation

It is well established that canonical Wnt signaling is required for NC induction [69, 299, 300]. In *Xenopus*, overexpression of Wnts or Wnt receptors, as well as downstream signaling components, can all induce NC. Conversely, inhibition of Wnts, Wnt receptors and β-catenin blocks NC induction [93, 97, 98, 299]. Since Krm2 is a negative Wnt modulator and is itself Wnt regulated, I therefore hypothesized that Krm2 may also play a positive role in Wnt/LRP6-mediated NC induction. Hence, I tested whether LRP6 knock-down mimics Krm2 loss-of-function during NC development.

I designed a MO targeting both *X. laevis* and *X. tropicalis* LRP6 genes. Injection of this LRP6 MO results in strongly anteriorized embryos with enlarged cement gland, shorter and ventrally bent tail and triangular body shape (Fig. 31A). This phenotype closely mimics the anteriorization induced by overexpression of the LRP6 antagonist *dkk1* (Fig. 31A). Of note, a morphologically highly sensitive structure to injection of low doses of LRP6 MO is the

dorsal fin (Fig. 31D, arrowheads). The LRP6 MO phenotype is fully rescued by co-injecting human *LRP6* mRNA (Fig. 31A, panels c, e), confirming specificity of the MO. Furthermore, injection of LRP6 MO in *X. tropicalis* embryos results in the same phenotype as in *X. laevis* (Fig. 31B). Similar to Krm2 MO, LRP6 MO inhibits *slug* expression (Fig. 31C). Thus, MO mediated knock-down of both LRP6 as well as its modulator Krm2 results in inhibition of NC formation.

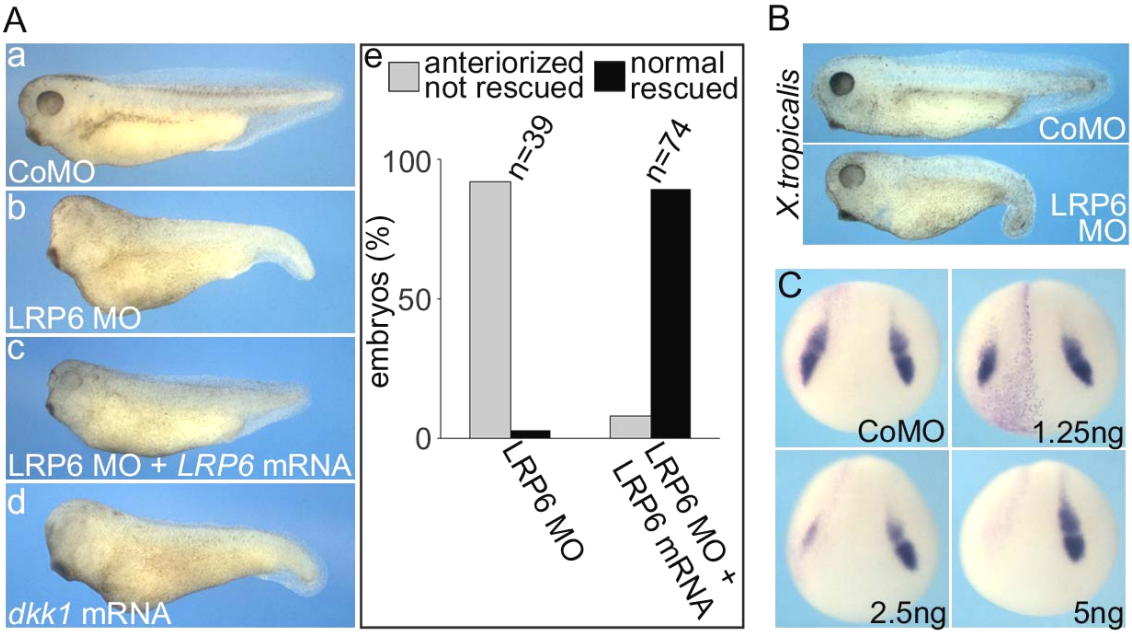

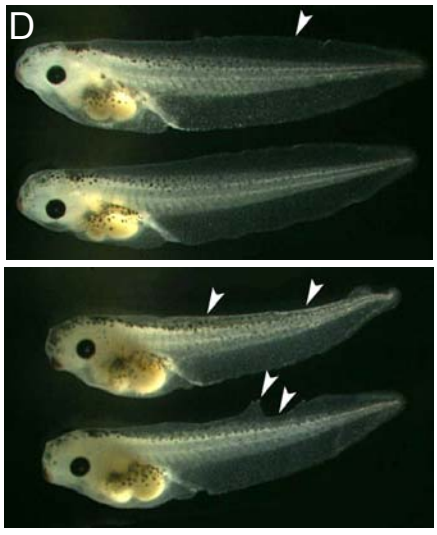

Figure 31. Morpholino-mediated knock-down of LRP6 expression. (A, B) Phenotypic analysis of LRP6 MO in *X. laevis* **(A)** and *X. tropicalis* **(B)**. All embryos were injected equatorially at 2-cell stage. **(A) (a)** Injection of 5 ng CoMO. **(b, c)** Co-injection of 5 ng LRP6 MO and either 1 ng control (*PPL*) **(b)** or 400-600 pg human *LRP6* mRNA **(c)**. **(e)** Statistical overview. **(d)** Injection of 20 pg *dkk1* mRNA. **(B)** *X. tropicalis* embryos injected with 1.25 ng CoMO or LRP6 MO show the displayed phenotypes at frequencies of 89%, n=38, upper panel and 98%, n=44, lower panel. **(C)** 2-cell stage *X. laevis* embryos were injected equatorially in one blastomere with 5 ng CoMO or increasing LRP6 MO doses as indicated. Neurula stage embryos were processed for *slug* expression by *in situ* hybridization and are shown in anterior view. ß-gal lineage tracer is stained in red. **(D)** Effect of mild LRP6 knock-down on development of the dorsal fin. Upper panel, control embryos. Lower panel, phenotypes of embryos injected animally with 1.5 ng LRP6 MO. Note reduction of the dorsal fin (arrows) in embryos with otherwise normal morphology.

Krms stimulate LRP6-mediated Wnt signaling in 293T cells

The results obtained so far suggest that Krm2, besides its well established role in Wnt inhibition, may also, in the absence of Dkk1, positively regulate Wnt signaling. Previously this lab found no effect of Krm1 or 2 in Wnt responsive reporter assays triggered by transfection of *wnt/fz* or *wnt/fz/LRP6* in HEK293T cells. I now find that *Xkrm1*, but also *Xkrm2*, significantly stimulate Wnt signaling when co-transfected with *LRP6* alone, whereas no effect is observed with *fz8* or *dvl* (Figs. 32A, 33). I conclude that Krms can specifically promote LRP6-mediated signaling.

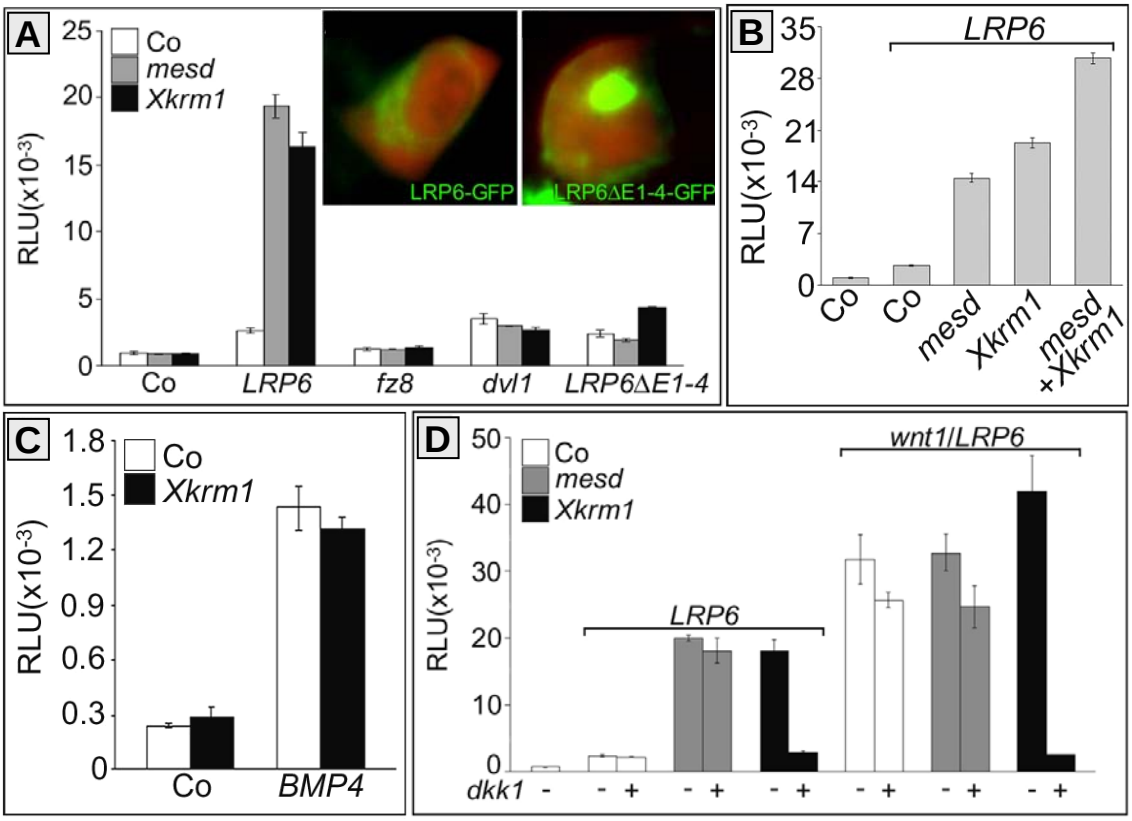

Figure 32. Krm promotes LRP6-mediated Wnt signaling. **(A-D)** TOPFLASH luciferase reporter assays in HEK293T cells. RLU, relative light units. Co, empty pCS2 vector. **(A)** XKrm1 cooperates specifically with LRP6. The inset shows the subcellular localization of transfected LRP6-GFP (left panel) and LRP6ΔE1-4-GFP (right panel) in HEK 293T cells; co-transfected cytoplasmic dsRed (red) demarcates the cell shape. **(B)** Co-transfection of *mesd* and *Xkrm1*. **(C)** BMP luciferase reporter assay in HEK293T cells. **(D)** Effect of XKrm1 on LRP6 signaling is Dkk1 dependent.

One possibility how Krm may stimulate LRP6 signaling is by promoting its trafficking or stability. I therefore compared its effects to Mesd, an LRP6 chaperone, which also

stimulates LRP6-mediated Wnt signaling [172, 173] (Fig. 32A). As previously shown, Mesd is required for maturation of β-propeller/EGF modules of LDLR family members [180]. Consequently, *mesd* transfection does not promote signaling stimulated by LRP6ΔE1-4, a cell surface-localized constitutive active LRP6 construct with truncated extracellular domain (Fig. 32A). In contrast, *krm1* does moderately stimulate LRP6ΔE1-4-mediated signaling (Fig. 32A). Co-transfection of *krm1* and *mesd* shows a merely additive effect (Fig. 32B), suggesting that these genes do not functionally interact.

To test the specificity of the Wnt promoting effect of Krm1, I analyzed a BMP responsive reporter and found it unaffected (Fig. 32C).

I next analyzed the effect of XKrm1 and Mesd on Wnt signaling in presence of Dkk1. Co-transfection of *dkk1* expectedly reduces the Krm1/LRP6 signal to background levels, but it does not affect the Mesd/LRP6 signal (Fig. 32D), as previously shown [301]. When *wnt1* is co-transfected additionally, the same result is observed (Fig. 32D).

I furthermore compared the effect of different Krm constructs in Wnt reporter assay. Similarly to XKrm1, albeit to a lesser extent, mouse Krm1 and *Xenopus* Krm2 promote LRP6-mediated Wnt signaling; however, mouse Krm2 consistently does not (Fig. 33). This may be due to an unspecific inhibition of downstream Wnt components by mKrm2 (unpublished observation). Interestingly, a mKrm1 construct with truncated cytoplasmic domain (mKrm1ΔC) has reduced activity when compared to wildtype mKrm1, indicating that the cytoplasmic tail is partially required for Krm1 activity (Fig. 33).

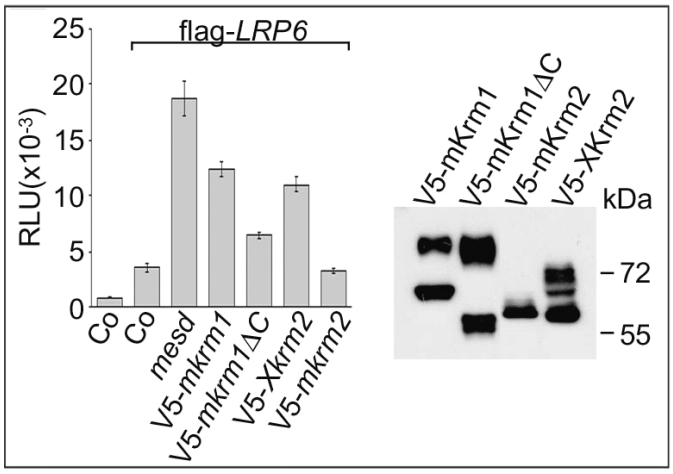

Figure 33. Krm constructs in Wnt reporter gene assay. Left panel: TOPFLASH luciferase reporter assay in HEK293T cells. RLU, relative light units. Co, empty pCS2 vector. Right panel: SDS-PAGE and Western blot analysis of *krm* constructs shows that they are expressed at a comparable level.

Taken together, these data indicate a context-dependent role of Krms in Wnt signaling. Together with Dkk1, Krms inhibit Wnt/LRP6 signaling; however, in the absence of Dkk1, Krms promote LRP6 signaling.

Krms bind to LRP6

This lab previously reported that Dkk1 binds to both Kremen and LRP6, thereby bridging the two receptors in a ternary complex, which is then removed from the cell surface [198, 211]. Since my results indicate that Krms can also function without Dkk1, C.C. tested if they may bind directly to LRP6, in absence of Dkk1. She used HEK293T cells, which express very low levels of *dkk1* (unpubl. observation). In Co-immunoprecipitation (CoIP) experiments Krm1 and 2 are specifically precipitated with LRP6 (Fig. 34A, A', lane 2), but not with the control transmembrane proteins FLRT3 and LDLRΔC (Fig. 34A, A', lanes 3, 4). This is also the case in CoIPs with added anti-Dkk1 antibody, to block any endogenous Dkk1 protein (unpublished observation of C.C.). To corroborate the directness of binding and to demonstrate extracellular interaction, C.C. also performed *in vitro* binding assays using secreted, recombinant proteins, which show that LRP6 co-precipitates with both Krm1 and 2, but not Dkk3 (Fig. 34B). I conclude that Krm1 and 2 specifically and directly bind to LRP6.

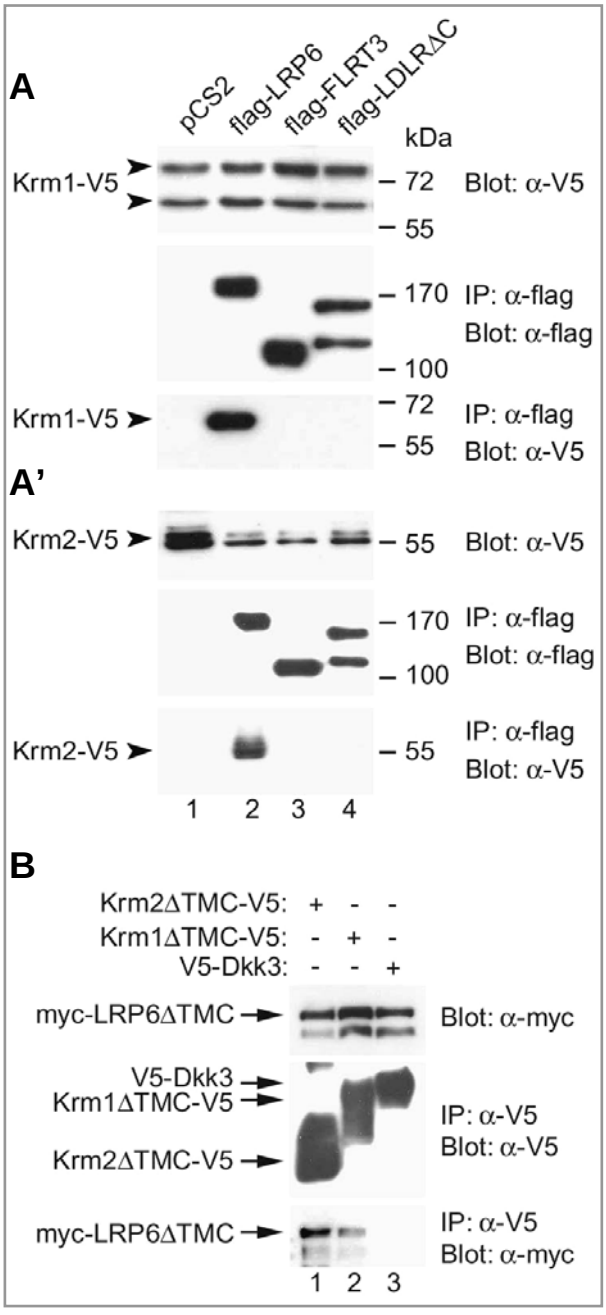

Figure 34. Krms bind to LRP6 specifically and directly. (A, A') Co-immunoprecipitation (CoIP) assays of HEK293T cell lysates transfected with *krm1*-V5 **(A)** or *krm2*-V5 **(A')** and the indicated constructs. CoIPs were performed with anti-flag antibody and analyzed by SDS-PAGE and Western blotting. **(B)** *In vitro* binding assay with secreted recombinant proteins as indicated. IPs were performed with anti-V5 antibody and analyzed by SDS-PAGE and Western blotting. **(A, A', B)** Upper panel: Protein expression. Middle and lower panels: IPs. All experiments shown in this figure were perfomed by C.C.

Krm2 promotes cell surface localization of LRP6

To explore the possibility that Krm may influence protein expression or trafficking of LRP6, I performed co-transfection experiments.

In Western blot analysis of transfected HEK293T cell lysates, LRP6 is detected as an upper and a lower band, which are thought to correspond to the mature cell surface (ma), and immature cytoplasmic (im) forms of LRP6 (Fig. 35, lane 1) [173]. I confirmed this by treatment with Endoglycosidase H (EndoH), which cleaves immature glycans that have not yet traversed the Golgi apparatus. Only the lower band is EndoH sensitive and downshifts due to deglycosylation (dg) (Fig. 35, lane 2). Co-transfection of *mesd* increases mature LRP6, consistent with it being a reported chaperone [172, 173] (Fig. 35, lanes 5, 6). Co-transfection of *krm2* has a very similar effect on LRP6. Mature LRP6 increases at the expense of the immature form (Fig. 35, lanes 7, 8), the total amount of LRP6 protein being mostly unaffected. Co-transfection of empty vector (Fig. 35, lanes 1, 2) or *dkk3* (Fig. 35, lanes 3, 4), a gene not affecting the Wnt pathway [35], has no effect on LRP6 protein expression.

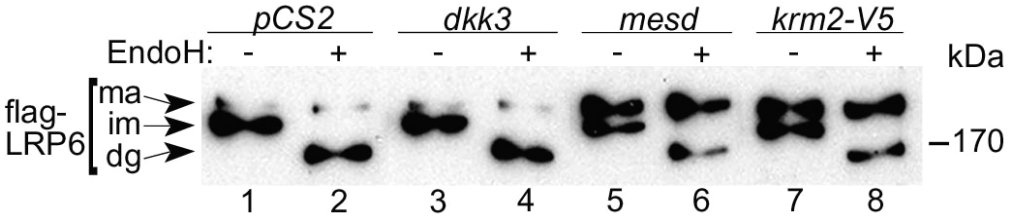

Figure 35. Krm promotes maturation of LRP6. Western blot analysis of HEK293T cells transfected with *flag-LRP6* and the indicated constructs. Samples were treated with Endoglycosidase H (EndoH) as indicated. Arrows indicate the EndoH resistant mature (ma) and EndoH sensitive immature (im) forms of LRP6. dg, deglycosylated form.

To corroborate this finding, I monitored plasma membrane levels of LRP6 by cell surface biotinylation. Following co-transfection with *krm2*, cell surface levels of LRP6 are increased, while the total LRP6 is mostly unaffected (Fig. 36A). This effect mimics *mesd* co-transfection (Fig. 36A). The cytoplasmic protein Nucleoside diphosphate kinase A (NME1) serves as control and is not biotinylated (Fig. 36A'). These data indicate that Krm2 promotes cell surface localization of the Wnt receptor LRP6.

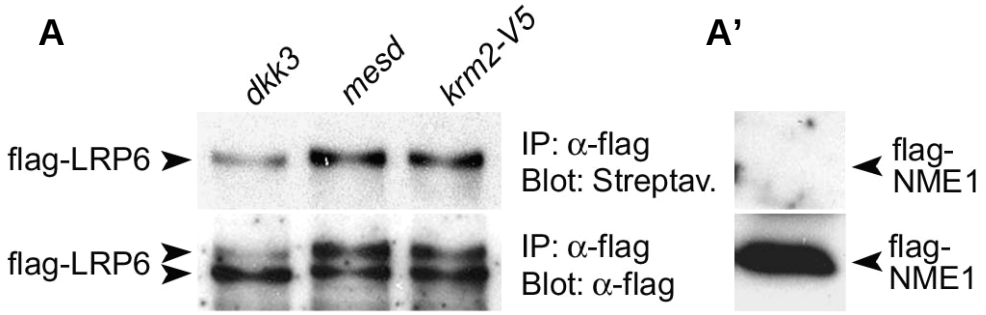

Fig. 36. Krm2 promotes cell surface localization of LRP6. (A, A') Cell surface biotinylation assay. **(A)** HEK293T cells were co-transfected with *flag-LRP6* and the indicated constructs. After cell surface biotinylation, cell lysates were immunoprecipitated with anti-flag antibody and subjected to SDS-PAGE and Western blot analysis. Membranes were probed with streptavidin-HRP to detect plasma membrane LRP6 (upper panel) and anti-flag antibody to detect total LRP6 (lower panel). **(A')** The cytoplasmic protein NME1 is not biotinylated (upper panel). Lower panel: Total NME1 protein.

ER-localized Krm2 has little effect on LRP6 maturation

As shown above, the effect of Krm2 on LRP6 protein localization closely resembles the effect of Mesd, an ER-localized chaperone (Figs. 35 and 36). I therefore considered the possibility that Krms may also promote LRP6 maturation in the ER. However, Krms are not ER resident; they lack a conserved di-lysine (KKXX) motif in their cytoplasmic tail, which mediates ER retention of transmembrane proteins [302, 303], and the presence of Krm2 protein on the cell surface is established [211, 263]. I therefore tested if ER-trapped Krm2, which is prevented from leaving the ER, can still promote cell surface localization of LRP6. It is well established that a reporter protein tagged with the KKXX motif is retained within the ER [302-305]. Amino acids flanking the core KK motif (indicated as XX) additionally influence ER retention [304]. I therefore cloned three Krm2 constructs carrying different KKXX motifs (extracted from literature as indicated in Fig. 37) on the C-terminus (Krm2-ER) (Fig. 37A).

To test the ER-retention efficiency of the Krm2-ER constructs, I first analyzed their plasma membrane levels by cell surface biotinylation. While wildtype Krm2 is readily labeled at the cell surface by biotin, Krm2-ER constructs are undetectable (Fig. 37B). Note that a faint residual band detected by streptavidin-HRP is likely unspecific, as it is also present when the control protein NME1 is transfected (Fig. 37B).

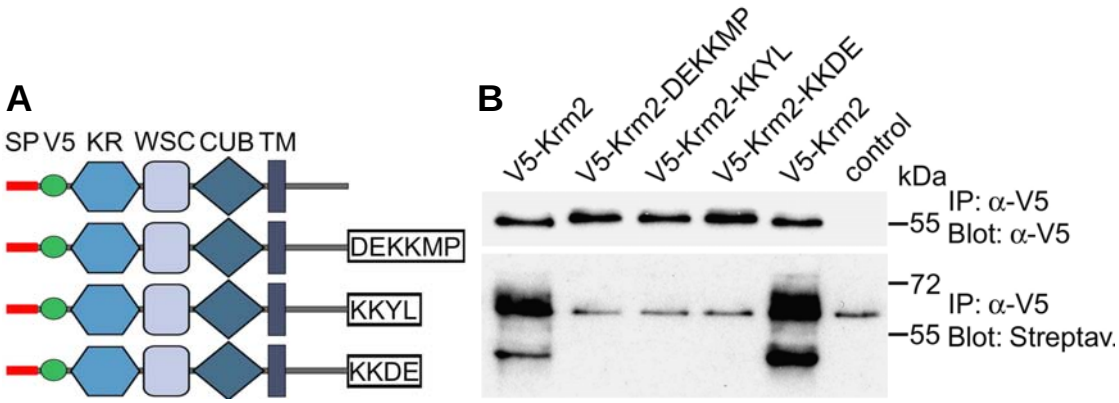

Figure 37. Characterization of Krm2-ER constructs. (A) Domain structure of wildtype mouse V5-Krm2 (top) and constructs containing ER localization motifs on the C-terminus (DEKKMP [303], KKYL [304] , KKDE [305]). SP, signal peptide; V5, V5 tag; KR, WSC and CUB, kringle WSC and CUB domains; TM, transmembrane domain. **(B)** Cell surface biotinylation of Krm2-ER. Cells were transfected with the indicated constructs. After biotinylation, cell lysates were immunoprecipitated with anti-V5 antibody and subjected to SDS-PAGE and Western blot analysis. Membranes were probed with anti-V5 antibody to detect total Krm2 (upper panel) and Streptavidin-HRP to detect plasma membrane Krm2 (lower panel). As control, *NME1* was transfected (protein not shown); the lane is included to show unspecificity of the residual band.

To test in a functional approach if Krm2-ER constructs are present at the cell surface, I made use of the fact that Krm2 and Dkk1 strongly cooperatively inhibit Wnt signaling in reporter gene assays [211, 223]. This cooperation depends on both Dkk1 and Krm2 being present in the same subcellular compartment. I performed Wnt reporter assays transfected with *wnt1/LRP6* and wildtype *krm2*/*krm-ER* constructs, and either co-transfected *dkk1* DNA, or added Dkk1 protein as conditioned media. Importantly, transfected *dkk1* is translated and traverses the ER to be finally secreted, whereas added Dkk1 protein is present only extracellularly. Thus, added Dkk1 protein can only cooperate with cell surface-localized Krm2 in Wnt inhibition.

Expectedly, wildtype Krm2 cooperates at a comparable level with co-transfected *dkk1* and Dkk1 conditioned media in Wnt inhibition (Fig. 38). Krm2-ER constructs also cooperate with co-transfected *dkk1* to various degrees, indicating that they are still functional despite altered subcellular localization (Fig. 38). However, no cooperation occurs between ER-localized Krm2 and Dkk1 conditioned media, indicating that Krm2-ER is not present at the cell surface (Fig. 38).

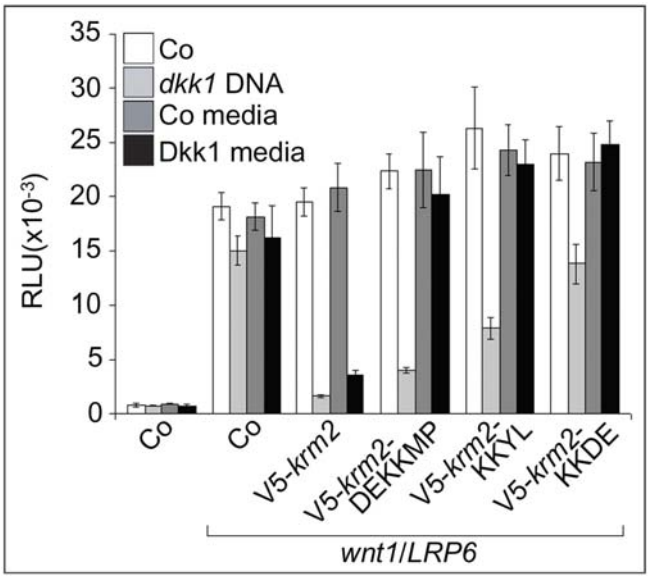

Figure 38. Functional cooperation of Krm2-ER with Dkk1. TOPFLASH luciferase reporter assay in HEK293T cells. RLU, relative light units. Co, empty pCS2 vector. Note that Dkk1 was either co-transfected as DNA or added as protein contained in conditioned media.

I next asked whether ER-localized Krm2 promotes LRP6 maturation similarly to wildtype Krm2 and Mesd. To this end, I co-transfected HEK293T cells with flag-*LRP6* and *krm2-ER* constructs and analyzed protein lysates by SDS-PAGE and Western blotting.

Whereas Mesd and wildtype Krm2 induce an increase of the upper (cell surface) band of LRP6 at expense of the lower (intracellular) band (Fig. 39, lanes 2 and 4), Krm2-ER constructs hardly affect LRP6 localization (Fig. 39, lanes 5-7) in comparison to controls (Fig. 39, lanes 1 and 3). This suggests that Krm2 exerts its effect on LRP6 maturation in a subcellular compartment other than the ER.

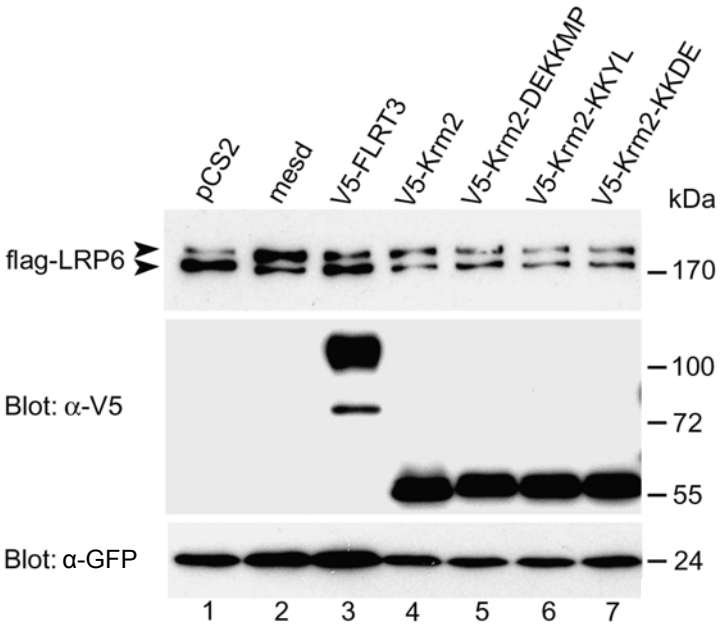

Figure 39. Krm2-ER has little effect on LRP6 maturation. Western blot analysis of HEK293T cells transfected with *flag-LRP6* and the indicated constructs. Negative controls are pCS2 vector and *Xenopus* FLRT3. Middle panel: Co-transfected V5-tagged constructs are expressed at a similar level. Bottom panel: Co-transfected GFP serves as further control.

5. DISCUSSION

This thesis work started out with the mechanistic analysis of Krm-mediated Wnt inhibition, which led to the identification of Erlectin, a novel N-glycan binding protein. Surprisingly, though, during the course of the study a novel role of Krm2 protein in *Xenopus* neural crest formation emerged.

Mechanistic analysis of Krm-mediated Wnt inhibition. To identify and characterize Krm interaction partners, I followed three different approaches: i) An *in vivo* injection screen for functional interaction partners of Krm2 in *Xenopus*; ii) an *in vitro* screen for modifiers of Krm2/LRP6/Wnt3a protein expression (screen done by G.D. [154]); iii) screenings for binding partners of Krms, including bacterial and yeast 2-hybrid screens, and proteomic pull-down (pull-down done by C.C. [263]). Whereas the injection screen did not reveal any candidate interaction partner of Krm2, the modification screen led to the identification of various potential Krm2 and LRP6 modifying factors. These were further analyzed *in vivo*, but did not include a factor specifically involved in Wnt regulation in *Xenopus* (discussed below). Screenings for Krm binding partners resulted in identification of two novel Krm binding proteins, TAX1BP and Erlectin. Both did not cooperate with Krm in Wnt inhibition in *Xenopus* embryos. However, a comprehensive analysis of Erlectin function led to significant novel insights, the implications of which will be discussed below.

Role of Krm proteins during development. The second main focus of my thesis was the characterization of the role of Krm2 during NC development. Using combined *in vivo* and *in vitro* approaches, I established that 1) in *Xenopus*, *krm2* expression is positively regulated by zygotic Wnt signaling; 2) in *Xenopus,* Krm2 is required for NC formation, which is a Wnt-dependent process; and 3) in cultured cells, Krms promote LRP6-mediated Wnt signaling as well as cell surface localization of LRP6. The implications of these findings will be discussed below.

Screenings - advantages, disadvantages and conclusions

The **injection screen** was characterized by the use of *Xenopus* embryos as *in vivo* system to identify novel interaction partners of Krm2. Such an approach is very promising to reveal biologically relevant, and functionally diverse (i.e., not limited to binding) interaction partners of baits; however, it is highly time-consuming, rendering a large-scale application difficult. In contrast, ***in vitro* screens** based on cultured cells are generally faster and more easily feasible. However, a major drawback of *in vitro* screens is that identified candidates may be not of physiological relevance, which means that the candidate's function, or interaction with the bait, is not required when assessed in the context of an organism (*in vivo*). Thus, further analysis of *in vitro* identified candidates using *in vivo* systems is crucial for the evaluation of their biological significance.

In his **modification screen**, G.D. used protein expression of the baits Krm2, LRP6 and Wnt3a as readout to identify novel and specific Wnt regulators at the level of receptor/ligand biogenesis. Of note, the kinase CK1γ was identified in the modification screen, and successfully characterized as specific Wnt regulator by G.D. et. al. [154]. However, my further analysis of the remaining 28 single clones did not lead to the identification of another specific Wnt regulator. Here, I want to discuss two circumstances which in my opinion contributed to this outcome.

Foremost, I would like to state that the idea of the modification screen was novel and pioneering, and the screening protocol unprecedented in its design. Further, similar screens may include some minor improvements as suggested below.

The identified candidates include numerous general cell components of transcription, translation, protein transport and degradation, which may be explained by the fact that protein expression is a very general screening readout. General cell components affect a broad range of target proteins, and likely are not specifically involved in bait modification. To optimize the screen output, it is therefore crucial to distinguish between general cell components and specific bait modifiers. Selectivity already at the level of the screen could be achieved by co-transfecting control proteins, which ideally closely mimic the bait of interest concerning structure and subcellular localization, but must remain unaffected by candidate clones. By co-transfecting three baits within the same sample in the modification

screen, this was done to some degree; however, the transmembrane proteins LRP6 and Krm2 are functionally linked and can form a complex [211], thus not being independent controls for each other. Furthermore, unlike LRP6, Krm2 does not show a clear distinction of cell surface (upper band) and intracellular form (lower band) in Western blot analysis, which impedes a direct comparison. Last, LRP6 and Krm2 are suboptimal controls for the secreted Wnt3a, and vice versa, due to distinct subcellular localization. Therefore, a possible improvement includes the incorporation of independent control proteins into the screen; this may facilitate the selection of bait-specific modifiers.

Taking a closer look at the screen results (Table 1), the distribution of identified single clones within original pools is noticeable: Of the 28 single clones, six were not identified from independent pools, but from pools already containing another identified clone (Table 1, same pool number). In other words, 4 pools contained 2, and 1 pool contained even 3 of the identified single clones. This is unlikely due to chance, as in total >1000 pools were screened, and only 28 single clones remained for analysis. One possible explanation is that additional, initially hidden single clones were found during sib selection of a given pool, when pool size decreased and single clones became more concentrated. Alternatively, it is possible that the initial pool effect was due to an accumulation of effects from several active single clones. In both scenarios, however, a single active clone is not concentrated enough in the initial pool to be detected. Of note, the specific bait modifier CK1γ is an enzyme, affecting baits in a catalytic manner (>>1:1 stochiometry). Other specific modifiers may act non-catalytically (approx. 1:1 stochiometry) and thus have a rather weak effect on bait expression; this is likely true for the chaperone Mesd, which was not found in the screen. Again, weak modification activity may be too diluted in the initial pool, therefore being undetectable. To minimize such intrinsic bias towards identification of highly active modifiers, a reduction of clone number per pool may be suggested; this eventually facilitates identification of less penetrant modifiers.

Of final note, several identified clones comprise novel genes of unknown function; my gain- and loss-of-function analysis may provide first insight into their developmental role, and ideally spark further analysis.

The **proteomic pull-down** performed by C.C. led to the identification of the novel Krm binding protein Erlectin. Although the binding of Erlectin to Krm *per se* was well

established by C.C., we could neither show a functional interaction of these two proteins in Wnt inhibition *in vitro* (reporter gene assays performed by C.C.; not shown), nor *in vivo* (see Results, p. 46). Rather, our study of Erlectin enlightened its role as a general ER component involved in N-glycan recognition.

Characterization of the Krm2 binding protein Erlectin

In eukaryotic cells, the ER is the entry site for proteins destined for the secretory pathway, and the site where folding, disulfide bond formation, N- and O- glycosylation, oligomerisation and quality control of newly synthesized proteins occur [279, 306-309].

MRH domain proteins are a small family of N-glycan recognizing proteins, which have been shown to reside in the ER or Golgi apparatus, respectively. Glucosidase II beta subunit (PRKCSH) functions in glycan processing in the ER, while yeast OS-9 functions in ER-associated degradation of misfolded proteins [269-272, 275-279]. GNPTAG is the non-catalytic gamma subunit of GlcNAc-1-phosphotransferase, which is involved in the synthesis of Mannose-6-phosphate on lysosomal hydrolases and localizes to the Golgi apparatus [274]. Erlectin is the fourth and novel member of the MRH domain family, and the results presented in this study indicate that it also functions in the ER. It is member of the ER synexpression group, which strongly predicts an ER function, and it localizes to the ER lumen in transfected cells. The fact that it lacks a canonical KDEL or HDEL retention signal raises the possibility that Erlectin is part of a protein complex retained in the ER. Since binding of Erlectin is abolished by N-glycosidase F treatment of Krm2 this strongly suggests, that like other MRH domain proteins, Erlectin recognizes N-glycans.

Erlectin contains two MRH domains that do not appear equivalent in substrate binding abilities. MRH domain 1 is dispensable for binding to Krm2 and it remains an open question if it is inactive in N-glycan recognition or if it has other specificities. Interestingly, a point mutation in the MRH domain 2, which mimics a homologous mutation in GNPTAG linked to mucolipidosis type III [273], abolishes binding of Erlectin to Krm2, indicating that this is a functionally conserved amino acid.

Co-transfection with Erlectin can specifically inhibit transport of Krm2 to the cell surface and induce its intracellular accumulation (experiment performed by C.C.; not shown; [263]). This is likely due to binding and trapping of Krm2 by ER-localized Erlectin. However, the physiological effect of this interaction is unclear. Since Krm2 in cooperation with Dkk1 is a negative regulator of Wnt signaling, one would predict that Erlectin derepresses Wnt signaling. However, in Wnt reporter assays *erlectin* co-transfection with *krm2* is mildly inhibitory on Wnt signaling (not shown), suggesting that Erlectin overexpression may have other effects as well. On the other hand, knock down of Erlectin in *Xenopus* embryos results in disturbed axial development and head defects, which are generally associated with enhanced Wnt signaling. Phenotypically these embryos do resemble embryos depleted of Krm1/2. However, early a-p markers are unaffected, in contrast to Krm1/2 depleted embryos, in which reduction of the forebrain marker *bf1* is observed [220]. Moreover, I could not rescue the Erlectin MO injected embryos with *krm2* mRNA or other Wnt inhibitors like *dkk1*, *dnWnt8* mRNA or β-catenin MO, providing further evidence that this phenotype is not due to excessive Wnt signaling. Thus, Erlectin is not required for Wnt mediated early a-p patterning. Yet, the severe phenotypic defects observed after depletion of Erlectin indicate an essential, pleiotropic function of this gene, since multiple tissues, including brain, notochord and heart are affected. Maternal Erlectin, which would be unaffected by MO injection, may account for normal early development.

What may be the physiological role of Erlectin? Since Erlectin is member of the ER synexpression group a specific role in any one given developmental pathway seems unlikely and this rather points to a more general involvement of the protein in ER mediated processes. Similar to Glucosidase II beta subunit, Erlectin may be part of an enzyme complex involved in recognizing and/or processing N-glycans. This would be supported by its lack of an ER retention signal as well as of any other functional protein domain. Erlectin was suggested as a possible functional homolog to Yos9p [269], an MRH protein playing a role in ER-associated degradation [269-272]. It is therefore an interesting possibility that the phenotype of Erlectin depletion in *Xenopus* embryos reflects disturbed protein degradation. Of note, two other MRH domain proteins, Glucosidase II beta subunit and GNPTAG cause human disease when mutated [274, 276], and my loss of function analysis suggests that Erlectin too, may be essential in humans as it is in frogs.

The role of Krm2 in *Xenopus* neural crest formation

The expression pattern of *krm2* in early *Xenopus* embryos is highly dynamic

Krms have been shown to be co-expressed with *dkk1* in the prechordal plate (PC) of neurula stage embryos, and to functionally cooperate with Dkk1 in a-p patterning. Interestingly, during gastrula and neurula stages *krm2* is as well expressed in regions devoid of Dkk1 transcript; these include ventro-lateral mesoderm and lateral neural folds, respectively [220]. In the light of the results presented in this study, an intriguing dynamics of *krm2* expression is emerging.

A novel finding described here is that *krm2* is co-expressed with zygotic *Wnts*, and that its expression is positively regulated by Wnt/β-catenin signaling and abolished upon Wnt inhibition (Fig. 27). Since at neurula stages *krm2* is expressed in the PC [220], which is characterized by very low Wnt signaling activity [34, 61, 310], this suggests a fundamental switch in the regulation of *krm2* expression with regard to Wnt responsiveness. Further analysis may reveal which specific transcription factors of the organizer are involved in the activation of *krm2* expression in the PC. Furthermore, it will be of interest to in-depth analyze the onset of *krm2* expression in the PC. So far, *krm2* expression in the PC was only shown from early neurula stage (stage 14) onwards [220]. Since Dkk1 and Krms cooperate in CNS patterning, but neuroectodermal cells lose competence to induce anterior CNS in response to Dkk1 at stage 13 [202], this would predict that *krm2* is expressed in dorsal mesoderm at earlier stages, albeit maybe at low levels.

Of note, neither *krm1* nor *2* are expressed in anterior neuroectoderm, although they regulate its a-p patterning [220]. Since Krms are transmembrane proteins and act cell-autonomously during Dkk1-mediated Wnt inhibition, this strongly suggests that Krms are required for maintenance of the PC, as shown similarly for Dkk1 [202]. This hypothesis deserves further testing.

During neurula stages, *krm2* is differentially expressed in the lateral neural plate [220]. In collaboration with R. Mayor and his lab, we show here that this expression domain of *krm2*

comprises the prospective NC region. This is consistent with the finding that Krm2 is required for NC formation.

Krm2 is required and sufficient for NC formation

An important finding of this study is that Krm2 is required for NC induction in *Xenopus*. What may be the function of Krm2 during this process? Since Krm2 is both regulated by Wnts and promotes LRP6 activity in cultured cells (discussed below), this suggests that in the context of NC induction Krm2 functions by promoting Wnt signaling. Consistent with this, depletion of LRP6 inhibits NC induction similar to Krm2 knock-down; this is, however, merely correlative evidence. A complete picture requires further experiments to determine the direct effect of Krm2 loss-of-function on Wnt/LRP6 signaling in the NC region. Of note, Krm1 and 2 null mutant mice do not show NC defects, indicating that the requirement of Krm2 for NC induction is likely not evolutionary conserved among anamniotes and mammals (unpublished data kindly provided by Kristina Ellwanger).

Concerning the LRP6 Morpholino, I made two interesting observations: i) LRP6 knock-down can completely block NC marker expression (Fig. 31C), indicating that LRP6 acts non-redundantly from LRP5 in NC formation in *Xenopus*. ii) Mild LRP6 knock-down has a highly specific inhibitory effect on development of the dorsal fin, a NC derivative, but does not (or very marginally; this has to be determined yet) affect NC marker expression and development of other NC derivatives, such as melanocytes (Fig. 31D). This raises the possibitity that different NC derivatives may show differential sensitivity to Wnt level perturbation during NC induction. Alternatively, this observation allows the speculation that the fin defect of LRP6 MO injected embryos may be caused by perturbation of a process subsequent to NC induction. Intriguingly, knock-down of Wnt11-R, a gene involved in migration of fin precursors, leads to fin defects reminiscent of LRP6 knock-down [311].

The finding that anteriorly overexpressed Krm2 inhibits, while posterior overexpression enhances NC formation suggests a dual Krm2 action. Anteriorly overexpressed Krm2 likely cooperates with Dkk1 in Wnt inhibition, while in posterior regions Krm2 on its own promotes Wnt signaling. This dual activity is also supported by my reporter assays in cultured cells.

Currently, I cannot exclude the possibility that Krm2 may act also on other pathways which are involved in NC formation, e.g. BMP signaling. However, in cell culture reporter assays BMP signaling is unaffected by Krms.

Interestingly, based on EST (expressed sequence tag) expression data *krm2* is significantly upregulated in several human cancers, e.g. brain, testis, kidney and gastrointestinal tract tumors [312]. Since Krm2 is a Wnt target (this study), this raises the possibility that it may be a tumor associated gene or may even have an oncogenic role.

Krms promote LRP6 mediated Wnt signaling

Another surprising finding of this study is that Krms not only act as negative, but also as positive Wnt regulators in cultured cells. In reporter gene assays, they specifically promote LRP6-mediated Wnt signaling in the absence of Dkk1; accordingly, Krm2 co-transfection promotes cell surface localization of LRP6. This is reminiscent of the LRP6 chaperone Mesd, which promotes LRP6 folding and cell surface localization ([172, 173]; this study). Since cell surface levels of LRP6 are rate limiting for Wnt signal transduction [156, 172, 173], enhanced surface localization by either Mesd or Krms translates into more Wnt signaling.

Do Krms then act as chaperones of LRP6? Three lines of evidence argue against this: i) Unlike Mesd, Krms are not ER-resident [172, 173, 263]; ii) Krms can, albeit weakly, promote Wnt signaling induced by LRP6ΔE1-4 (Fig. 32A), a construct lacking all four ß-propeller/EGF regions, which are the target of Mesd [180]. LRP6ΔE1-4, in contrast to full length LRP6, is predominantly cell surface-localized (Fig. 32A and [156]), indicating that this construct does not require support in trafficking; iii) artificially ER-trapped Krm2 has a strongly reduced effect on LRP6 surface localization compared to wild type Krm2, indicating that a subcellular localization other than in the ER is required for Krm to exert its full effect on LRP6 (Fig. 39).

As a sideline, the analysis of ER-trapped Krm2 led to the interesting observation that co-transfection of Dkk1 and ER-localized Krm2 (foremost DEKKMP) can inhibit Wnt signaling, which, besides confirming functionality of ER-trapped Krm2 constructs, also indicates that transfected Wnt signaling components already signal within the ER (before reaching the cell surface) (Fig. 38).

What then could be the mechanism of action of Krms? Krms may enhance cell surface localization by binding to LRP6 and attenuating endocytosis. This would be the reverse of their action in presence of Dkk1, which induces rapid LRP6 internalization [211]. Krms may therefore be context-dependent endocytosis regulators of LRP6. Indeed, a hallmark of LDLR family members is their regulated endocytosis [177, 178, 313].

A model of Krm2 function during NC induction

Integrating both *in vivo* and *in vitro* data, currently the following model of the role of Krm2 in *Xenopus* NC induction can be suggested (Fig. 40): Wnt signaling is activated in the prospective NC region, probably by Wnt8 secreted from the paraxial mesoderm [88, 100], and induces transcription of several target genes, including *krm2*. Krm2 may positively regulate protein expression of LRP6, probably by attenuating endocytosis and elevating surface levels of LRP6, which in turn facilitates Wnt signaling. Thus, in this scenario Krm2 acts as positive feedback activator of Wnt signaling. Since Krm2 is predicted to act at the level of inductive signals in the NC induction cascade (Fig. 6), this explains why the *krm2* expression domain is broader than the prospective NC region as determined by *slug* staining (Fig. 26B). It remains an open question why Krm2 may be required for Wnt signaling particularly in the NC region; possibly, Krm2 compensates for absence of another LRP6 stabilizing factor or antagonizes a NC-specific negative regulator of LRP6 stability.

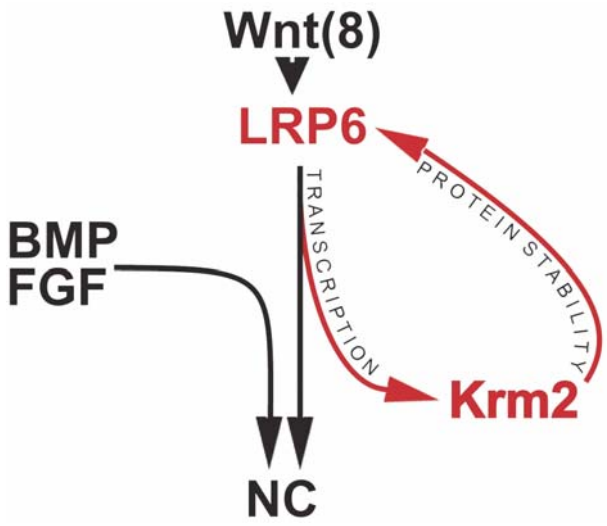

Figure 40. Model of the role of Krm2 during NC induction. Wnt signaling induces *krm2* transcription. Krm2 protein may then positively feed back on Wnt signaling by promoting stability of LRP6 protein.

6. MATERIALS AND METHODS

Equipment and Materials

Equipment

Stereomicroscopes (Nikon, Leica), microinjectors and micromanipulators (Inject+Matic, Harvard Medical Systems), gastromaster (Xenotek Engineering), needle puller (Sutter Instruments), glass vials (NeoLab), calibration glass (Gera GmbH), surgical knives (M.S.P. Medical Sterile Products, CAT 7503), rotators (IDL GMBH+CO.KG), homogenisers (embryos: Kontes; cells: B. Braun Melsungen, Wheaton), PCR thermocyclers, heating blocks, centrifuges and microcentrifuges, fluorescent microscop (Nikon), digital cameras (Sony, Visitron Systems), spectrophotometer, luminometer (Luminoscan Ascent, Labsystems), power supplies, gel UV photodocumentation system, electroporator (BioRad), waterbaths, balances, photolaboratory (Agfa), micropipettes, multi-channel pipettes, vortexes, agarose gel and PAGE minigel chambers, microwave oven, shakers.

Chemicals

Acrylamide, ammonium persulfate, ampicilline, agarose, acetic acid, acetic anhydride, anti-digoxigenin-AP (Fab fragment), Bouin's fixative (ACCUSTAIN, Sigma-Aldrich), BSA, Boehringer Block, biotin, $CaCl_2$, chloroform, chloramphenicol, CHAPS, cysteine, dNTPs, DTT, diethylpyrocarbonate (DEPC), digoxigenin (DIG) RNA labelling mix, EDTA, EGTA, ethanol, ethidium bromide, Fugene, freon, ficoll, formamid, formaldehyde, glycogen, goat serum, glycerol, HCl, hydrogen peroxide, HEPES, heparin, isopropanol, KCl, LB agar, LiCl, maleic acid, $MgSO_4$, methanol, MOPS (3-(N-Morpholino)Propansulfonsäure), NaOH, NaCl, Na_2HPO_4, NaH_2PO_4, NaOAc, 8-oxychinoline, paraffin, phenol, paraformaldehyde (PFA), proteinase K, PMSF, RNA cap structure analog, RNA guard, sodium citrate, SDS, trypsin, Tween-20, Triton X-100, Trizol, Tris base, TEMED, triethanolamine. Suppliers: Biochrom AG, Bio-Rad, BioZym, Boehringer Mannheim, Eppendorf, Falcon, Fluka, Fuji, Gibco, Kodak, Nunc, Merck, Roche, Roth, Sarstedt, Serva, Sigma, Whatman and others.

Emzymes

DNaseI, Super Script II RNase H$^-$ Reverse transcriptase, Polynucleotide kinase (PNK), Proteinase K, various restriction enzymes, Shrimp alkaline phosphatase, T4 DNA ligase, T4 DNA polymerase, Taq DNA polymerase, Endoglycosidase H. Suppliers: New England Biolabs, Gibco, Promega, Fermentas and Roche.

Antibodies

	ANTIBODY	DILUTION	SOURCE
PRIMARY	anti-Calnexin, mouse	1:5000	BD Biosciences Pharmingen
	anti-α-Tubulin, mouse	1:10000	Sigma, cl. B512
	anti-V5, mouse	1:5000	Invitrogen
	anti-flag, mouse	1:2000	Sigma
	anti-myc, mouse	1:2000	M. Eilers lab
	anti-HA, rat	1:10000	Roche
	anti-GFP, mouse	1: 5000	Dianova
2nd ARY	Streptavidin-HRP	1:15000	Pierce
	Anti-mouse HRP	1:10000	Dianova
	Anti-rat HRP	1:10000	Chemicon
	Anti-mouse TrueBlot	1:2000	eBioscience

Kits

QIAprep spin mini-prep kit, QIAex gel extraction kit, QIAquick PCR purification kit (all Qiagen); Expand High Fidelity PCR system (Roche); T3, T7, SP6 MEGAscript *in vitro* transcription kits (Ambion); TOPO TA cloning kit (Invitrogen); pGEM-T-Easy cloning kit (Promega), Dual-Luciferase Reporter Assay System (Promega).

Buffers and solutions

- Barth solution (10x): 880 mM NaCl, 10 mM KCl, 24 mM $NaHCO_3$, 8.2 mM $MgSO_4 \cdot 7H_2O$, 3.3 mM $Ca(NO_3)_2 \cdot 4H_2O$, 4.1 mM $CaCl_2 \cdot 2H_2O$, 100 mM HEPES, pH 7.6
- Bleaching solution for embryos: 1% H_2O_2, 5% formamide, 0.5x SSC
- DEPC-H_2O: 0.01% (v/v) DEPC/ddH_2O, mixed for 2 hours at room temperature (RT) and autoclaved
- DNase buffer (10x): 50 mM $MgCl_2$, 10 mM DTT, 200 mM Tris-HCl, pH 7.2
- DNase mix: 100 mM Tris-HCl, pH 7.2, 25 mM $MgCl_2$, 5 mM DTT, 5 U DNase I, 10 U RNA guard (MBI)
- DNase stop mix: 5 mM EDTA, 100 mM Tris-HCl, pH 8.3
- dNTP mix: 2 or 5 mM dATP, dCTP, dGTP, dTTP, stored at -20°C

- Ethanol/NaAc mix: 100 mM sodium acetate in absolute ethanol
- Eosin stock solution: 2.5 g Eosin G (Roth) in 250 ml ddH_2O
- Eosin staining solution: 30 ml Eosin stock solution, 270 ml 70% ethanol, 3 ml acetic acid (100%)
- Gurdon's injection buffer (G+E): 88 mM NaCl, 1 mM KCl, 0.01 mM EDTA, 15 mM Tris-HCl, ph 7.5; ev. DEPC treated, autoclaved, stored at -20°C
- HANKS's buffer: Prepared separately: **Hanks salts x10 (g/l)**: 1.85 $CaCl_2 \bullet 2H_2O$*, 4 KCl, 0.6 KH_2PO_4, 1 $MgCl_2 \bullet 6H_2O$*, 1 $MgSO_4 \bullet 7H_2O$*, 80 NaCl, 0.6 $Na_2HPO_4 \bullet 2H_2O$; **$NaHCO_3$ x10:** 3.5 g/l; *mixed and dissolved separately; sterile filtered both solutions, stored at 4°C, mixed before use
- Hybridization buffer for *in situ*: 5x SSC, 50% (v/v) deionized formamide, 1% (w/v) Boehringer Block: dissolved 1h at 65°C; 1 mg/ml yeast tRNA, 0.1 mg/ml heparin, 0.1% (v/v) Tween-20, 0.1% (w/v) CHAPS, 5 mM EDTA, filtered, stored at -20°C
- Hypotonic buffer: 1 mM EDTA, 5 mM HEPES, pH 7.5, 0.1 mM PMSF, one protease inhibitor cocktail tablet/ 25 ml (Roche)
- Hypotonic ER isolation buffer: 10 mM HEPES pH 7.6, 25 mM potassium chloride, 1 mM EGTA (can be prepared as 10x stock and stored at 4 degrees)
- Isotonic ER isolation buffer: 10 mM HEPES pH 7.6, 250 mM sucrose, 25mM potassium chloride, 1mM EGTA (can be prepared as 10x stock, and stored at 4 degrees)
- Laemmli loading buffer (4x): 200 mM Tris-HCl, pH 6.8, 400 mM DTT, 8% SDS, 0.4% bromophenol blue, 40% glucerol
- LB Broth (1 liter): 10 g NaCl, 10 g bactotryptone, 5 g yeast extract, 20 g agar, pH 7.0, autoclaved
- Maleic Acid Buffer (MAB): 100 mM maleic acid, 150 mM NaCl, pH 7.5, autoclaved (can be prepared as 10x stock and stored at -20°C)
- MEMFA fixative: 3.7% formaldehyde, 2 mM EGTA, 1 mM $MgSO_4$, 0.1 M MOPS, ph 7.4 (not autoclaved!)
- Modified Ringer solution (MR): 0.1 M NaCl, 1.8 mM KCl, 2.0 mM $CaCl_2$, 5.0 mM HEPES-NaOH, pH 7.6, 1.0 mM $MgCl_2$
- Murray's clearing medium: 2:1 (v/v) benzyl benzoate:benzyl alcohol
- NP-40 buffer: 150 mM NaCl, 50 mM Tris pH 7.4, 7.5% glycerol, 1 mM EDTA, 1 mM ß-mercaptoethanol (or DTT), 25 mM NaF, one protease inhibitor cocktail tablet/ 25 ml (Roche), 0.8-2% NP-40

- Phenol/Chloroform: 50% (v/v) phenol, saturated with 10 mM Tris-HCL, pH 7.8, 48% (v/v) chloroform, 2% (v/v) isoamyl alcohol, stored at 4°C
- Phosphate-buffered saline (10x PBS): 1.36 M NaCl, 26.8 mM KCl, 14.7 mM KH_2PO_4, 162.9 mM Na_2HPO_4, autoclaved, stored at RT
- PTW: 1x PBS + 0.1% (v/v) Tween-20
- Proteinase K mix: 75 µl proteinase K stock (2 mg/ml in H_2O, this solution can be stored aliquotted at -80°C), before use add 30 µl EDTA (0.5 M) and 45 µl TE buffer
- Ringer's solution (10x): 1.16 M NaCl, 29 mM KCl, 18 mM $CaCl_2$, 50 mM HEPES, pH 7.2, stored at 4°C
- SSC (20x): 3 M NaCl, 0.3 M sodium citrate, pH 7.5, filtered, autoclaved
- Stain buffer (lacZ staining): Wash buffer + 30 mM $K_3Fe(CN)_6$, 30 mM $K_4Fe(CN)_6 \cdot 3H_2O$
- TBS (20x): 3 M NaCl, 5.36 mM KCl, 1 M Tris-HCl, pH 7.4, autoclaved
- TE buffer: 1 mM EDTA, 10 mM Tris-HCl, pH 7.5, autoclaved
- Wash buffer (lacZ staining): PBS, pH 7.4 + 0.01 % (v/v) sodium deoxycholate, 0.02% (v/v) NP-40, 2 mM $MgCl_2$

General molecular biology methods

General molecular biology methods such as preparation of electrocompetent XL1-blue *E. coli* cells, transformation, plasmid preparation, photometric quantification of DNA and RNA samples, restriction digests, dephosphorylation and ligation of DNA, agarose and SDS-PAGE gel electrophoresis and PCR were carried out essentially as described [314]. DNA isolation from bacteria, agarose gels and PCR reactions were done with kits from Qiagen; DNA oligonucleotides for PCR and sequencing were synthesized by Qiagen Operon. DNA samples were sequenced by SEQLAB Sequence Laboratories Göttingen GmbH.

Cloning

Cloning was performed using the Expand High Fidelity PCR system (Roche) according to the manufacturer's instructions. Expression constructs were restriction digested and cloned into the vector pCS2. *In situ* probes were directly cloned into TOPO or pGEM-T vectors using the respective cloning kits. All constructs were sequenced.

Mutagenesis

Site-directed mutagenesis (point mutations) was performed by including the desired mutation into a primer, and amplifying of the whole vector plus insert. Deletions were constructed by using PCR primers that amplify the whole vector plus insert excluding the region to be deleted. The following protocol was used:

- PCR: Elongation time: approx. 1 min per 1000 bp; cycle number: either very low (16-18) with high amount of template (1 µg for 50 µl mix) or high (28) with low amount of template (200 ng). Note: Expand High Fidelity PCR system produces an A/T overhang; alternatively, Pfu polymerase does not produce an overhang.
- After gel purification of band, elution in 50 µl elution buffer, then digest with DpnI overnight. This enzyme cuts only methylated DNA, so all template is removed.
- PCR products containing A/T overhang were blunted with T4 DNA polymerase (otherwise frameshift): 1/10 vol. 2 mM dNTPs, 1-2 µl T4 DNA polymerase, 14°C for 15 min. Samples were kept on ice, and heat inactivation of was done at 75°C for 10 min (very important)
- Purification with PCR elution kit; elution in 30 µl elution buffer
- Phosphorylation of DNA ends: 8 µl eluted DNA, 1 µl ligation buffer (same as for DNA ligase, contains ATP), 0.5 µl PNK, 37°C for 30 min
- Addition of 1 µl DNA ligase, ligation at RT for 1-2 hours, then transformation of bacteria (plated up to 200-300 µl)
- Usually, picking 5 colonies was enough. All deletion constructs were restriction digested and analyzed on agarose gels (compared size with wildtype), then sequenced. Note: Point mutations can be detected if new restriction site arises.

cDNA libraries

The following cDNA libraries were used:

- *X. laevis* eye library (constructed by Andrei Glinka). cDNA prepared from adult *X. laevis* eyes was cloned into the pCS2-SfiI vector using EcoRI/NotI restriction sites. Host: XL1-blue (Amp^R). Total independent clones: 1 x 10^6; average insert size: 1.6 kb. Pools à 200 clones were prepared and injected as mRNA. For sib selection of a single active clone, several successive steps involving plating and pooling of bacteria, preparation of mRNA and injection (of as many subpools as necessary until re-detection of activity) were performed.

- *X. tropicalis* embryonic library (constructed by W.W.). Normalized cDNA [315] was prepared from stage 10, 20 and 30 *X. tropicalis* embryos and cloned into the pRKW2 vector (modified from pRK5) using XhoI/BamHI restriction sites. Host: DH10B (Amp^R). Total independent clones: 2 x 10^6; average insert size: 1.5 kb. 10^6 primary transformants were arrayed in 261 384-well plates (RZPD Berlin); each 384-well plate was grouped into 4 x 96 clones (4 96-well plates); each 96-well plate comprises a pool (96 single clones). Total number of pools: 1044 (11 96-well plates).

Constructs

The following plasmids were obtained from external sources and subcloned into the pCS2 vector. Abbreviations: *X* or *X.l.*, *X. laevis*; *X.t.*, *X. tropicalis*; m, mouse; h, human; ID, sequence identity in public database; RZPD, Deutsches Ressourcenzentrum fuer Genomforschung GmbH; the upper and lower sequences comprise the forward and reverse primer, respectively; both are in 5' – 3' orientation. '-' indicates that the primer sequence is continued in the next line.

Obtained plasmids

GENE NAME	ID	SOURCE	VECTOR
h*TAX1BP1*	BC024600; AL136586	RZPD	pSPORT1
h*erlectin*	NM_015701	RZPD	pCMV-SPORT6
X.t. erlectin	MGC69308	RZPD	pCMV-SPORT6
X.l. erlectin	AAH74469	RZPD	pCMV-SPORT6
X.l. erlectin	CB558691	RZPD	pCMV-SPORT6
m*erlectin*	BC018468	RZPD	pCMV-SPORT6
X.l. sox10	XL053o11	NIBB	pBS SK^-
h*ARF4*	BC022866	RZPD	pDNR-LIB
X.l. slug (0.8 kb)		H. Steinbeisser	SP72

Cloned constructs

CONSTRUCT	PRIMERS	TEMPLATE
pCS2-h*TAX1BP1*	GTCTTTCCACTGGATCCACAATG GCACTCGAGCTCTATGGTCTCCTC	h*TAX1BP1* AL136586
pCS2-*erlectin* (*X.t.*)	ACGGATCCGCCGCCACCATGCGCAGAAGTGACCG- CTTACG GTTCTAGACGTCAGTTGGGAATTGAAAGG	*X.t. erlectin* MGC69308
pCS2-*erlectin*-HA (*X.t.*)	ACGGATCCGCCGCCACCATGCGCAGAAGTGACCG- CTTACG TGTCTAGACTCGAGGTTGGGAATTGAAAGGAGTC- CGTTC	*X.t. erlectin* MGC69308

pCS2-flag-h*erlectin* ΔD1	ATCGAAGGTCAGATGACACCATAC TTGTTTAAATAGTGGCTCCAAAAGC	pCS2-flag-h*erlectin*
pCS2-flag-h*erlectin* ΔD2	GATATTTGTGATATAACTGACAAAC ACCACTAAGAAACTCTTTTATGAG	pCS2-flag-h*erlectin*
pCS2-flag-h*erlectin* ΔD1/2	GATATTTGTGATATAACTGACAAAC ACCACTAAGAAACTCTTTTATGAG	pCS2-flag-h*erlectin* ΔD1
pCS2-flag-h*erlectin* G379S	AGCACATGGAACCAAGAAGAGC GACAACCACAGAGGTTTTCCCAC	pCS2-flag-h*erlectin*
pCS2-*ARF4* (*X.t.*)	AAGGATCCGCCGCCATGGGCCTCACCATCTCC GCTCTAGATTAGCGCTTGGAGAGTTCGTTTGAG	pRKW2-*ARF4* (*X.t.*)
pCS2-*T31N* (*X.t.*)	AATACTATTCTGTACAAATTAAAG CTTGCCGGCAGCATCCAAAC	pCS2-*ARF4* (*X.t.*)
pCS2-*Q71L* (*X.t.*)	CTAGATAAAATCCGCCCCCT GCCACCCACGTCCCACACAG	pCS2-*ARF4* (*X.t.*)
pCS2-*Xkrm1ΔC*	CCCAAGCTTGATTTAGGTGACAC GGGTCTAGACTATGCCGAAATAGCAATGATGGT	pCS2-*Xkrm1*
pCS2-h*LRP6ΔE1-4-GFP*	Constructed by restriction digest and ligation	pCS2-h*LRP6-GFP*
pCS2-V5-m*krm2-DEKKMP*	CCCAAGCTTGATTTAGGTGACAC GGGTCTAGATCAAGGCATTTTCTTTTCATCGAGAG-CAGAGACGAGCGAGCGCA	pCS2-V5-m*krm2*
pCS2-V5-m*krm2-KKDE*	CCCAAGCTTGATTTAGGTGACAC GGGTCTAGATCATTCATCCTTCTTGAGAGCAGAGA-CGAGCGAGCGCA	pCS2-V5-m*krm2*
pCS2-V5-m*krm2-KKYL*	CCCAAGCTTGATTTAGGTGACAC GGGTCTAGATCAGAGATATTTCTTGAGAGCAGAG-ACGAGCGAGCGCA	pCS2-V5-m*krm2*

Reverse transcriptase – polymerase chain reaction (RT-PCR)

For RT-PCR experiments, RNA was isolated and reverse-transcribed to yield cDNA, which was then normalized by PCR amplification of the housekeeping gene H4. Subsequently, cDNA species of genes of interest were amplified using specific primers. All RT-PCR assays were carried out in the exponential phase of amplification, and PCR samples were loaded on the same agarose gel to compare intensity.

RNA isolation

- Embryos or explants were collected at the proper developmental stage in 1.5 ml Eppendorf tubes (2 whole embryos, 10 DMZs and VMZs, or 20 animal caps)
- Buffer was pipetted off as much as possible, and 0.5 ml Trizol (Gibco) were added; samples were vortexed for 5-10 min at RT, and stored at -20°C
- After addition of 100 µl chloroform, samples were vortexed and spun at 4°C for 20 min with maximal speed
- Precipitation of upper phase with 300 µl isopropanol, mixed, -20°C for at least 30 min

- Samples were spun down at 4°C for 20 min (always visible pellet)
- Pellets were washed with 70% ethanol, kept at RT for 5-10 min
- Samples were spun, ethanol was poured off, pellets were dried briefly and dissolved in 24 µl DEPC-treated H_2O
- 6 µl DNase mix was added and samples were incubated at 37°C for 15 min
- 33 µl DNase stop mix (and 2 µl of 4 mg/ml glycogen if less than 4 animal caps) were added, samples were vortexed and extracted with 60 µl phenol-chloroform
- Precipitation of RNA with 3 volumes ethanol/NaAc mix at -20°C overnight
- Samples were spun at 4°C for 15 min with max. speed (always visible pellet)
- Pellets were washed in 70% ethanol at RT for 5-10 min, spun down, briefly dried at RT for 2-3 min
- Pellets were dissolved in DEPC-treated H_2O: 1 µl per animal cap, 40 µl per embryo
- RNA was denatured at 70°C for 2 min, chilled on ice-water mix, and stored at -20°C

Reverse transcription

10 µl mixes were prepared (always prepared a master mix for all samples):

2 µl	5 x RT buffer (Gibco)
2 µl	DEPC-H_2O
1 µl	random primer dN(6) (100 pmol/µl)
1 µl	dNTPs mix (5 mM each)
1 µl	DTT (0.1 M)
0.15 µl	RNA guard (RNA guard, MBI)
1 µl	BSA acetylated (1 mg/ml, Promega)
1 µl	Super Script II RNase H^- reverse transcriptase, or H_2O as -RT control

Then 1 µl denatured RNA was added, samples were mixed, spun briefly and incubated at 45°C for 1 hour and subsequently at 55°C for 30 min.

RT-PCR

For normalization with H4, samples giving the weakest bands were kept, and H_2O was added to those samples that gave stronger bands, until all samples showed the same amount of PCR product after proper amplification (for H4, 18-20, maximal 22 cycles). Always 1 µl of RT-reaction was used in the PCR system.

PCR mix:

18 µl H_2O
1 µl primer mix (12.5 pmol/µl each)
2.5 µl dNTPs mix (2 mM each)
2.5 µl 10 x PCR buffer (Perkin-Elmer)
1 µl RT reaction (cDNA sample)
0.3 µl Taq DNA polymerase (homemade)

The PCR program settings were:

95°C 1 min
55°C 1 min depending on primers
72°C 1 min
20-35 cycles depending on target
72°C 10 min
20°C 10 min

After PCR, 5 µl of 6x loading buffer was added, and 20 µl of the mix was loaded on a 2% agarose gel, separated at 6V/cm for 20-30 min and visualized with ethidium bromide/UV staining.

Primers used for RT-PCR

The upper and lower sequences comprise the forward and reverse primer, respectively; both are in 5' – 3' orientation.

GENE/PROTEIN NAME	**PRIMERS OR REFERENCE**
X. laevis Hatching enzyme	GCAGTGGCCAAAGAGGACATTC TCATCCCGGTCACTTCTGTTCTG
Simil. to Ubiquit. carboxyl-terminal hydrolase family2	TAACAGGGAGCGGTTGGCCTT CCAGCTTAGCCAGATACTAGGCCG
Embryonic serine protease-1 (Xesp-1)	GGCTTCTTTATGTGATGGGTC GCTGTCAGAATCCACTGGTCA
Embryonic serine protease-2 (Xesp-2)	TGAACCGCCTCCCTATACAA ATTGGGAAGACCGGACACAA
X. laevis nuclear orphan receptor XGCNF	GGGTTCTTCAAGCGCAGCATCT GCCGTAAGCAGCTGGTTAATGAGTG
Serine/threonine-protein kinase ANKRD3	AAAACTTGGCTGGCCATCAA TTCACATGGTAATGGCCATC
Receptor tyrosine kinase, c-mer like	TGCCAGGCTGTTTGTCTTTT ATGCCCCAGGTTCTGCCA

ADP-ribosylation factor 4, ARF-4	TGCTTTACTGTGTGGGACGTGG GATGTTACGAGCCTAGGCCGATTC
Glycosyl transferase	TTATCCTGTTCCAGATGGGTT TTGCTCTCTCCTCTGCTTTCA
Sialyltransferase	GGTAGTAGCACCAAGAAGAGGAGCG GCCTAATTTGTGTCCAACGGAGTC
Signal peptide peptidase-like 3, SPP-like 3	AAGACAAGGAGAAGGACAGCA CACAGCACCCAAAGGAAATT
Similar to DnaJ (Hsp40) homolog	GTGCCACAGAAGCTTTTAAA GGATATAAACTGTATGGTGGG
Embryonic 7-span transmembrane protein-like	ATCTGTGGCTCGTGCGTTTTA TTCCTTCCTCCGAGCCGTA
Similar to thioredoxin domain containing 4	TCTTCGTCCCTTACTTTTGCC CAGAATGTTGATCACAGTCCA
Weak simil. to putat. G-prot. coupled receptor, TRC8	GCTCAGACTGCTGGGTGTT ATGAGAACGAGGGCAGAAAT
Potential novel G-protein-coupled receptor	TGTGCATGGGAGCTTGGATA TGGGATATACCATTTGTGGG
Uncharacterised multi TM protein - hemolytic activity	TCTGCATGTTGTGTTCAGTGG ATCGAAGTTCCAACACCTCCA
Similar to presenilin stabilisation factor b, APH1	AACAAGAATGACGCCAACCT AAGTAATACTGCGAGTCGCCA
Unknown WD40 repeat containing protein	TGACTTTAGTCCAACTGGTGA TGAACGTATCATCCACAGGA
XH4	[316]
Xerlectin, allele1	TGAAGGAGAAGTTCTCCAGT GTTTGCACTTTAGTTTCACTATC
Xerlectin, allele2	TGAAAGAGAAGTTCTCCACC GTTTGCACTTTAATTTCACAACG
XBiP	CTGGGCACTTTTGACTTGACCGG GCATCCTGATGGCTTTCTAACCACTC
XHsp70	AGACAGCAGGAGGAGTAATG GCCTTGTACTTTTCTGCCTC
Xkeratin	CACCAGAACACAGAGTAC CAACCTTCCCATCAACCA
Xintegrin	CCGGAGACGGAAAATTAGGCG ACACTTCCTTCCGTCTTCCCC
Xkrm2	GGAACCAGACCACACAGCACTTG CCGCCTCCACACCTGCATACT
Xbra	CACAGTTCATAGCAGTGACCG TTCTGTGAGTGTACGGACTGG
Xhox3	[317]
Xchordin	[37]
XWnt8	[49]

Preparation of mRNA for embryo injections

mRNA for injections was prepared from linearized template using the MEGAscript *in vitro* transcription kits from Ambion. RNA cap structure analog was added to increase stability and translation efficiency of the mRNA. Since free cap analog is a potent translation inhibitor and toxic to cells, it must be removed carefully during RNA purification.

Linearization of DNA template

- Plasmids were linearized by restriction digest. If 3' protruding ends were generated, they were blunted by incubation with T4 DNA polymerase (in 0.2 mM dNTPs) at 16°C for 15 min
- 2 µl of glycogen (4 mg/ml) and 0.1 volumes of proteinase K mix were added, and the mixture was incubated at 45°C for 30 min
- After 2x phenol-chloroform extraction, the upper phase was precipitated with 3 volumes ethanol/NaAc mix at RT for 30 min
- Precipitate was pelleted at max. speed for 2 min, washed in 75% ethanol, dried and resuspended in DEPC-H_2O (10 µl for 1-2 µg of DNA)

RNA synthesis by *in vitro* transcription

20 µl mixes were prepared:

2.25 µl	RNAase-free dH_2O
2 µl	10x reaction buffer
2 µl	ATP solution (75 mM for T3 and T7, 50 mM for SP6)
2 µl	CTP solution (75 mM for T3 and T7, 50 mM for SP6)
2 µl	UTP solution (75 mM for T3 and T7, 50 mM for SP6)
0.4 µl	GTP solution (75 mM for T3 and T7, 50 mM for SP6)
1.6 µl	RNAase-free dH_2O
3.75 µl	RNA cap structure analog (40 mM)
2 µl	RNA polymerase (10x stock)
2 µl	DNA template

Samples were incubated at 37°C for 2 hours, and subsequently treated with 1 µl DNase I (RNase free, Roche) at 37°C for 15 min.

Purification of RNA transcript

- Ammonium acetate (final 0.5 M) was added to the samples and filled with RNAase-free H_2O to a total volume of 150 µl
- Samples were extracted two times with 150 µl phenol/chloroform by vortexing for at least 20 seconds; for a faster separation of the phases a short centrifugation step was performed

- RNA was precipitated by addition of 150 µl isopropanol; samples were kept at -20°C for at least 30 min
- Precipitates were pelleted by centrifugation at 4°C for 15 min with 15000 rpm
- The supernatant was removed with a pipette, and the pellets were washed once with 70% ethanol and dried briefly
- Dried pellets were dissolved in 20 µl G+E buffer, concentrations were quantified photometrically, and RNA quality was checked on an agarose gel

Preparation of DIG-labeled *in situ* probes

Digoxygenin (DIG)-labeled RNA for *in situ* hybridizations was prepared using the MEGAscript *in vitro* transcription kits (Ambion) and a DIG-labeled nucleotide mix (Roche) instead of dNTPs, according to the following protocol:

- Linearized DNA template was prepared as described for mRNA preparation
- 20 µl transcription mix:

2 µl	10x transcription buffer
2 µl	DIG-labeled nucleotide mix
2 µl	RNA polymerase
2 µl	DNA template

- Samples were incubated at 37°C for 2 hours
- Digestion with 1 µl DNase I at 37 °C for 30 min
- Volume was filled up to 80 µl with DEPC-H_2O
- Addition of 8 µl EDTA (0.5 M, pH 8) to stop DNase
- Addition of 10 µl 4 M LiCl and 250 µl absolute ethanol; samples were vortexed and put on -20°C over night
- Samples were spun at 4°C for 15 min at max. speed, washed with 75% ethanol, dried and resuspended in 20 µl dH_2O
- After measuring concentrations photometrically and checking the samples on agarose gel, they were denatured at 95°C for 3 min and added to hybridization buffer to a final stock of 20 ng/µl
- For final concentration of *in situ* probes: Dilution of this stock 1:100 (200 ng/ml)

Embryological methods

In vitro fertilization, embryo culture, staging and microinjection of *X. laevis* embryos were generally carried out as described [13, 14, 318, 319]. LiCl treatment was carried out as described in [318].

Priming, fertilization and microinjection

For priming, *X. laevis* females were injected with 600 U of human chorionic gonadotropin (Sigma). The next day, eggs were *in vitro* fertilized by mixing them with a piece of testis minced in 1x Ringer's solution. After 3 min, eggs were covered with 0.1x Barth to promote sperm activation. After 20-30 min, embryos were dejellied in 2% cysteine in H_2O, pH 7.8-8. Embryos were washed 3x in a tap:VE H_2O mix (2/3:1/3), and cultivated in 0.3x Barth. Microinjections were performed in glass dishes containing 0.3x Barth using calibrated glass capillary needles. Embryos were injected at 2, 4 or 8 cell stage in 0.3x Barth. Generally, a volume of 5 nl was injected per blastomere. Embryos were cultured in glass petri dishes in 0.1x Barth at temperatures between 14°C – RT.

Constructs for mRNA injection

PLASMID	LINEARIZATION	TRANSCRIPTION	REFERENCE
pCS2-*Xkrm1* and *2*	NotI	SP6	[220]
pCS2-*XRspo-2*	NotI	SP6	[238]
pCS2-*Xdkk1*	Asp718	SP6	[29]
dnXWnt8	Asp718	SP6	[56]
pRN-*preprolactin*	SfiI	T3	[236]
pCS2-*BMP4*	Asp718	SP6	
pCS2-h*LRP6*	NotI	SP6	[176]
pCS2-*ARF4* pCS2-*T31N* pCS2-*Q71L* } human and *X.t.*	NotI	SP6	this study
pCS2-h*TAX1BP1*	NotI	SP6	this study
pCS2-*erlectin* (*X.t.*)	NotI	SP6	this study
pCS2-h*erlectin*-flag/V5	NotI	SP6	[263]
pCS2-m*Wnt3a*	injected as DNA		[320]
pBS-*XWnt8*	injected as DNA		[321]
pCS2-cβGal	NotI	SP6	A. Braendli

Morpholino injections

Morpholinos (MOs) were designed according to the general guidelines suggested by Gene Tools, LLC; [322]; if possible, MOs targeting *X. laevis* as well as *X. tropicalis* alleles were chosen. All obtained MOs were dissolved in autoclaved dH_2O (not DEPC-treated) to a final concentration of 5 ng/nl, aliquotted and stored at -20°C. Before use, MOs were thawed and briefly warmed to 50°C, and then kept on RT during injection. MO injected embryos were preferentially grown at RT, to minimize off-target effects of the MOs.

Obtained MOs

TARGETED GENE	**TARGET**		**MORPHOLINO SEQUENCE** (5' – 3' ORIENTATION)
	X.l.	***X.t.***	
Embryonic serine protease-1 (Xesp-1)	no	yes	TCACATAAAGAAGCCCTTGTCTCAT
Receptor tyrosine kinase, c-mer like	no	yes	ACATCATCAGCTGCAATAACACCGT
ADP-ribosylation factor 4, ARF-4	no	yes	CTGCCCCGCTCGCCGCCTCTATCCG
Signal peptide peptidase-like 3, SPP-like 3	yes	yes	CACTCAACGGCGGCTCTGTGATTCG
Similar to DnaJ (Hsp40) homolog	yes	yes	TCCCTATTGCTCTCCATGATGCCGG
Embryonic 7-span transmembrane protein-like	no	yes	AAACTCTCCGTCCCCTTCCCTCCCT
Weak simil. to putat. G-prot. coupled receptor, TRC8	yes	yes	CTCCGGAATCCAATTGCCCCCTCAT
Uncharacterised multi TM protein - hemolytic activity	no	yes	CATTGTGCAGTTATTGGTGTTTTAA
Unknown WD40 repeat containing protein	no	yes	GCTTCATGATGACCCAATGTGCTGG
Erlectin MO1	yes	yes	GAGAATGTGCAGGAGTTACCGGTTA
Erlectin MO2	yes	yes	AGAGAATGCGCAGGAGCGACAGGTT
Krm2 MO-1	yes	yes	[220]
Krm2 MO-2	yes	no	ATCCTCACATGAAGACGTGCTGGAA
LRP6	yes	yes	CCCCGGCTTCTCCGCTCCGACCCCT

Explants

Explants and conjugates were generally performed as described (Villanueva et al 2002). In brief, removal of explants was performed in dishes covered with a layer of 1% agarose (dissolved in 0.5x Barth), and filled with 0.5x Barth. The vitelline membrane of embryos was removed with two watchman forceps (Dumont number 5), and explants were cut using self-made eyebrow knives. Explants were cultured in agarose coated dishes in 0.5x Barth until the desired stage.

Lineage tracing

For lineage tracing, *ß-gal* mRNA (250 pg per blastomere) was co-injected with experimental samples. For LacZ staining, embryos were first fixed in MEMFA for max. 1 hour in glass vials on a roller, then washed 2x 15 min with wash buffer, then washed 2x 15 min with stain buffer. Next, embryos were incubated with stain buffer containing 0.8 mg/ml blue (X-gal; 5-Bromo-4-chloro-3-indolyl-β-D-galactopyranoside) or red (Magenta-gal; 5-Bromo-6-chloro-3-indolyl-β-D-galactopyranoside) substrate until the desired staining appeared (substrate stocks were dissolved in dimethylformamide and stored at -20°C). Embryos were washed several times in PBT, and refixed in MEMFA for 1 hour at RT. This protocol was adapted from [323].

Whole-mount *in situ* hybridization (WISH)

The *Xenopus* WISH protocol [14, 324] was modified following suggestions of Prof. Thomas Pieler (Universitaet Goettingen).

Preparation of embryos

- Best results for WISH are obtained using albino embryos, but pigmented embryos are similarly suitable, since their pigment can be bleached at the end of the procedure
- Fixation was performed in 5 ml glass vials with plastic screw caps (< 250 embryos) in freshly prepared 1x MEMFA buffer on a rotator for 1 to 1.5 hours (or overnight at 4ºC)
- The embryos were then processed through a series of methanol in PTW:
  5 min 25% methanol
  5 min 50% methanol
  5 min 75% methanol
  4 times 5 min 100% methanol
- The embryos were stored at –20ºC up to one year

Hybridization

- The embryos were rehydrated by successive 5 min incubations (on a roller) in 5 ml of:
  100% methanol,
  75% methanol in PTW

50% methanol in PTW

25% methanol in PTW

4 times in PTW

- A proteinase K step was included to increase the permeability for RNA probes and for antibodies; embryos were incubated with 10 µg/ml proteinase K in PTB for 5 min, without agitation
- Embryos were washed 3x 5 min with 5 ml PTW to remove Proteinase K
- Embryos were rinsed 2 times 5 min with 5 ml 0.1 M triethanolamine (pH 7.5) on the rotator; 12.5 µl acetic anhydride were added to the embryos per 5 ml triethanolamine, and vials were rolled for 5 min (acetic anhydride is an hydrophobic chemical that forms a bubble when added to aqueous solutions). Another 12.5 µl acetic anhydride were added, and vials rolled again for 5 min.
- Embryos were washed 3-5x 5 min with 5 ml PTW prior to refixation. Embryos were refixed for 20 min in 5 ml 4% paraformaldehyde (or formaldehyde) in PTW (freshly prepared solution)
- Embryos were rinsed 5x 5 min with 5 ml PTW; all but 1 ml of PTW was removed, and 250 µl of hybridisation buffer were added. When all embryos had settled, the solution was exchanged 2x with 500 µl hybridisation buffer. Embryos were incubated in hybridisation buffer for 30 min at 65ºC with gentle shaking in a water bath. Then the hybridisation buffer was renewed, and embryos were prehybridised for least 6-12 hours at 60ºC with gentle shaking in a water bath.
- DIG RNA probes (200 ng/ml) were brought to 70ºC, exchanged with the prehybridisation buffer and hybridised overnight at 60ºC with gentle shaking in a water bath.

Antibody incubation

- RNA probe solutions were replaced with 500 µl prewarmed hybridisation buffer and samples were incubated at 65ºC for 10 min
- 1 volume of prewarmed 4x SSC was added, and samples were incubate at 65ºC for 20 min; embryos were washed 3 times 20 min with prewarmed 2x SSC + 0.1% CHAPS, at 65ºC
- Embryos were washed 2 times 30 min with 0.2x SSC+ 0.1% CHAPS, at 65º
- Embryos were rinsed 2x 15 min with 5 ml Maleic Acid buffer (MAB) and rolled gently at RT
- MAB was replaced with 2.5 ml MAB + 2% BMB; embryos were rolled for 15 min

- The solution was exchanged with 2.5 ml MAB + 2% BMB + 10% goat serum, and samples were incubated for at least 2 hours, at RT, on a roller
- The solution was replaced with 1ml MAB + 2% BMB + 10% goat serum including a 1:12000 dilution of the affinity purified sheep anti-DIG antibody coupled to alkaline phosphatase (Roche), and samples were incubated overnight at 4ºC, on a roller
- Embryos were washed 10-12x for 1 hour with MAB; at least one over night wash with MAB was included

Chromogenic reaction

- Embryos were rinsed 2 times 5 min with dH_2O
- Embryos were transferred to a plastic 24-well plate, and solution was replaced with Purple AP Substrate (Boehringer Mannheim); embryos were incubated at RT, or over night at 4°C, until desired staining appeared
- Staining was stopped by rinsing the embryos several times with MAB, and subsequently PTW
- Embryos were either stored in MEMFA at 4ºC, or, if subsequent bleaching of pigment was necessary, were fixed over night in Bouin's fixative (ACCUSTAIN, Sigma-Aldrich) at RT

Bleaching of embryos

For bleaching, pigmented embryos were first fixed in Bouin's fixative, then extensively washed in 70% ethanol in TE buffer to remove dye, and finally incubated in bleaching solution on ice, under direct light. After bleaching, embryos were refixed in MEMFA.

In situ probes

PLASMID	**LINEARIZATION**	**TRANSCRIPTION**	**REFERENCE**
pBS-*Xkrm1* and *2*	Anti-sense: EcoRI	T3	[220]
pGEM-T-*Xerlectin* (AAH74469)	Anti-sense: NotI Sense: SphI	T7 SP6	this study
pGEM-T-*Xerlectin* (CB558691)	Anti-sense: NcoI Sense: NotI	SP6 T7	this study
pGEM-T-*Xsox10*	Anti-sense: NcoI	SP6	this study
SP72-*Xslug* (0.8 kb)	Anti-sense: ClaI	SP6	H. Steinbeisser
Xbf-1	was ready to use		[294]
Xkrox-20	was ready to use		[295]

Histology

Embryos were dehydrated in ethanol and xylene, and then embedded in paraffin wax. Samples were sectioned using a microtome and stained with Mayer's hemalaun/Eosin solutions.

Embedding of embryos in paraffin wax

- Before harvest of embryos at desired stages: removed vitelline membranes manually
- Fixed embryos over night at 4°C in 4% PFA in PBS
- Washed embryos 2x 5 min in PBS
- Washed embryos 3x 30 min in 70% ethanol (embryos can be stored at 4°C for up to 6 months)
- Washed embryos 1x 1 hour in 85% ethanol
- Washed embryos 1x 1 hour in 95% ethanol
- Washed embryos 3x 1 hour in 100% ethanol
- Washed embryos 1x 1 hour in xylene (in glass cuvettes, under hood)
- Exchanged xylene and left over night
- Next day: exchanged xylene
- Prewarmed cuvette for 30-60 min in the embedding machine
- Washed embryos 3x 1 hour in paraffin
- Embedded embryos in specific embedding molds (after orienting them), and let them cool down for 1 hour
- Paraffin blocks were stored at 4°C

Microtome sectioning

Paraffin blocks containing embedded embryos were cut into 10 µm sections using the Jung Biocut microtom (Leica). Sections were immediately transferred to a water bath heated to 42°C (to smoothen/stretch the paraffin). After 20-30 min, sections were mounted on microscope slides (SuperFrost Plus, Menzel-Glaeser), and dried at the rim of the water bath. Slides were then further dried in an oven at 55°C (best: horizontally; vertical drying may lead to small paraffin drops at lower edge of slides).

Mayer's hemalaun/Eosin staining

- Slides were transferred through an ethanol series (in special glass containers for

histology): 2x 10 min xylene; 2x 5 min 100% ethanol; 1x 5 min 96% ethanol; 1x 5 min 80% ethanol; 2x 5 min 70% ethanol

- Slides were rinsed briefly in H_2O
- Incubation in Mayer's hemalaun (Roth) (solution must be filtered!) for 10 min
- Transfer to H_2O for 1 min, then ethanol-HCl (0.5% HCl in 70% ethanol) for 1 min
- Put slides under running tap H_2O for 10 min (or longer)
- Transferred slides for 1 min to ddH_2O, then to Eosin staining solution for 0.5-1 min
- Dipped slides in H_2O
- Transferred slides to 70% ethanol for 3 min
- Slides were again transferred through ethanol series: 70%, 80%, 96%, 100% ethanol (each very short), then again 100% ethanol for 1 min, then xylene (short)
- Samples were embedded immediately (important; samples must not dry) in Roti-Histokitt II (Roth) and covered with cover glasses
- After drying, samples were analyzed under microscope

X. tropicalis methods

X. tropicalis adults and embryos were usually kept at RT. Fertilization was also done at RT; after cysteine treatment, one batch was put on 18°C. Importantly, embryos were always grown/kept in petri dishes covered with 0.5-1 % agarose in 1/18 MR, in order to avoid embryos sticking to the dish. For a general description of *X. tropicalis* husbandry, as well as methods and protocols, see [325].

Priming, fertilization and microinjection

- Females were preprimed the evening before the experiment with 10 units human chorionic gonadotropin (Sigma); males were primed at the same time with 100 units of the hormone
- The next morning, females were primed with 200 units of gonadotropin; frogs start laying eggs after 4-6 hours.
- Females were first squeezed to obtain eggs, then testis was prepared. Prepared testis was stored in 1x Ringer at 18°C for a few hours. One whole testis was used per fertilization (3-4 egg batches, 100 µl minced testis per batch). After 3 min, 0.1x Barth was added to cover the eggs

- Embryos were incubated for 20 min, then dejellied with 2% cysteine (or even 3%) in 1/9 MR (pH 7.8-8) at RT
- Embryos were washed 3x with 0.1x Barth and 2x with 1/9 MR, and kept in 1/9 MR at RT and 18°C, respectively. There was never much time difference; both batches are almost equally fast
- Injections were carried out in 1/9 MR + 2% Ficoll; embryos were generally injected at 2, 4 or 8 cell stage with a volume of 2.5 nl per blastomere
- After injection, embryos were grown in 1/18 MR at RT

Cell culture and transfection

HEK 293T cells were maintained in DMEM (Bio Whittaker) supplemented with 1% L-Glutamine, 1% PEN-STREP, and 10% FCS (all Bio Whittaker) and grown at 10% CO_2. Cells were always seeded one day before transfection. All transfections were done using FuGENE6 transfection reagent (Roche) according to the manufacturer's instructions. After transfection, cells were kept in DMEM and harvested after 24-48 hours, depending on the experiment.

Constructs used for transfection of 293T cells

PLASMID	**REFERENCE**
pCS2-*Xkrm1/2*	[220]
pCS2-V5-*Xkrm2*	[220]
pCS2-V5-m*krm1/2*	[211]
pCS2-m*krm1/2*-V5	[211]
pCS2-m*krm1/2*-ΔTMC-V5	[211]
pCS2-h*LRP6*	[176]
pCS2-flag-h*LRP6*	[211]
pCS2-6myc-h*LRP6*	[154]
pCS2-h*LRP6*-GFP	[211]
pCS2-myc-h*LRP6ΔTMC*	[211]
pCS2-flag-h*LRP6ΔE1-4*	[198]
pCMV-SPORT6-m*mesd*	from RZPD; GenBank Accession BI657640
pCS2-V5-m*dkk3*	constructed by Bingyu Mao
pCS2-myc-m*dkk3*	constructed by Bingyu Mao
pCS2-flag-h*LDLRΔC*	Constructed by W.W.
pCS2-flag-h*NME1*	[263]
pCS2-flag-X*FLRT3*	constructed by Ralph Boettcher
pCS2-X*dkk1*	[29]
pcDNA3.1-*BMP4*	
pRK5-m*fz8*	provided by J. Nathans
m*wnt1*	provided by H. Clevers
pCS2-h*dvl*	[154]

pTK-Renilla	Promega
BREx4-E1b-dLuc plasmid	(modified from [326])
TOPFLASH	[327]

Luciferase reporter gene assays

Luciferase reporter gene assays were carried out in triplicates in 96-well plates using Promega's Dual-Luciferase Reporter Assay System as described [210]. After transfection, cells were grown for 48 hours, then lysed in 50 µl passive lysis buffer (Promega) per well. Firefly and Renilla luciferase activities were measured using a Fluoroskan Ascent FL (Labsystems), and Firefly activity was normalized against Renilla activity.

In all experiments a total of 50 ng DNA per well was transfected, and 1 ng pCMV-SPORT6-*mmesd* or 5 ng pCS2-*Xkrm1* DNA were used as indicated. For Wnt reporter assays transfected DNAs per well were: 10 ng TOPFLASH and 1 ng pTK-Renilla reporter plasmids; 12 ng (Fig. 32B) or 24 ng (Figs. 32A, D and 33) *hLRP6*; 2 ng *mfrizzled8* (*fz8*); 0.25 ng *hdishevelled1* (*dvl1*); 0.5 ng *hLRP6ΔE1-4*; 5 ng/ 3 ng *mwnt1*/ *hLRP6* (Fig. 32D); 0.5 ng *Xdkk1*. For experiment shown in Fig. 33, 5 ng were transfected of each *krm* construct. For BMP responsive reporter assays transfected DNAs per well were: 20 ng BREx4-E1b-dLuc plasmid and 1 ng pTK-Renilla; 10 ng pcDNA3.1-*BMP4* as indicated.

Biochemical methods

SDS-PAGE and Western blotting

SDS-polyacrylamide gel electrophoresis (SDS-PAGE) and Western blotting were carried out as described in [314]. Signal detection was performed using the enhanced chemiluminescence system of Pierce.

Co-immunoprecipitation and *in vitro* binding assays

For Co-immunoprecipitation (CoIP) assays, HEK293T cells were transfected in 10 cm plates with 0.1 µg pCS2-*mkrm1*-V5 or pCS2-*mkrm2*-V5 together with 1.5 µg pCS2-flag-

hLRP6, 0.5 µg pCS2-flag-*XFLRT3*, 0.1 µg pCS2-flag-*hLDLRΔC* or 1.5 µg empty vector pCS2 using Fugene6 (Roche). After 48 hours cells were washed in PBS and lysed in NP-40 buffer containing 0.8% NP-40. Lysates were subjected to CoIP with anti-flag antibody beads (Sigma) over night at 4°C. CoIPs were washed with NP-40 buffer and analyzed by SDS-PAGE and Western blotting.

In vitro binding assays were carried out essentially as described [263]. Recombinant proteins were produced as conditioned media by transient transfection of HEK293T cells with pCS2-*mkrm1ΔTMC*-V5, pCS2-*mkrm2ΔTMC*-V5, pCS2-V5-*mdkk3* or pCS2-myc-*hLRP6ΔTMC* in serum-free media (Optimem I, Gibco). Media were concentrated about 50-fold using Centricon Plus-20 filters (Millipore). Equal amounts of V5-tagged proteins were resuspended in NP-40 buffer containing 0.2% (w/v) NP-40, and incubated with anti-V5 antibody beads (Sigma) under gentle shaking over night at 4^{o}C. IPs were washed and incubated for five hours with media containing pCS2-myc-*hLRP6ΔTMC*. CoIPs were washed again and analyzed by SDS-PAGE and Western blotting.

Endoglycosidase H (EndoH) treatment

For deglycosylation of LRP6, HEK293T cells were grown in 10 cm plates and transfected with 1 µg flag-*LRP6* together with 0.4 µg pCS2-myc-*mdkk3*, pCMV-SPORT6-*mmesd*, pCS2-*mkrm2*-V5 or empty pCS2. After 2 days, cells were washed in Hank's buffer and resuspended in 1 ml hypotonic buffer. Samples were dounced 25 times, and after removal of cell debris by centrifugation at 2500 rpm, membranes were pelleted by centrifugation at 30.000 rpm. Pellets were lysed in NP-40 buffer (without NaF) containing 2% NP-40 and subjected to EndoH (Roche) treatment (0.25 U/ ml) in 100 mM NaOAc, pH 5.5, for 30 min at 37°C. Samples were analyzed by SDS-PAGE and Western blotting.

Cell surface biotinylation

For cell surface biotinylation of LRP6, HEK293T cells were transfected in 6 cm dishes with 0.25 µg pCS2-flag-*hLRP6* together with 0.1 µg pCS2-myc-*mdkk3*, pCMV-SPORT6-*mmesd* or pCS2-*mkrm2*-V5, or pCS2-flag-*hNME*. For cell surface biotinylation of ER-trapped Krm2 constructs, HEK293T cells were transfected in 6-well dishes with 0.1 µg pCS2-V5-

mkrm2, pCS2-V5-*mkrm2-DEKKMP,* pCS2-V5-*mkrm2-KKYL,* pCS2-V5-*mkrm2-KKDE,* or 0.4 µg pCS2-V5-h*NME1*.

Special materials

EZ-link Sulfo-NHS-LC-Biotin, No 21335, Mol weight 556,59 (Pierce)

Anti-FLAG M2-Agarose from mouse, A2220-25ML (Sigma)

Anti-V5-Agarose, Affinity gel, from mouse (Sigma)

Complete, EDTA free protease inhibitor tablet, 11 873 580 001 (Roche)

Protocol for cell surface biotinylation

- Used poly-L-lysine plates for 293T cells (diluted 1 ml of Poly-L-Lysine hydrobromide (Sigma, P-5899) in 50 ml dH_2O (not necessary to autoclave); incubated plates for 30 min, then dried plates with open lid under hood with switched on UV light; plates were stored at RT)
- Seeded cells very thin (maybe 1:15); after desired period of growth (2 days) cells should be max. **70% confluent**; transfection of constructs was done as described above
- Next day: exchanged 75% of supernatant with fresh DMEM
- Harvest: After 2 days; everything on ice, all solutions were precooled
- Washed 2x with HANK's, 1x with HANK's + 100 mM Hepes, pH 7.5 (HANK's-Hepes)
- Pre-weighed biotin (prewarmed tube in hand, so that it attracts less humidity when opened, prewarmed also falcon)
- Dissolved biotin (**final conc: 0.5 mM**) in precooled HANK's - Hepes, pH 7.5 and immediately put on cells;
- Incubated ½ hour on ice; importantly, cells must be completely covered
- Quenched reaction by adding HANK's + 20 mM Monoethanolamine, incubated 10 min
- Scraped cells in this solution using a gummy scraper
- Spun 5 min, 4°C, 2000 rpm, to keep cells intact
- Washed cells 2x in 5 ml HANK's in a volume of 5 ml (spun 5 min, 4°C, 2000 rpm)
- Resuspended cells in hypotonic buffer
- Dounced 25 times in small homogenizer (on ice); transferred samples to Eppendorf tubes
- Spun 5 min, 4°C, 2500 rpm, in Falcon centrifuge (to get rid of debris)
- Transferred 0.9 ml to fresh tubes
- Ultracentrifugation: 30 min, 4°C, 30 K (30.000 rpm), TLA-55 rotor, in tabletop ultracentrifuge

- Resuspended membrane pellet in 300 µl NP-40 buffer containing 2% NP-40
- Lysed on ice for 1 hour, vortexed several times
- Spun 2x 3 min, 4°C, max. speed, transferred and kept supernatant
- Prewashed antibody-coupled beads 3x with NP-40 buffer containing 0.2% NP-40 in Falcon, spun 2 min, 500 rpm
- Took pre-beads (load, input) aliquot, then added 40 µl beads to lysate, put on rotator for 4 hours (when over night, a lot of LRP6 is degraded)
- Took post-beads (flow-through) aliquot, then washed beads 5x in 1 ml NP-40 buffer containing 0.2% NP-40; always spun 2 min at 500 rpm, 4°C
- Elution: 50 µl 4x Laemmli for 5 min, at 99°C, shaking
- For pre- and post-beads aliquots: added same ratio of 4x Laemmli, e.g. for 15 µl added 5 µl of 4x Laemmli
- PAGE and Western blotting: for LRP6 normally 7.5% PA, and detection with anti-flag and Streptavidin-HRP antibodies; for Krm2 constructs 10-12.5 % PA, and detection with anti-V5 and Streptavidine-HRP antibodies

Protease protection assay

The microsomal fraction was isolated from HEK293T cells after transfection of Erlectin-HA using an ER Isolation Kit protocol: SIGMA, Endoplasmic Reticulum Isolation Kit, Product Code ER0100. The endogenous ER protein Calnexin was used as control [293].

ER membrane isolation

- Plated 293T cells in 15 cm dish; when confluent, harvested with gummi cell scraper in 10 ml ice cold PBS, on ice
- Transferred cells to 15 ml falcon, spun at 2500 rpm (600xg), 4°C
- Resuspended pellet in 10x vol. ice cold PBS, spun again
- Suspended pellet in 3x vol. hypotonic ER isolation buffer (1 ml), transferred samples to Eppendorf tubes
- Rested for 20 min on ice (this helps to break up cells later by making cells unstable)
- Spun for 5 min, 2000 rpm, 4°C
- Resuspended pellets in 2x vol. isotonic ER isolation buffer (0.5 ml) and dounced 10x
- Spun in Eppendorf cool centrifuge, 10 min, 4°C, 2200 rpm (1000xg) (this removes cell debris)

- Spun in Eppendorf cool centrifuge, 15 min, 7700 rpm (12000xg) (this removes mitochondria)
- Spun in table top ultracentrifuge, TLA-55 rotor, 1h, 4°C, 41.000 rpm (approx. 100.000xg)
- Resuspended pellet in isotonic ER isolation buffer (150 µl); (kept supernatant = cytosolic fraction)
- Spun 1 min at 2500 rpm in Eppendorf cool centrifuge to remove clumps
- Samples were used immediately or frozen at -80

Proteinase K treatment

- Aliquots were pretreated +/- 1% TritonX-100 for 30 min on ice, then incubated +/- 250 µg/ml Proteinase K (Gerbu) (prepared very fresh from powder, since this enzyme eats itself), for 1 hour on ice
- PMSF was added to a final concentration of 1 mM to inhibit Proteinase K, and samples were analyzed by SDS-PAGE and Western blotting

Bioinformatics

General webpages are (mainly *Xenopus*): AxelDB, Ensembl, JGI *Xenopus*, NCBI, NIBB XDB, Sanger Institute, XGI (TIGR), Xenbase. *Xenopus* EST sequences for alignments (MO design) were withdrawn from: Sanger Institute, JGI *Xenopus* and NCBI.

Erlectin sequences were extracted from public databases, using browsers of the NCBI and Sanger centers: human (NM_015701, GeneID: 27248), mouse (NM_025745), chicken (XM_419295), *D. rerio* (BC044498), *X. tropicalis* (AAH67973), *C. intestinalis* (AK114497), *S. purpuratus* (XP_784270) and *D. melanogaster* (NM_135693). The two *X. laevis* alleles are: BC074469 (allele1) and CB558691 (allele2). CB558691 is a partial sequence of contig XGI TC228200. Alignments and homology trees were generated using the program DNAMAN (Lynnon Corporation).

7. REFERENCES

1. Wolpert, L., *Principles of Development*. 3rd ed. 2007: Oxford University Press.
2. Pires-daSilva, A. and R.J. Sommer, *The evolution of signalling pathways in animal development.* Nat Rev Genet, 2003. **4**(1): p. 39-49.
3. Gerhart, J., *1998 Warkany lecture: signaling pathways in development.* Teratology, 1999. **60**(4): p. 226-39.
4. Shi, Y. and J. Massague, *Mechanisms of TGF-beta signaling from cell membrane to the nucleus.* Cell, 2003. **113**(6): p. 685-700.
5. Ingham, P.W. and A.P. McMahon, *Hedgehog signaling in animal development: paradigms and principles.* Genes Dev, 2001. **15**(23): p. 3059-87.
6. Bray, S.J., *Notch signalling: a simple pathway becomes complex.* Nat Rev Mol Cell Biol, 2006. **7**(9): p. 678-89.
7. Tan, P.B. and S.K. Kim, *Signaling specificity: the RTK/RAS/MAP kinase pathway in metazoans.* Trends Genet, 1999. **15**(4): p. 145-9.
8. Logan, C.Y. and R. Nusse, *The Wnt signaling pathway in development and disease.* Annu Rev Cell Dev Biol, 2004. **20**: p. 781-810.
9. Sundaram, M.V., *The love-hate relationship between Ras and Notch.* Genes Dev, 2005. **19**(16): p. 1825-39.
10. Pera, E.M., et al., *Integration of IGF, FGF, and anti-BMP signals via Smad1 phosphorylation in neural induction.* Genes Dev, 2003. **17**(24): p. 3023-8.
11. Glinka, A., et al., *Head induction by simultaneous repression of Bmp and Wnt signalling in Xenopus.* Nature, 1997. **389**(6650): p. 517-9.
12. Callery, E.M., *There's more than one frog in the pond: a survey of the Amphibia and their contributions to developmental biology.* Semin Cell Dev Biol, 2006. **17**(1): p. 80-92.
13. Nieuwkoop, P.D. and J. Faber, *Normal Table of Xenopus laevis.* North Holland Publishing Company, Amsterdam, 1967.
14. Sive, H.L., R.M. Grainger, and R.M. Harland, *Early Development of Xenopus laevis. A Laboratory Manual.* Cold Spring Harbor Laboratory Press, 2000.
15. Hausen, P. and M. Riebesell, *The Early Development of Xenopus Laevis.* Springer-Verlag, Berlin Heidelberg New York, 1991.
16. Hirsch, N., L.B. Zimmerman, and R.M. Grainger, *Xenopus, the next generation: X. tropicalis genetics and genomics.* Dev Dyn, 2002. **225**(4): p. 422-33.
17. Carruthers, S. and D.L. Stemple, *Genetic and genomic prospects for Xenopus tropicalis research.* Semin Cell Dev Biol, 2006. **17**(1): p. 146-53.
18. Goda, T., et al., *Genetic screens for mutations affecting development of Xenopus tropicalis.* PLoS Genet, 2006. **2**(6): p. e91.
19. Spemann, H. and H. Mangold, *Über Induktion von Embryonalanlagen durch Implantation artfremder Organisatoren.* Arch Mikrosk Anat Entwicklungsmechan, 1924. **100**: p. 599-638.

20. Heasman, J., *Patterning the early Xenopus embryo.* Development, 2006. **133**(7): p. 1205-17.
21. De Robertis, E.M. and H. Kuroda, *Dorsal-ventral patterning and neural induction in Xenopus embryos.* Annu Rev Cell Dev Biol, 2004. **20**: p. 285-308.
22. De Robertis, E.M., et al., *The establishment of Spemann's organizer and patterning of the vertebrate embryo.* Nat Rev Genet, 2000. **1**(3): p. 171-81.
23. Grunz, H., *The Vertebrate Organizer*. 2004, Berlin, Heidelberg, New York: Springer-Verlag. 1-428.
24. Niehrs, C., *Regionally specific induction by the Spemann-Mangold organizer.* Nat Rev Genet, 2004. **5**(6): p. 425-34.
25. De Robertis, E. and J. Arechaga, *The Spemann-Mangold Organizer.* Int J Dev Biol, 2001. **Vol. 45 No. 1 Special issue 2001**.
26. Keller, R., L.A. Davidson, and D.R. Shook, *How we are shaped: the biomechanics of gastrulation.* Differentiation, 2003. **71**(3): p. 171-205.
27. Keller, R., *Shaping the vertebrate body plan by polarized embryonic cell movements.* Science, 2002. **298**(5600): p. 1950-4.
28. Niehrs, C., *Head in the WNT: the molecular nature of Spemann's head organizer.* Trends Genet, 1999. **15**(8): p. 314-9.
29. Glinka, A., et al., *Dickkopf-1 is a member of a new family of secreted proteins and functions in head induction.* Nature, 1998. **391**(6665): p. 357-62.
30. Leyns, L., et al., *Frzb-1 is a secreted antagonist of Wnt signaling expressed in the Spemann organizer.* Cell, 1997. **88**(6): p. 747-56.
31. Wang, S., et al., *Frzb, a secreted protein expressed in the Spemann organizer, binds and inhibits Wnt-8.* Cell, 1997. **88**(6): p. 757-66.
32. Pera, E.M. and E.M. De Robertis, *A direct screen for secreted proteins in Xenopus embryos identifies distinct activities for the Wnt antagonists Crescent and Frzb-1.* Mech Dev, 2000. **96**(2): p. 183-95.
33. Pfeffer, P.L., E.M. De Robertis, and J.C. Izpisua-Belmonte, *Crescent, a novel chick gene encoding a Frizzled-like cysteine-rich domain, is expressed in anterior regions during early embryogenesis.* Int J Dev Biol, 1997. **41**(3): p. 449-58.
34. Yamaguchi, T.P., *Heads or tails: Wnts and anterior-posterior patterning.* Curr Biol, 2001. **11**(17): p. R713-24.
35. Niehrs, C., *Function and biological roles of the Dickkopf family of Wnt modulators.* Oncogene, 2006. **25**(57): p. 7469-81.
36. Kawano, Y. and R. Kypta, *Secreted antagonists of the Wnt signalling pathway.* J Cell Sci, 2003. **116**(Pt 13): p. 2627-34.
37. Sasai, Y., et al., *Xenopus chordin: a novel dorsalizing factor activated by organizer-specific homeobox genes.* Cell, 1994. **79**(5): p. 779-90.
38. Smith, W.C. and R.M. Harland, *Expression cloning of noggin, a new dorsalizing factor localized to the Spemann organizer in Xenopus embryos.* Cell, 1992. **70**(5): p. 829-40.
39. Fainsod, A., et al., *The dorsalizing and neural inducing gene follistatin is an antagonist of BMP-4.* Mech Dev, 1997. **63**(1): p. 39-50.
40. Hansen, C.S., et al., *Direct neural induction and selective inhibition of mesoderm and epidermis inducers by Xnr3.* Development, 1997. **124**(2): p. 483-92.
41. Smith, W.C., et al., *A nodal-related gene defines a physical and functional domain within the Spemann organizer.* Cell, 1995. **82**(1): p. 37-46.
42. Meno, C., et al., *Mouse Lefty2 and zebrafish antivin are feedback inhibitors of nodal signaling during vertebrate gastrulation.* Mol Cell, 1999. **4**(3): p. 287-98.

43. Thisse, C. and B. Thisse, *Antivin, a novel and divergent member of the TGFbeta superfamily, negatively regulates mesoderm induction.* Development, 1999. **126**(2): p. 229-40.
44. Branford, W.W. and H.J. Yost, *Nodal signaling: CrypticLefty mechanism of antagonism decoded.* Curr Biol, 2004. **14**(9): p. R341-3.
45. Schier, A.F., *Nodal signaling in vertebrate development.* Annu Rev Cell Dev Biol, 2003. **19**: p. 589-621.
46. Bouwmeester, T., et al., *Cerberus is a head-inducing secreted factor expressed in the anterior endoderm of Spemann's organizer.* Nature, 1996. **382**(6592): p. 595-601.
47. Piccolo, S., et al., *The head inducer Cerberus is a multifunctional antagonist of Nodal, BMP and Wnt signals.* Nature, 1999. **397**(6721): p. 707-10.
48. http://www.xenbase.org/xine/xine2-1.html.
49. Christian, J.L., et al., *Xwnt-8, a Xenopus Wnt-1/int-1-related gene responsive to mesoderm-inducing growth factors, may play a role in ventral mesodermal patterning during embryogenesis.* Development, 1991. **111**(4): p. 1045-55.
50. del Barco Barrantes, I., et al., *Dkk1 and noggin cooperate in mammalian head induction.* Genes Dev, 2003. **17**(18): p. 2239-44.
51. Perea-Gomez, A., et al., *Nodal antagonists in the anterior visceral endoderm prevent the formation of multiple primitive streaks.* Dev Cell, 2002. **3**(5): p. 745-56.
52. Agathon, A., C. Thisse, and B. Thisse, *The molecular nature of the zebrafish tail organizer.* Nature, 2003. **424**(6947): p. 448-52.
53. Stern, C.D., *Neural induction: old problem, new findings, yet more questions.* Development, 2005. **132**(9): p. 2007-21.
54. Hoppler, S. and R.T. Moon, *BMP-2/-4 and Wnt-8 cooperatively pattern the Xenopus mesoderm.* Mech Dev, 1998. **71**(1-2): p. 119-29.
55. Christian, J.L. and R.T. Moon, *Interactions between Xwnt-8 and Spemann organizer signaling pathways generate dorsoventral pattern in the embryonic mesoderm of Xenopus.* Genes Dev, 1993. **7**(1): p. 13-28.
56. Hoppler, S., J.D. Brown, and R.T. Moon, *Expression of a dominant-negative Wnt blocks induction of MyoD in Xenopus embryos.* Genes Dev, 1996. **10**(21): p. 2805-17.
57. Marom, K., A. Fainsod, and H. Steinbeisser, *Patterning of the mesoderm involves several threshold responses to BMP-4 and Xwnt-8.* Mech Dev, 1999. **87**(1-2): p. 33-44.
58. Kiecker, C. and C. Niehrs, *A morphogen gradient of Wnt/beta-catenin signalling regulates anteroposterior neural patterning in Xenopus.* Development, 2001. **128**(21): p. 4189-201.
59. McGrew, L.L., C.J. Lai, and R.T. Moon, *Specification of the anteroposterior neural axis through synergistic interaction of the Wnt signaling cascade with noggin and follistatin.* Dev Biol, 1995. **172**(1): p. 337-42.
60. McGrew, L.L., S. Hoppler, and R.T. Moon, *Wnt and FGF pathways cooperatively pattern anteroposterior neural ectoderm in Xenopus.* Mech Dev, 1997. **69**(1-2): p. 105-14.
61. Kiecker, C. and C. Niehrs, *The role of prechordal mesendoderm in neural patterning.* Curr Opin Neurobiol, 2001. **11**(1): p. 27-33.
62. Erter, C.E., et al., *Wnt8 is required in lateral mesendodermal precursors for neural posteriorization in vivo.* Development, 2001. **128**(18): p. 3571-83.
63. Niehrs, C., *The Spemann organizer and embryonic head induction.* Embo J, 2001. **20**(4): p. 631-7.

64. Northcutt, R.G. and C. Gans, *The genesis of neural crest and epidermal placodes: a reinterpretation of vertebrate origins.* Q Rev Biol, 1983. **58**(1): p. 1-28.
65. Glenn Northcutt, R., *The new head hypothesis revisited.* J Exp Zoolog B Mol Dev Evol, 2005. **304**(4): p. 274-97.
66. Manzanares, M. and M.A. Nieto, *A celebration of the new head and an evaluation of the new mouth.* Neuron, 2003. **37**(6): p. 895-8.
67. Huang, X. and J.P. Saint-Jeannet, *Induction of the neural crest and the opportunities of life on the edge.* Dev Biol, 2004. **275**(1): p. 1-11.
68. Knecht, A.K. and M. Bronner-Fraser, *Induction of the neural crest: a multigene process.* Nat Rev Genet, 2002. **3**(6): p. 453-61.
69. LaBonne, C. and M. Bronner-Fraser, *Molecular mechanisms of neural crest formation.* Annu Rev Cell Dev Biol, 1999. **15**: p. 81-112.
70. Farlie, P.G., S.J. McKeown, and D.F. Newgreen, *The neural crest: basic biology and clinical relationships in the craniofacial and enteric nervous systems.* Birth Defects Res C Embryo Today, 2004. **72**(2): p. 173-89.
71. Mollaaghababa, R. and W.J. Pavan, *The importance of having your SOX on: role of SOX10 in the development of neural crest-derived melanocytes and glia.* Oncogene, 2003. **22**(20): p. 3024-34.
72. Hutson, M.R. and M.L. Kirby, *Neural crest and cardiovascular development: a 20-year perspective.* Birth Defects Res C Embryo Today, 2003. **69**(1): p. 2-13.
73. His, W., *Untersuchungen ueber die erste Anlage des Wirbelltierleibes. Die erste Entwicklung des Huehnchens im Ei.* Leipzig: F.C.W. Vogel., 1868.
74. Baker, C.V. and M. Bronner-Fraser, *The origins of the neural crest. Part I: embryonic induction.* Mech Dev, 1997. **69**(1-2): p. 3-11.
75. Basch, M.L., M.I. Garcia-Castro, and M. Bronner-Fraser, *Molecular mechanisms of neural crest induction.* Birth Defects Res C Embryo Today, 2004. **72**(2): p. 109-23.
76. Bonstein, L., S. Elias, and D. Frank, *Paraxial-fated mesoderm is required for neural crest induction in Xenopus embryos.* Dev Biol, 1998. **193**(2): p. 156-68.
77. Marchant, L., et al., *The inductive properties of mesoderm suggest that the neural crest cells are specified by a BMP gradient.* Dev Biol, 1998. **198**(2): p. 319-29.
78. Moury, J.D. and A.G. Jacobson, *The origins of neural crest cells in the axolotl.* Dev Biol, 1990. **141**(2): p. 243-53.
79. Mayor, R. and M.J. Aybar, *Induction and development of neural crest in Xenopus laevis.* Cell Tissue Res, 2001. **305**(2): p. 203-9.
80. Mayor, R., R. Young, and A. Vargas, *Development of neural crest in Xenopus.* Curr Top Dev Biol, 1999. **43**: p. 85-113.
81. LaBonne, C. and M. Bronner-Fraser, *Neural crest induction in Xenopus: evidence for a two-signal model.* Development, 1998. **125**(13): p. 2403-14.
82. Villanueva, S., et al., *Posteriorization by FGF, Wnt, and retinoic acid is required for neural crest induction.* Dev Biol, 2002. **241**(2): p. 289-301.
83. Monsoro-Burq, A.H., R.B. Fletcher, and R.M. Harland, *Neural crest induction by paraxial mesoderm in Xenopus embryos requires FGF signals.* Development, 2003. **130**(14): p. 3111-24.
84. Monsoro-Burq, A.H., E. Wang, and R. Harland, *Msx1 and Pax3 cooperate to mediate FGF8 and WNT signals during Xenopus neural crest induction.* Dev Cell, 2005. **8**(2): p. 167-78.
85. Mayor, R., N. Guerrero, and C. Martinez, *Role of FGF and noggin in neural crest induction.* Dev Biol, 1997. **189**(1): p. 1-12.
86. Jones, C.M. and J.C. Smith, *Establishment of a BMP-4 morphogen gradient by long-range inhibition.* Dev Biol, 1998. **194**(1): p. 12-7.

87. Aybar, M.J. and R. Mayor, *Early induction of neural crest cells: lessons learned from frog, fish and chick.* Curr Opin Genet Dev, 2002. **12**(4): p. 452-8.
88. Lewis, J.L., et al., *Reiterated Wnt signaling during zebrafish neural crest development.* Development, 2004. **131**(6): p. 1299-308.
89. Garcia-Castro, M.I., C. Marcelle, and M. Bronner-Fraser, *Ectodermal Wnt function as a neural crest inducer.* Science, 2002. **297**(5582): p. 848-51.
90. Ikeya, M., et al., *Wnt signalling required for expansion of neural crest and CNS progenitors.* Nature, 1997. **389**(6654): p. 966-70.
91. Raible, D.W. and J.W. Ragland, *Reiterated Wnt and BMP signals in neural crest development.* Semin Cell Dev Biol, 2005. **16**(6): p. 673-82.
92. Schmidt, C. and K. Patel, *Wnts and the neural crest.* Anat Embryol (Berl), 2005. **209**(5): p. 349-55.
93. Yanfeng, W., J.P. Saint-Jeannet, and P.S. Klein, *Wnt-frizzled signaling in the induction and differentiation of the neural crest.* Bioessays, 2003. **25**(4): p. 317-25.
94. Saint-Jeannet, J.P., et al., *Regulation of dorsal fate in the neuraxis by Wnt-1 and Wnt-3a.* Proc Natl Acad Sci U S A, 1997. **94**(25): p. 13713-8.
95. Chang, C. and A. Hemmati-Brivanlou, *Neural crest induction by Xwnt7B in Xenopus.* Dev Biol, 1998. **194**(1): p. 129-34.
96. Deardorff, M.A., et al., *A role for frizzled 3 in neural crest development.* Development, 2001. **128**(19): p. 3655-63.
97. Wu, J., J. Yang, and P.S. Klein, *Neural crest induction by the canonical Wnt pathway can be dissociated from anterior-posterior neural patterning in Xenopus.* Dev Biol, 2005. **279**(1): p. 220-32.
98. Abu-Elmagd, M., C. Garcia-Morales, and G.N. Wheeler, *Frizzled7 mediates canonical Wnt signaling in neural crest induction.* Dev Biol, 2006. **298**(1): p. 285-98.
99. Bastidas, F., J. De Calisto, and R. Mayor, *Identification of neural crest competence territory: role of Wnt signaling.* Dev Dyn, 2004. **229**(1): p. 109-17.
100. Raible, D.W., *Development of the neural crest: achieving specificity in regulatory pathways.* Curr Opin Cell Biol, 2006. **18**(6): p. 698-703.
101. Steventon, B., C. Carmona-Fontaine, and R. Mayor, *Genetic network during neural crest induction: from cell specification to cell survival.* Semin Cell Dev Biol, 2005. **16**(6): p. 647-54.
102. Sauka-Spengler, T. and M. Bronner-Fraser, *Development and evolution of the migratory neural crest: a gene regulatory perspective.* Curr Opin Genet Dev, 2006. **16**(4): p. 360-6.
103. Meulemans, D. and M. Bronner-Fraser, *Gene-regulatory interactions in neural crest evolution and development.* Dev Cell, 2004. **7**(3): p. 291-9.
104. Vallin, J., et al., *Cloning and characterization of three Xenopus slug promoters reveal direct regulation by Lef/beta-catenin signaling.* J Biol Chem, 2001. **276**(32): p. 30350-8.
105. Burstyn-Cohen, T., et al., *Canonical Wnt activity regulates trunk neural crest delamination linking BMP/noggin signaling with G1/S transition.* Development, 2004. **131**(21): p. 5327-39.
106. Kalcheim, C. and T. Burstyn-Cohen, *Early stages of neural crest ontogeny: formation and regulation of cell delamination.* Int J Dev Biol, 2005. **49**(2-3): p. 105-16.
107. Dunn, K.J., et al., *Neural crest-directed gene transfer demonstrates Wnt1 role in melanocyte expansion and differentiation during mouse development.* Proc Natl Acad Sci U S A, 2000. **97**(18): p. 10050-5.

108. Jin, E.J., et al., *Wnt and BMP signaling govern lineage segregation of melanocytes in the avian embryo.* Dev Biol, 2001. **233**(1): p. 22-37.
109. Takeda, K., et al., *Induction of melanocyte-specific microphthalmia-associated transcription factor by Wnt-3a.* J Biol Chem, 2000. **275**(19): p. 14013-6.
110. Tachibana, M., *MITF: a stream flowing for pigment cells.* Pigment Cell Res, 2000. **13**(4): p. 230-40.
111. Honore, S.M., M.J. Aybar, and R. Mayor, *Sox10 is required for the early development of the prospective neural crest in Xenopus embryos.* Dev Biol, 2003. **260**(1): p. 79-96.
112. Wegner, M., *Secrets to a healthy Sox life: lessons for melanocytes.* Pigment Cell Res, 2005. **18**(2): p. 74-85.
113. Shah, N.M., A.K. Groves, and D.J. Anderson, *Alternative neural crest cell fates are instructively promoted by TGFbeta superfamily members.* Cell, 1996. **85**(3): p. 331-43.
114. Lee, P.N., et al., *A WNT of things to come: evolution of Wnt signaling and polarity in cnidarians.* Semin Cell Dev Biol, 2006. **17**(2): p. 157-67.
115. Guder, C., et al., *The Wnt code: cnidarians signal the way.* Oncogene, 2006. **25**(57): p. 7450-60.
116. Korswagen, H.C., *Canonical and non-canonical Wnt signaling pathways in Caenorhabditis elegans: variations on a common signaling theme.* Bioessays, 2002. **24**(9): p. 801-10.
117. Brandhorst, B.P. and W.H. Klein, *Molecular patterning along the sea urchin animal-vegetal axis.* Int Rev Cytol, 2002. **213**: p. 183-232.
118. Croce, J.C. and D.R. McClay, *The canonical Wnt pathway in embryonic axis polarity.* Semin Cell Dev Biol, 2006. **17**(2): p. 168-74.
119. Imai, K., et al., *(beta)-catenin mediates the specification of endoderm cells in ascidian embryos.* Development, 2000. **127**(14): p. 3009-20.
120. Holland, L.Z., *Heads or tails? Amphioxus and the evolution of anterior-posterior patterning in deuterostomes.* Dev Biol, 2002. **241**(2): p. 209-28.
121. Nichols, S.A., et al., *Early evolution of animal cell signaling and adhesion genes.* Proc Natl Acad Sci U S A, 2006. **103**(33): p. 12451-6.
122. Borycki, A.G. and C.P. Emerson, Jr., *Multiple tissue interactions and signal transduction pathways control somite myogenesis.* Curr Top Dev Biol, 2000. **48**: p. 165-224.
123. Snider, L. and S.J. Tapscott, *Emerging parallels in the generation and regeneration of skeletal muscle.* Cell, 2003. **113**(7): p. 811-2.
124. Church, V.L. and P. Francis-West, *Wnt signalling during limb development.* Int J Dev Biol, 2002. **46**(7): p. 927-36.
125. Pongracz, J.E. and R.A. Stockley, *Wnt signalling in lung development and diseases.* Respir Res, 2006. **7**: p. 15.
126. Esteve, P. and P. Bovolenta, *Secreted inducers in vertebrate eye development: more functions for old morphogens.* Curr Opin Neurobiol, 2006. **16**(1): p. 13-9.
127. Wurst, W. and L. Bally-Cuif, *Neural plate patterning: upstream and downstream of the isthmic organizer.* Nat Rev Neurosci, 2001. **2**(2): p. 99-108.
128. Packard, M., D. Mathew, and V. Budnik, *Wnts and TGF beta in synaptogenesis: old friends signalling at new places.* Nat Rev Neurosci, 2003. **4**(2): p. 113-20.
129. Salinas, P.C., *Synaptogenesis: Wnt and TGF-beta take centre stage.* Curr Biol, 2003. **13**(2): p. R60-2.
130. Giraldez, A.J. and S.M. Cohen, *Wingless and Notch signaling provide cell survival cues and control cell proliferation during wing development.* Development, 2003. **130**(26): p. 6533-43.

131. Shtutman, M., et al., *The cyclin D1 gene is a target of the beta-catenin/LEF-1 pathway.* Proc Natl Acad Sci U S A, 1999. **96**(10): p. 5522-7.
132. He, T.C., et al., *Identification of c-MYC as a target of the APC pathway.* Science, 1998. **281**(5382): p. 1509-12.
133. Reya, T. and H. Clevers, *Wnt signalling in stem cells and cancer.* Nature, 2005. **434**(7035): p. 843-50.
134. Kuhl, M., *The WNT/calcium pathway: biochemical mediators, tools and future requirements.* Front Biosci, 2004. **9**: p. 967-74.
135. Seifert, J.R. and M. Mlodzik, *Frizzled/PCP signalling: a conserved mechanism regulating cell polarity and directed motility.* Nat Rev Genet, 2007. **8**(2): p. 126-38.
136. Veeman, M.T., J.D. Axelrod, and R.T. Moon, *A second canon. Functions and mechanisms of beta-catenin-independent Wnt signaling.* Dev Cell, 2003. **5**(3): p. 367-77.
137. Baron, R., G. Rawadi, and S. Roman-Roman, *Wnt signaling: a key regulator of bone mass.* Curr Top Dev Biol, 2006. **76**: p. 103-27.
138. Alonso, L. and E. Fuchs, *Stem cells in the skin: waste not, Wnt not.* Genes Dev, 2003. **17**(10): p. 1189-200.
139. Staal, F.J. and H.C. Clevers, *WNT signalling and haematopoiesis: a WNT-WNT situation.* Nat Rev Immunol, 2005. **5**(1): p. 21-30.
140. Gregorieff, A. and H. Clevers, *Wnt signaling in the intestinal epithelium: from endoderm to cancer.* Genes Dev, 2005. **19**(8): p. 877-90.
141. Clevers, H., *Wnt/beta-catenin signaling in development and disease.* Cell, 2006. **127**(3): p. 469-80.
142. De Ferrari, G.V. and R.T. Moon, *The ups and downs of Wnt signaling in prevalent neurological disorders.* Oncogene, 2006. **25**(57): p. 7545-53.
143. Moon, R.T., et al., *WNT and beta-catenin signalling: diseases and therapies.* Nat Rev Genet, 2004. **5**(9): p. 691-701.
144. Wodarz, A. and R. Nusse, *Mechanisms of Wnt signaling in development.* Annu Rev Cell Dev Biol, 1998. **14**: p. 59-88.
145. Nusse, R., *Wnt signaling in disease and in development.* Cell Res, 2005. **15**(1): p. 28-32.
146. Gordon, M.D. and R. Nusse, *Wnt signaling: multiple pathways, multiple receptors, and multiple transcription factors.* J Biol Chem, 2006. **281**(32): p. 22429-33.
147. Barrow, J.R., *Wnt/PCP signaling: a veritable polar star in establishing patterns of polarity in embryonic tissues.* Semin Cell Dev Biol, 2006. **17**(2): p. 185-93.
148. Strutt, D., *Frizzled signalling and cell polarisation in Drosophila and vertebrates.* Development, 2003. **130**(19): p. 4501-13.
149. Klein, T.J. and M. Mlodzik, *Planar cell polarization: an emerging model points in the right direction.* Annu Rev Cell Dev Biol, 2005. **21**: p. 155-76.
150. Kohn, A.D. and R.T. Moon, *Wnt and calcium signaling: beta-catenin-independent pathways.* Cell Calcium, 2005. **38**(3-4): p. 439-46.
151. Kuhl, M., et al., *The Wnt/Ca2+ pathway: a new vertebrate Wnt signaling pathway takes shape.* Trends Genet, 2000. **16**(7): p. 279-83.
152. Cadigan, K.M. and Y.I. Liu, *Wnt signaling: complexity at the surface.* J Cell Sci, 2006. **119**(Pt 3): p. 395-402.
153. http://www.stanford.edu/~rnusse/wntwindow.html.
154. Davidson, G., et al., *Casein kinase 1 gamma couples Wnt receptor activation to cytoplasmic signal transduction.* Nature, 2005. **438**(7069): p. 867-72.
155. Zeng, X., et al., *A dual-kinase mechanism for Wnt co-receptor phosphorylation and activation.* Nature, 2005. **438**(7069): p. 873-7.

156. Cong, F., L. Schweizer, and H. Varmus, *Wnt signals across the plasma membrane to activate the beta-catenin pathway by forming oligomers containing its receptors, Frizzled and LRP.* Development, 2004. **131**(20): p. 5103-15.
157. Holmen, S.L., et al., *Wnt-independent activation of beta-catenin mediated by a Dkk1-Fz5 fusion protein.* Biochem Biophys Res Commun, 2005. **328**(2): p. 533-9.
158. Brennan, K., et al., *Truncated mutants of the putative Wnt receptor LRP6/Arrow can stabilize beta-catenin independently of Frizzled proteins.* Oncogene, 2004. **23**(28): p. 4873-84.
159. Cliffe, A., F. Hamada, and M. Bienz, *A role of Dishevelled in relocating Axin to the plasma membrane during wingless signaling.* Curr Biol, 2003. **13**(11): p. 960-6.
160. Lustig, B., et al., *Negative feedback loop of Wnt signaling through upregulation of conductin/axin2 in colorectal and liver tumors.* Mol Cell Biol, 2002. **22**(4): p. 1184-93.
161. Niida, A., et al., *DKK1, a negative regulator of Wnt signaling, is a target of the beta-catenin/TCF pathway.* Oncogene, 2004. **23**(52): p. 8520-6.
162. Hausmann, G., C. Banziger, and K. Basler, *Helping Wingless take flight: how WNT proteins are secreted.* Nat Rev Mol Cell Biol, 2007.
163. Mikels, A.J. and R. Nusse, *Wnts as ligands: processing, secretion and reception.* Oncogene, 2006. **25**(57): p. 7461-8.
164. Schlesinger, A. and B.Z. Shilo, *ER retention of signaling modules.* Dev Cell, 2005. **8**(2): p. 136-7.
165. Kadowaki, T., et al., *The segment polarity gene porcupine encodes a putative multitransmembrane protein involved in Wingless processing.* Genes Dev, 1996. **10**(24): p. 3116-28.
166. Takada, R., et al., *Monounsaturated fatty acid modification of Wnt protein: its role in Wnt secretion.* Dev Cell, 2006. **11**(6): p. 791-801.
167. Bartscherer, K., et al., *Secretion of Wnt ligands requires Evi, a conserved transmembrane protein.* Cell, 2006. **125**(3): p. 523-33.
168. Banziger, C., et al., *Wntless, a conserved membrane protein dedicated to the secretion of Wnt proteins from signaling cells.* Cell, 2006. **125**(3): p. 509-22.
169. Coudreuse, D.Y., et al., *Wnt gradient formation requires retromer function in Wnt-producing cells.* Science, 2006. **312**(5775): p. 921-4.
170. Prasad, B.C. and S.G. Clark, *Wnt signaling establishes anteroposterior neuronal polarity and requires retromer in C. elegans.* Development, 2006. **133**(9): p. 1757-66.
171. Yamamoto, A., et al., *Shisa promotes head formation through the inhibition of receptor protein maturation for the caudalizing factors, Wnt and FGF.* Cell, 2005. **120**(2): p. 223-35.
172. Culi, J. and R.S. Mann, *Boca, an endoplasmic reticulum protein required for wingless signaling and trafficking of LDL receptor family members in Drosophila.* Cell, 2003. **112**(3): p. 343-54.
173. Hsieh, J.C., et al., *Mesd encodes an LRP5/6 chaperone essential for specification of mouse embryonic polarity.* Cell, 2003. **112**(3): p. 355-67.
174. Wehrli, M., et al., *arrow encodes an LDL-receptor-related protein essential for Wingless signalling.* Nature, 2000. **407**(6803): p. 527-30.
175. Pinson, K.I., et al., *An LDL-receptor-related protein mediates Wnt signalling in mice.* Nature, 2000. **407**(6803): p. 535-8.
176. Tamai, K., et al., *LDL-receptor-related proteins in Wnt signal transduction.* Nature, 2000. **407**(6803): p. 530-5.
177. May, P., H.H. Bock, and J. Herz, *Integration of endocytosis and signal transduction by lipoprotein receptors.* Sci STKE, 2003. **2003**(176): p. PE12.

178. Schneider, W.J. and J. Nimpf, *LDL receptor relatives at the crossroad of endocytosis and signaling.* Cell Mol Life Sci, 2003. **60**(5): p. 892-903.
179. He, X., et al., *LDL receptor-related proteins 5 and 6 in Wnt/beta-catenin signaling: arrows point the way.* Development, 2004. **131**(8): p. 1663-77.
180. Culi, J., T.A. Springer, and R.S. Mann, *Boca-dependent maturation of beta-propeller/EGF modules in low-density lipoprotein receptor proteins.* Embo J, 2004. **23**(6): p. 1372-80.
181. Willert, K., et al., *Wnt proteins are lipid-modified and can act as stem cell growth factors.* Nature, 2003. **423**(6938): p. 448-52.
182. Zecca, M., K. Basler, and G. Struhl, *Direct and long-range action of a wingless morphogen gradient.* Cell, 1996. **87**(5): p. 833-44.
183. Neumann, C.J. and S.M. Cohen, *Long-range action of Wingless organizes the dorsal-ventral axis of the Drosophila wing.* Development, 1997. **124**(4): p. 871-80.
184. Zhu, A.J. and M.P. Scott, *Incredible journey: how do developmental signals travel through tissue?* Genes Dev, 2004. **18**(24): p. 2985-97.
185. Eaton, S., *Release and trafficking of lipid-linked morphogens.* Curr Opin Genet Dev, 2006. **16**(1): p. 17-22.
186. Panakova, D., et al., *Lipoprotein particles are required for Hedgehog and Wingless signalling.* Nature, 2005. **435**(7038): p. 58-65.
187. Greco, V., M. Hannus, and S. Eaton, *Argosomes: a potential vehicle for the spread of morphogens through epithelia.* Cell, 2001. **106**(5): p. 633-45.
188. Ramirez-Weber, F.A. and T.B. Kornberg, *Cytonemes: cellular processes that project to the principal signaling center in Drosophila imaginal discs.* Cell, 1999. **97**(5): p. 599-607.
189. Lin, X., *Functions of heparan sulfate proteoglycans in cell signaling during development.* Development, 2004. **131**(24): p. 6009-21.
190. Melkonyan, H.S., et al., *SARPs: a family of secreted apoptosis-related proteins.* Proc Natl Acad Sci U S A, 1997. **94**(25): p. 13636-41.
191. Uren, A., et al., *Secreted frizzled-related protein-1 binds directly to Wingless and is a biphasic modulator of Wnt signaling.* J Biol Chem, 2000. **275**(6): p. 4374-82.
192. Hsieh, J.C., et al., *A new secreted protein that binds to Wnt proteins and inhibits their activities.* Nature, 1999. **398**(6726): p. 431-6.
193. Gorfinkiel, N., et al., *The Drosophila ortholog of the human Wnt inhibitor factor Shifted controls the diffusion of lipid-modified Hedgehog.* Dev Cell, 2005. **8**(2): p. 241-53.
194. Bell, E., et al., *Cell fate specification and competence by Coco, a maternal BMP, TGFbeta and Wnt inhibitor.* Development, 2003. **130**(7): p. 1381-9.
195. Itasaki, N., et al., *Wise, a context-dependent activator and inhibitor of Wnt signalling.* Development, 2003. **130**(18): p. 4295-305.
196. Li, X., et al., *Sclerostin binds to LRP5/6 and antagonizes canonical Wnt signaling.* J Biol Chem, 2005. **280**(20): p. 19883-7.
197. Bafico, A., et al., *Novel mechanism of Wnt signalling inhibition mediated by Dickkopf-1 interaction with LRP6/Arrow.* Nat Cell Biol, 2001. **3**(7): p. 683-6.
198. Mao, B., et al., *LDL-receptor-related protein 6 is a receptor for Dickkopf proteins.* Nature, 2001. **411**(6835): p. 321-5.
199. Semenov, M.V., et al., *Head inducer Dickkopf-1 is a ligand for Wnt coreceptor LRP6.* Curr Biol, 2001. **11**(12): p. 951-61.
200. Guder, C., et al., *An ancient Wnt-Dickkopf antagonism in Hydra.* Development, 2006. **133**(5): p. 901-11.

201. Shinya, M., et al., *Zebrafish Dkk1, induced by the pre-MBT Wnt signaling, is secreted from the prechordal plate and patterns the anterior neural plate.* Mech Dev, 2000. **98**(1-2): p. 3-17.
202. Kazanskaya, O., A. Glinka, and C. Niehrs, *The role of Xenopus dickkopf1 in prechordal plate specification and neural patterning.* Development, 2000. **127**(22): p. 4981-92.
203. Hashimoto, H., et al., *Zebrafish Dkk1 functions in forebrain specification and axial mesendoderm formation.* Dev Biol, 2000. **217**(1): p. 138-52.
204. Mukhopadhyay, M., et al., *Dickkopf1 is required for embryonic head induction and limb morphogenesis in the mouse.* Dev Cell, 2001. **1**(3): p. 423-34.
205. Morvan, F., et al., *Deletion of a single allele of the Dkk1 gene leads to an increase in bone formation and bone mass.* J Bone Miner Res, 2006. **21**(6): p. 934-45.
206. Li, J., et al., *Dkk1-mediated inhibition of Wnt signaling in bone results in osteopenia.* Bone, 2006. **39**(4): p. 754-66.
207. MacDonald, B.T., M. Adamska, and M.H. Meisler, *Hypomorphic expression of Dkk1 in the doubleridge mouse: dose dependence and compensatory interactions with Lrp6.* Development, 2004. **131**(11): p. 2543-52.
208. Grotewold, L. and U. Ruther, *The Wnt antagonist Dickkopf-1 is regulated by Bmp signaling and c-Jun and modulates programmed cell death.* Embo J, 2002. **21**(5): p. 966-75.
209. Mukhopadhyay, M., et al., *Dkk2 plays an essential role in the corneal fate of the ocular surface epithelium.* Development, 2006. **133**(11): p. 2149-54.
210. Wu, W., et al., *Mutual antagonism between dickkopf1 and dickkopf2 regulates Wnt/beta-catenin signalling.* Curr Biol, 2000. **10**(24): p. 1611-4.
211. Mao, B., et al., *Kremen proteins are Dickkopf receptors that regulate Wnt/beta-catenin signalling.* Nature, 2002. **417**(6889): p. 664-7.
212. Nakamura, T., et al., *Molecular cloning and characterization of Kremen, a novel kringle-containing transmembrane protein.* Biochim Biophys Acta, 2001. **1518**(1-2): p. 63-72.
213. http://smart.embl-heidelberg.de/smart/do_annotation.pl?DOMAIN=KR&BLAST=DUMMY.
214. http://smart.embl-heidelberg.de/smart/do_annotation.pl?DOMAIN=CUB&BLAST=DUMMY.
215. Bork, P. and G. Beckmann, *The CUB domain. A widespread module in developmentally regulated proteins.* J Mol Biol, 1993. **231**(2): p. 539-45.
216. Patthy, L., et al., *Kringles: modules specialized for protein binding. Homology of the gelatin-binding region of fibronectin with the kringle structures of proteases.* FEBS Lett, 1984. **171**(1): p. 131-6.
217. Castellino, F.J. and S.G. McCance, *The kringle domains of human plasminogen.* Ciba Found Symp, 1997. **212**: p. 46-60; discussion 60-5.
218. http://smart.embl-heidelberg.de/smart/do_annotation.pl?DOMAIN=WSC&BLAST=DUMMY.
219. Lodder, A.L., T.K. Lee, and R. Ballester, *Characterization of the Wsc1 protein, a putative receptor in the stress response of Saccharomyces cerevisiae.* Genetics, 1999. **152**(4): p. 1487-99.
220. Davidson, G., et al., *Kremen proteins interact with Dickkopf1 to regulate anteroposterior CNS patterning.* Development, 2002. **129**(24): p. 5587-96.
221. Croce, J.C., et al., *A genome-wide survey of the evolutionarily conserved Wnt pathways in the sea urchin Strongylocentrotus purpuratus.* Dev Biol, 2006.

222. Morris, J., et al., *The Macrostomum lignano EST database as a molecular resource for studying platyhelminth development and phylogeny.* Dev Genes Evol, 2006. **216**(11): p. 695-707.
223. Mao, B. and C. Niehrs, *Kremen2 modulates Dickkopf2 activity during Wnt/LRP6 signaling.* Gene, 2003. **302**(1-2): p. 179-83.
224. Osada, M., et al., *The Wnt signaling antagonist Kremen1 is required for development of thymic architecture.* Clin Dev Immunol, 2006. **13**(2-4): p. 299-319.
225. www.stratagene.com/homepage/.
226. Jin, D.-Y. and K.-T. Jeang, *direct GenBank accession, no. U33821.* 1995.
227. De Valck, D., et al., *The zinc finger protein A20 interacts with a novel anti-apoptotic protein which is cleaved by specific caspases.* Oncogene, 1999. **18**(29): p. 4182-90.
228. Ling, L. and D.V. Goeddel, *T6BP, a TRAF6-interacting protein involved in IL-1 signaling.* Proc Natl Acad Sci U S A, 2000. **97**(17): p. 9567-72.
229. Nagaraja, G.M. and R.P. Kandpal, *Chromosome 13q12 encoded Rho GTPase activating protein suppresses growth of breast carcinoma cells, and yeast two-hybrid screen shows its interaction with several proteins.* Biochem Biophys Res Commun, 2004. **313**(3): p. 654-65.
230. Ulrich, M., et al., *Tax1-binding protein 1 is expressed in the retina and interacts with the GABA(C) receptor rho1 subunit.* Biochem J, 2007. **401**(2): p. 429-36.
231. Saito, R., H. Suzuki, and Y. Hayashizaki, *Interaction generality, a measurement to assess the reliability of a protein-protein interaction.* Nucleic Acids Res, 2002. **30**(5): p. 1163-8.
232. Grammer, T.C., et al., *Use of large-scale expression cloning screens in the Xenopus laevis tadpole to identify gene function.* Dev Biol, 2000. **228**(2): p. 197-210.
233. Chen, J.A., et al., *Identification of novel genes affecting mesoderm formation and morphogenesis through an enhanced large scale functional screen in Xenopus.* Mech Dev, 2005. **122**(3): p. 307-31.
234. Voigt, J., et al., *Expression cloning screening of a unique and full-length set of cDNA clones is an efficient method for identifying genes involved in Xenopus neurogenesis.* Mech Dev, 2005. **122**(3): p. 289-306.
235. Smith, W.C. and R.M. Harland, *Injected Xwnt-8 RNA acts early in Xenopus embryos to promote formation of a vegetal dorsalizing center.* Cell, 1991. **67**(4): p. 753-65.
236. Glinka, A., et al., *Combinatorial signalling by Xwnt-11 and Xnr3 in the organizer epithelium.* Mech Dev, 1996. **60**(2): p. 221-31.
237. Amaya, E., *Xenomics.* Genome Res, 2005. **15**(12): p. 1683-91.
238. Kazanskaya, O., et al., *R-Spondin2 is a secreted activator of Wnt/beta-catenin signaling and is required for Xenopus myogenesis.* Dev Cell, 2004. **7**(4): p. 525-34.
239. McCormick, M., *Sib selection.* Methods Enzymol, 1987. **151**: p. 445-9.
240. Haramoto, Y., et al., *Xenopus tropicalis nodal-related gene 3 regulates BMP signaling: an essential role for the pro-region.* Dev Biol, 2004. **265**(1): p. 155-68.
241. Yamada, K., T. Takabatake, and K. Takeshima, *Isolation and characterization of three novel serine protease genes from Xenopus laevis.* Gene, 2000. **252**(1-2): p. 209-16.
242. Matsumoto, K., et al., *CIRP2, a major cytoplasmic RNA-binding protein in Xenopus oocytes.* Nucleic Acids Res, 2000. **28**(23): p. 4689-97.
243. Meylan, E., et al., *RIP4 (DIK/PKK), a novel member of the RIP kinase family, activates NF-kappa B and is processed during apoptosis.* EMBO Rep, 2002. **3**(12): p. 1201-8.

244. Behrens, E.M., et al., *The mer receptor tyrosine kinase: expression and function suggest a role in innate immunity.* Eur J Immunol, 2003. **33**(8): p. 2160-7.
245. D'Souza-Schorey, C. and P. Chavrier, *ARF proteins: roles in membrane traffic and beyond.* Nat Rev Mol Cell Biol, 2006. **7**(5): p. 347-58.
246. Nie, Z., D.S. Hirsch, and P.A. Randazzo, *Arf and its many interactors.* Curr Opin Cell Biol, 2003. **15**(4): p. 396-404.
247. Kim, S.W., et al., *ADP-ribosylation factor 4 small GTPase mediates epidermal growth factor receptor-dependent phospholipase D2 activation.* J Biol Chem, 2003. **278**(4): p. 2661-8.
248. Donaldson, J.G. and A. Honda, *Localization and function of Arf family GTPases.* Biochem Soc Trans, 2005. **33**(Pt 4): p. 639-42.
249. Williger, B.T., et al., *Arfaptin 1 forms a complex with ADP-ribosylation factor and inhibits phospholipase D.* FEBS Lett, 1999. **454**(1-2): p. 85-9.
250. Weihofen, A., et al., *Identification of signal peptide peptidase, a presenilin-type aspartic protease.* Science, 2002. **296**(5576): p. 2215-8.
251. Hegde, R.S., *Targeting and beyond: new roles for old signal sequences.* Mol Cell, 2002. **10**(4): p. 697-8.
252. Lo, J.F., et al., *Tid1, a cochaperone of the heat shock 70 protein and the mammalian counterpart of the Drosophila tumor suppressor l(2)tid, is critical for early embryonic development and cell survival.* Mol Cell Biol, 2004. **24**(6): p. 2226-36.
253. Miller, S.M. and D.L. Kirk, *glsA, a Volvox gene required for asymmetric division and germ cell specification, encodes a chaperone-like protein.* Development, 1999. **126**(4): p. 649-58.
254. Luders, F., et al., *Slalom encodes an adenosine 3'-phosphate 5'-phosphosulfate transporter essential for development in Drosophila.* Embo J, 2003. **22**(14): p. 3635-44.
255. Ishida, N., et al., *Molecular cloning and characterization of a novel isoform of the human UDP-galactose transporter, and of related complementary DNAs belonging to the nucleotide-sugar transporter gene family.* J Biochem (Tokyo), 1996. **120**(6): p. 1074-8.
256. Gemmill, R.M., et al., *The TRC8 hereditary kidney cancer gene suppresses growth and functions with VHL in a common pathway.* Oncogene, 2002. **21**(22): p. 3507-16.
257. Gemmill, R.M., et al., *The hereditary renal cell carcinoma 3;8 translocation fuses FHIT to a patched-related gene, TRC8.* Proc Natl Acad Sci U S A, 1998. **95**(16): p. 9572-7.
258. Tang, Y.T., et al., *PAQR proteins: a novel membrane receptor family defined by an ancient 7-transmembrane pass motif.* J Mol Evol, 2005. **61**(3): p. 372-80.
259. Serneels, L., et al., *Differential contribution of the three Aph1 genes to gamma-secretase activity in vivo.* Proc Natl Acad Sci U S A, 2005. **102**(5): p. 1719-24.
260. Hollmann, M., et al., *The essential Drosophila melanogaster gene wds (will die slowly) codes for a WD-repeat protein with seven repeats.* Mol Genet Genomics, 2002. **268**(4): p. 425-33.
261. Dascher, C. and W.E. Balch, *Dominant inhibitory mutants of ARF1 block endoplasmic reticulum to Golgi transport and trigger disassembly of the Golgi apparatus.* J Biol Chem, 1994. **269**(2): p. 1437-48.
262. Peters, P.J., et al., *Overexpression of wild-type and mutant ARF1 and ARF6: distinct perturbations of nonoverlapping membrane compartments.* J Cell Biol, 1995. **128**(6): p. 1003-17.

263. Cruciat, C.M., C. Hassler, and C. Niehrs, *The MRH protein Erlectin is a member of the endoplasmic reticulum synexpression group and functions in N-glycan recognition.* J Biol Chem, 2006. **281**(18): p. 12986-93.
264. Munro, S., *The MRH domain suggests a shared ancestry for the mannose 6-phosphate receptors and other N-glycan-recognising proteins.* Curr Biol, 2001. **11**(13): p. R499-501.
265. Ghosh, P., N.M. Dahms, and S. Kornfeld, *Mannose 6-phosphate receptors: new twists in the tale.* Nat Rev Mol Cell Biol, 2003. **4**(3): p. 202-12.
266. Kornfeld, S., *Structure and function of the mannose 6-phosphate/insulinlike growth factor II receptors.* Annu Rev Biochem, 1992. **61**: p. 307-30.
267. Litovchick, L., E. Friedmann, and S. Shaltiel, *A selective interaction between OS-9 and the carboxyl-terminal tail of meprin beta.* J Biol Chem, 2002. **277**(37): p. 34413-23.
268. Baek, J.H., et al., *OS-9 interacts with hypoxia-inducible factor 1alpha and prolyl hydroxylases to promote oxygen-dependent degradation of HIF-1alpha.* Mol Cell, 2005. **17**(4): p. 503-12.
269. Bhamidipati, A., et al., *Exploration of the topological requirements of ERAD identifies Yos9p as a lectin sensor of misfolded glycoproteins in the ER lumen.* Mol Cell, 2005. **19**(6): p. 741-51.
270. Buschhorn, B.A., et al., *A genome-wide screen identifies Yos9p as essential for ER-associated degradation of glycoproteins.* FEBS Lett, 2004. **577**(3): p. 422-6.
271. Kim, W., E.D. Spear, and D.T. Ng, *Yos9p detects and targets misfolded glycoproteins for ER-associated degradation.* Mol Cell, 2005. **19**(6): p. 753-64.
272. Szathmary, R., et al., *Yos9 protein is essential for degradation of misfolded glycoproteins and may function as lectin in ERAD.* Mol Cell, 2005. **19**(6): p. 765-75.
273. Raas-Rothschild, A., et al., *Genomic organisation of the UDP-N-acetylglucosamine-1-phosphotransferase gamma subunit (GNPTAG) and its mutations in mucolipidosis III.* J Med Genet, 2004. **41**(4): p. e52.
274. Raas-Rothschild, A., et al., *Molecular basis of variant pseudo-hurler polydystrophy (mucolipidosis IIIC).* J Clin Invest, 2000. **105**(5): p. 673-81.
275. D'Alessio, C., et al., *Genetic evidence for the heterodimeric structure of glucosidase II. The effect of disrupting the subunit-encoding genes on glycoprotein folding.* J Biol Chem, 1999. **274**(36): p. 25899-905.
276. Drenth, J.P., et al., *Germline mutations in PRKCSH are associated with autosomal dominant polycystic liver disease.* Nat Genet, 2003. **33**(3): p. 345-7.
277. Pelletier, M.F., et al., *The heterodimeric structure of glucosidase II is required for its activity, solubility, and localization in vivo.* Glycobiology, 2000. **10**(8): p. 815-27.
278. Treml, K., et al., *The alpha- and beta-subunits are required for expression of catalytic activity in the hetero-dimeric glucosidase II complex from human liver.* Glycobiology, 2000. **10**(5): p. 493-502.
279. Trombetta, E.S., J.F. Simons, and A. Helenius, *Endoplasmic reticulum glucosidase II is composed of a catalytic subunit, conserved from yeast to mammals, and a tightly bound noncatalytic HDEL-containing subunit.* J Biol Chem, 1996. **271**(44): p. 27509-16.
280. Wilkinson, B.M., J. Purswani, and C.J. Stirling, *Yeast GTB1 Encodes a Subunit of Glucosidase II Required for Glycoprotein Processing in the Endoplasmic Reticulum.* J Biol Chem, 2006. **281**(10): p. 6325-33.
281. Sive, H., K. Hattori, and H. Weintraub, *Progressive determination during formation of the anteroposterior axis in Xenopus laevis.* Cell, 1989. **58**: p. 171-180.

282. Niehrs, C. and N. Pollet, *Synexpression groups in eukaryotes.* Nature, 1999. **402**(6761): p. 483-7.
283. Baldessari, D., et al., *Global gene expression profiling and cluster analysis in Xenopus laevis.* Mech Dev, 2005. **122**(3): p. 441-75.
284. Thisse, B., et al., *Expression of the zebrafish genome during embryogenesis (NIH R01 RR15402).* ZFIN Direct Data Submission 2001.
285. Rutkowski, D.T. and R.J. Kaufman, *A trip to the ER: coping with stress.* Trends Cell Biol, 2004. **14**(1): p. 20-8.
286. Bernales, S., F.R. Papa, and P. Walter, *Intracellular signaling by the unfolded protein response.* Annu Rev Cell Dev Biol, 2006. **22**: p. 487-508.
287. Schroder, M. and R.J. Kaufman, *The mammalian unfolded protein response.* Annu Rev Biochem, 2005. **74**: p. 739-89.
288. Wu, J. and R.J. Kaufman, *From acute ER stress to physiological roles of the Unfolded Protein Response.* Cell Death Differ, 2006. **13**(3): p. 374-84.
289. Wang, Y., et al., *Activation of ATF6 and an ATF6 DNA binding site by the endoplasmic reticulum stress response.* J Biol Chem, 2000. **275**(35): p. 27013-20.
290. Lee, A.S., *The ER chaperone and signaling regulator GRP78/BiP as a monitor of endoplasmic reticulum stress.* Methods, 2005. **35**(4): p. 373-81.
291. Ponnambalam, S., et al., *The TGN38 glycoprotein contains two non-overlapping signals that mediate localization to the trans-Golgi network.* J Cell Biol, 1994. **125**(2): p. 253-68.
292. Wilson, J.M., et al., *EEA1, a tethering protein of the early sorting endosome, shows a polarized distribution in hippocampal neurons, epithelial cells, and fibroblasts.* Mol Biol Cell, 2000. **11**(8): p. 2657-71.
293. Tjoelker, L.W., et al., *Human, mouse, and rat calnexin cDNA cloning: identification of potential calcium binding motifs and gene localization to human chromosome 5.* Biochemistry, 1994. **33**(11): p. 3229-36.
294. Bourguignon, C., J. Li, and N. Papalopulu, *XBF-1, a winged helix transcription factor with dual activity, has a role in positioning neurogenesis in Xenopus competent ectoderm.* Development, 1998. **125**(24): p. 4889-900.
295. Bradley, L.C., et al., *The structure and expression of the Xenopus Krox-20 gene: conserved and divergent patterns of expression in rhombomeres and neural crest.* Mech Dev, 1993. **40**(1-2): p. 73-84.
296. Blitz, I.L. and K.W.Y. Cho, *Anterior neuroectoderm is progressively induced during gastrulation: the role of the Xenopus homeobox gene orthodenticle.* Development, 1995. **121**(4): p. 993-1004.
297. Heasman, J., M. Kofron, and C. Wylie, *Beta-catenin signaling activity dissected in the early Xenopus embryo: a novel antisense approach.* Dev Biol, 2000. **222**(1): p. 124-34.
298. Aoki, Y., et al., *Sox10 regulates the development of neural crest-derived melanocytes in Xenopus.* Dev Biol, 2003. **259**(1): p. 19-33.
299. Barembaum, M. and M. Bronner-Fraser, *Early steps in neural crest specification.* Semin Cell Dev Biol, 2005. **16**(6): p. 642-6.
300. Wu, J., J.P. Saint-Jeannet, and P.S. Klein, *Wnt-frizzled signaling in neural crest formation.* Trends Neurosci, 2003. **26**(1): p. 40-5.
301. Li, Y., et al., *Mesd binds to mature LDL-receptor-related protein-6 and antagonizes ligand binding.* J Cell Sci, 2005. **118**(Pt 22): p. 5305-14.
302. Jackson, M.R., T. Nilsson, and P.A. Peterson, *Identification of a consensus motif for retention of transmembrane proteins in the endoplasmic reticulum.* Embo J, 1990. **9**(10): p. 3153-62.

303. Nilsson, T., M. Jackson, and P.A. Peterson, *Short cytoplasmic sequences serve as retention signals for transmembrane proteins in the endoplasmic reticulum.* Cell, 1989. **58**(4): p. 707-18.
304. Zerangue, N., et al., *Analysis of endoplasmic reticulum trafficking signals by combinatorial screening in mammalian cells.* Proc Natl Acad Sci U S A, 2001. **98**(5): p. 2431-6.
305. Zhu, A.J., et al., *Altered localization of Drosophila Smoothened protein activates Hedgehog signal transduction.* Genes Dev, 2003. **17**(10): p. 1240-52.
306. Ellgaard, L. and A. Helenius, *Quality control in the endoplasmic reticulum.* Nat Rev Mol Cell Biol, 2003. **4**(3): p. 181-91.
307. Osborne, A.R., T.A. Rapoport, and B. van den Berg, *Protein Translocation by the Sec61/Secy Channel.* Annu Rev Cell Dev Biol, 2005. **21**: p. 529-550.
308. Sitia, R. and I. Braakman, *Quality control in the endoplasmic reticulum protein factory.* Nature, 2003. **426**(6968): p. 891-4.
309. Trombetta, E.S. and A.J. Parodi, *Quality control and protein folding in the secretory pathway.* Annu Rev Cell Dev Biol, 2003. **19**: p. 649-76.
310. Yao, J. and D.S. Kessler, *Goosecoid promotes head organizer activity by direct repression of Xwnt8 in Spemann's organizer.* Development, 2001. **128**(15): p. 2975-87.
311. Garriock, R.J. and P.A. Krieg, *Wnt11-R signaling regulates a calcium sensitive EMT event essential for dorsal fin development of Xenopus.* Dev Biol, 2007. **304**(1): p. 127-40.
312. http://cgap.nci.nih.gov/.
313. Howell, B.W. and J. Herz, *The LDL receptor gene family: signaling functions during development.* Curr Opin Neurobiol, 2001. **11**(1): p. 74-81.
314. Sambrook, J., E. Fritsch, and T. Maniatis, *Molecular Cloning. A Laboratory Manual*. 2nd ed. 1989: Cold Spring Harbor Laboratory Press.
315. Carninci, P., et al., *Normalization and subtraction of cap-trapper-selected cDNAs to prepare full-length cDNA libraries for rapid discovery of new genes.* Genome Res, 2000. **10**(10): p. 1617-30.
316. Niehrs, C., H. Steinbeisser, and E.M. De Robertis, *Mesodermal patterning by a gradient of the vertebrate homeobox gene goosecoid.* Science, 1994. **263**(5148): p. 817-20.
317. Ruiz i Altaba, A. and D.A. Melton, *Involvement of the Xenopus homeobox gene Xhox3 in pattern formation along the anterior-posterior axis.* Cell, 1989. **57**(2): p. 317-26.
318. Gawantka, V., et al., *Antagonizing the Spemann organizer: role of the homeobox gene Xvent-1.* Embo J, 1995. **14**(24): p. 6268-79.
319. Niehrs, C. and E.M. De Robertis, *Ectopic expression of a homeobox gene changes cell fate in Xenopus embryos in a position-specific manner.* Embo J, 1991. **10**(12): p. 3621-9.
320. Wolda, S.L., C.J. Moody, and R.T. Moon, *Overlapping expression of Xwnt-3A and Xwnt-1 in neural tissue of Xenopus laevis embryos.* Dev Biol, 1993. **155**(1): p. 46-57.
321. Sokol, S., et al., *Injected Wnt RNA induces a complete body axis in Xenopus embryos.* Cell, 1991. **67**(4): p. 741-52.
322. http://www.gene-tools.com/.
323. Sive, H.L., R.M. Grainger, and R.M. Harland, *Fate Mapping and Lineage Labeling*, in *Early Development of Xenopus laevis: A Laboratory Manual*, S. Curtis and M. Cozza, Editors. 2000, Cold Spring Harbor Laboratory Press: New York. p. 143-170.

324. Harland, R.M., *In situ hybridization: an improved whole-mount method for Xenopus embryos.* Methods Cell Biol, 1991. **36**: p. 685-95.
325. http://tropicalis.berkeley.edu/home/.
326. Hata, A., et al., *OAZ uses distinct DNA- and protein-binding zinc fingers in separate BMP-Smad and Olf signaling pathways.* Cell, 2000. **100**(2): p. 229-40.
327. Luckow, B. and G. Schutz, *CAT constructions with multiple unique restriction sites for the functional analysis of eukaryotic promoters and regulatory elements.* Nucleic Acids Res, 1987. **15**(13): p. 5490.

Acknowledgements

First of all, I would like to thank my supervisor Prof. Dr. Christof Niehrs for giving me the opportunity to be a member of his laboratory and for his support throughout all these years. I also thank the organizers of the Graduate college GRK791 (DFG) for providing me with a fellowship for three years.

I am very grateful to my collaborators Cristina Cruciat, Ya-Lin Huang, Gary Davidson, Sei Kuriyama and Roberto Mayor, who contributed significant results to my thesis work. Furthermore, I thank Emil Karaulanov, Andrei Glinka, Sonia Pinho, Olga Kazanskaya, Kristina Ellwanger, Xi He, Wei Wu, Herbert Steinbeisser and Hr. Eilers for sharing reagents and protocols. Special thanks go to Emil Karaulanov and Anshuman Kelkar for their critical reading of manuscripts.

I am deeply indebted to all members of the Niehrs lab, foremost Emil and Andrei, for helpful suggestions, practical advice and interesting discussions.

My warm thanks for a nice atmosphere in the lab, and Heidelberg in general, go to Alexandra, Andrea, Andrei, Caro, Cristina, Danila, Emil, Gabriel, Guillermo, Henry, Lili, Sonia, Suresh, Ursula, Ya-Lin and, of course, the Golden Grad Girls Caro, Gitta and Julia. It is difficult to imagine how the last years would have been without Anshumi.

Last, but not least, I dearly thank my family, including parents and brother, for their support and sympathy.

Publications derived from this work

Cruciat, C. M., Hassler, C. and Niehrs, C. (2006). The MRH protein Erlectin is a member of the endoplasmic reticulum synexpression group and functions in N-glycan recognition. *J Biol Chem* **281**, 12986-93

Hassler, C., Cruciat C. M., Kuriyama S., Mayor R., and Niehrs C. (2007). Kremen is required for neural crest induction in Xenopus and promotes LRP6-mediated Wnt signaling. Submitted to *Development*